

**UNIVERSIDAD DE INGENIERÍA Y TECNOLOGÍA**  
**CARRERA DE INGENIERÍA DE LA ENERGÍA**



**EVALUATION OF THE ENERGETIC COST OF  
BACTERIAL ELIMINATION OF E. COLI USING  
THE ELECTROPORATION TECHNIQUE IN  
CUVETTE VESSELS**

**TESIS**

Para optar el título profesional de Ingeniero de la Energía

**AUTOR**

Sergio Plasencia Gutiérrez (ORCID: 0000-0002-7132-2061)

**ASESOR**

Lei Zhang (ORCID: 0000-0001-6537-9814)

Lima – Perú

2021

**UNIVERSITY OF ENGINEERING AND TECHNOLOGY**  
**ENERGY ENGINEERING CAREER**



**EVALUATION OF THE ENERGETIC COST OF  
BACTERIAL ELIMINATION OF *E. COLI* USING THE  
ELECTROPORATION TECHNIQUE IN CUVETTE  
VESSELS**

**THESIS**

To obtain the college degree in Energy Engineering

**AUTHOR:**

Sergio Plasencia Gutiérrez (ORCID: 0000-0002-7132-2061)

**ADVISOR:**

Lei Zhang (ORCID: 0000-0001-6537-9814)

Lima – Perú

2021

*Dedication:*

To my dearest family, whom I love with all my heart.

To my brother Sebas, who is in Spain studying Cinema and Script, and to my  
brother Adrian who has just started his life in college.

To my grandparents, aunts, and cousins to my parents and brothers.

*Acknowledgments:*

Thank you, father and mother, teachers, Professor Lei, grandparents, siblings, and friends. Thank you, Hector, for lending me your book on circuit fundamentals during my first semester, you have been a great mentor mate.

Thank you, Luz Narciza and Giulianna Travi, with your help I was able to go through the cultivation process of my thesis and have a lot of fun during the experimentation process in the lab.

Thanks, God, for letting me achieve this experience which was very hard at the beginning.

# TABLE OF CONTENTS

	Pág.
ABSTRACT .....	15
INTRODUCTION .....	16
CHAPTER I:.....	22
THEORETICAL FRAMEWORK.....	22
1.1 <i>E. coli</i> cell.....	22
1.1.1 Cell dimensions.....	22
1.1.2 Dielectric <i>E. coli</i> parameters.....	23
1.2 Electroporation Principle.....	23
1.2.1 Irreversible Electroporation .....	24
1.2.2 Cell death .....	25
1.2.3 Membrane permeabilization .....	25
1.3 Actual irreversible electroporation studies .....	26
1.3.1 Actual mathematical models.....	26
1.3.2 Electroporation in the medical field.....	26
1.4 Equations and electrical formulas.....	27
1.4.1 External electrical field $E_e$ .....	27
1.4.2 Voltage-current relation of a capacitor .....	30
1.4.3 Ohm's Law.....	32
1.4.4 Kirchoff's Laws .....	32
1.4.4.1 Series Circuit.....	33
1.4.4.2 Parallel circuit .....	35
1.4.5 Electroporation phenomenon.....	37

1.4.6	Threshold electrical field <b><i>Ec</i></b> .....	38
1.4.7	Survivability equation.....	39
1.5	Electroporation equipment .....	40
1.5.1	Unipolar pulse generator.....	40
1.5.2	BTX Disposable Cuvettes Plus.....	40
1.5.3	Spectrophotometer Nanodrop - ND 1000.....	41
1.6	Softwares .....	42
1.6.1	Simulink from MATLAB <sup>®</sup> .....	42
CHAPTER		II:
	.....	43
	.....	
	METHODOLOGY	
	.....	43
2.1	Preparation of the contaminated tap water sample.....	45
2.2	Energy transfer simulation.....	46
2.2.1	Parameter's measurements.....	47
2.2.1.1	Electrical parameters .....	47
2.2.1.2	pH and temperature measurements .....	49
2.2.2	Simulink simulation explanation .....	50
2.2.3	Energy measurements with Simulink .....	53
2.3	Survivability analysis of <i>E. coli</i> .....	54
2.3.1	Colonies counting in Petri Plates .....	54
2.3.2	Spectrophotometric analysis UV-VIS OD600.....	55
2.4	Regression formula of survivability of the <i>E. coli</i> .....	57
2.5	Threshold value of the electrical field required for elimination 50 % of <i>E. coli</i> colonies	

CHAPTER		III:
.....		59
RESULTS	AND	DISCUSSIONS
.....		59
3.1	Energy transfer simulation.....	59
3.1.1	Thermo-physical parameters.....	59
3.1.2	Electrical parameters' measurements .....	62
3.1.2.1	RLC-meter's measurements.....	62
3.1.3	AMPROBE AC50A current measurements.....	63
3.1.3.1	Analysis Consideration 1: Change in the resistivity $\rho$ of the medium .....	64
3.1.3.2	Analysis Consideration 2: Change in the electrical conductivity K of the medium 66	
3.1.3.3	Final current discussion.....	67
3.1.4	Simulink simulation.....	68
3.1.4.1	Enthalpy $\Delta H$ simulation .....	69
3.2	Survivability equation of <i>E. coli</i> .....	73
3.2.1	Colonies counting in Petri plates .....	73
3.2.1.1	Discussion of the survivability trend.....	75
3.2.2	Spectrophotometric analysis UV-VIS OD600.....	76
3.3	Regression formula for <i>E. coli</i> survivability .....	78
3.4	Threshold electrical value for killing 50% of <i>E. coli</i> .....	79
3.5	Final discussion .....	81
.....	.....CONCLUSIONS	
.....	.....	82

.....	RECOMENDATIONS	
.....		84
.....	BIBLIOGRAPHY	
.....		86
.....	APPENDIXES	
.....		94



## TABLES' INDEX

<b>Table 2.1.</b> Voltages attainable by each cuvette according to distance from the Gap. ....	47
<b>Table 2.2.</b> Parameters read RLC-meter cuvette 4 mm. ....	48
<b>Table 2.3.</b> Impedance, Phase angle and reactance per electric field (100-100000 Hz) .....	49
<b>Table 2.4.</b> pH and temperature measurements .....	50
<b>Table 2.5.</b> Colony count for each field value .....	55
<b>Table 2.6.</b> Spectrophotometry tests .....	57
<b>Table 3.1.</b> pH and temperature measurements before and after electroporation .....	59
<b>Table 3.2.</b> Thermal energy and power transferred to the cuvette per pulse .....	61
<b>Table 3.3.</b> Inductance, capacitance, and series resistance measured by the RLC instrument, before and after the electroporation procedure. Last three columns show the variation of the parameters with respect to the initial values. ....	63
<b>Table 3.4.</b> Dielectric constant K and capacitance C values according to pre- and post-electroporation temperatures. ....	66
<b>Table 3.5.</b> Capacitance Cs and Resistance Rs measured from the 2mm cuvette .....	68
<b>Table 3.6.</b> Capacitance and resistivity (average and standard deviation) .....	68
<b>Table 3.7.</b> Values of Cs, Rp and Rs per simulated scenario .....	70
<b>Table 3.8.</b> Thermal energy dissipated in the cuvette vessel according to scenario and actual enthalpy .....	71
<b>Table 3.9.</b> Percentage of energy dissipated as heat to the vessel .....	73
<b>Table 3.10.</b> Surviving colonies per electric field value .....	74
<b>Table 3.11.</b> Control samples .....	74
<b>Table 3.12.</b> Percentage of colonies that survived the treatment (3 samples per e-field pulse) .....	74
<b>Table 3.13.</b> Pre- and post-electroporation treatment absorbance values .....	77

<b>Table 3.14.</b> Average survivability per e-field value applied.....	78
<b>Table 3.15.</b> Energy for eliminating a specific percentage of colonies per e-field pulse applied .....	79
<b>Table 3.16.</b> Result after analysis of data and results .....	81
<b>Table 7.1.</b> Matrix of cuvettes per electric field value .....	100
<b>Table 7.2.</b> Final electrical parameters .....	101
<b>Table 7.3.</b> Pulses applied to each dilution.....	104
<b>Table 7.4.</b> Parameter variation - 10 kV/cm- Dilution 1 .....	105
<b>Table 7.5.</b> Parameter variation - 20 kV/cm - Dilutions 2 and 3.....	105
<b>Table 7.6.</b> Parameter variation - 20 kV/cm - Dilutions 1, 2 and 3.....	105
<b>Table 7.7.</b> Frequency analysis of inductance, capacitance, and resistance.....	106
<b>Table 7.8.</b> Frequency analysis of impedance. ....	106
<b>Table 7.9.</b> Variation of the current measured for each pulse with respect to time. ....	117
<b>Table 7.10.</b> Resistivity, conductance and resistance values of water samples from Rimac basin and Lurin tapwater (Autoridad Nacional del Agua [76], INEI [77], Lurín [78]).....	119

## FIGURES' INDEX

<b>Figure 1.1.</b> Rod shape of <i>E. coli</i> bacteria. [24] .....	23
<b>Figure 1.2.</b> Parallel plate capacitor concept [43] .....	28
<b>Figure 1.3.</b> Polarization of bacteria due to the application of an electric field pulse [44] ...	30
<b>Figure 1.4.</b> Quadratic pulse [45] .....	31
<b>Figure 1.5.</b> Current Loop according to Kirchoff's Voltage Law - Reference Image. ....	33
<b>Figure 1.6.</b> Equivalent parallel circuit and current flow. ....	35
<b>Figure 1.7.</b> ECM 830 Pulse Generator [48] .....	40
<b>Figure 1.8.</b> Disposable Electroporation Cuvettes Plus [48] .....	41
<b>Figure 1.9.</b> Spectrophotometer ND-1000. ....	42
<b>Figure 1.10.</b> Simulink from MATLAB® .....	42
<b>Figure 2.1.</b> Application of voltage to the cuvette .....	43
<b>Figure 2.2.</b> Methodology flowchart .....	45
<b>Figure 2.3.</b> RLC-meter IET DE-5000 .....	47
<b>Figure 2.4.</b> Amprobe AC50A – Current sensor .....	49
<b>Figure 2.5.</b> Power flow from the pulse generator to the cuvette .....	51
<b>Figure 2.6.</b> Series and Parallel Circuit. Source: Manual RLC-meter IET D-5000 .....	51
<b>Figure 2.7.</b> a) Complete equivalent circuits modeling a real capacitor [69], b) Classical equivalent circuit of a capacitor [70] c) Cuvette filled with biological medium [71]. ....	52
<b>Figure 2.8.</b> Final simulation of the circuit in Simulink .....	53
<b>Figure 2.9.</b> Parameters of the simulated DC Pulse Voltage Generator .....	53
<b>Figure 2.10.</b> Simulink sensors and displays (a) voltage sensor, (b) current sensor, (c) multiplier, (d) integrator, (e) scope) .....	54
<b>Figure 2.11.</b> Inoculation model for spectrophotometer usage .....	56

<b>Figure 3.1.</b> Variation of peak current with respect to time .....	64
<b>Figure 3.2.</b> Increase in current during applied pulses in an irreversible electroporation experiment [64].....	65
<b>Figure 3.3.</b> Plots of dissipated energy per electric field value (red: experimentation, blue: simulation with average values, yellow: simulation with values measured with RLC-meter). .....	72
<b>Figure 3.4.</b> Increased electroporation efficiency in <i>E. coli</i> removal with increasing resistivity. [15].....	76
<b>Figure 3.5.</b> Experimental survival curves .....	78
<b>Figure 3.6.</b> Comparison of experimental survival vs. theoretical survival.....	80
<b>Figure 7.1.</b> Capacitance equations .....	96
<b>Figure 7.2.</b> Quality factor relations.....	96
<b>Figure 7.3.</b> LB and serial dilutions .....	98
<b>Figure 7.4.</b> Test tubes containing 6 different concentrations of bacteria in tap water (from highest concentration to lowest concentration in left to right direction).....	99
<b>Figure 7.5.</b> Cuvette yellow (4 mm), cuvette blue (2 mm), cuvette gray (1 mm).....	100
<b>Figure 7.6.</b> Left: pre-treatment control, right: electroporated sample after treatment. ....	102
<b>Figure 7.7.</b> Left: pre-treatment control, right: electroporated sample after treatment. ....	102
<b>Figure 7.8.</b> Left: pre-treatment control, right: electroporated sample after treatment. ....	102
<b>Figure 7.9.</b> Left: pre-treatment control, right: electroporated sample after treatment. ....	102
<b>Figure 7.10.</b> Left: pre-treatment control, right: electroporated sample after treatment. ....	103
<b>Figure 7.11.</b> Left: pre-treatment control, right: electroporated sample after treatment. ....	103
<b>Figure 7.12.</b> Variation of Z with respect to the variation of Rs in %. .....	107
<b>Figure 7.13.</b> Variation of Z with respect to the variation of Ls in %.....	107
<b>Figure 7.14.</b> Variation of Z with respect to the variation of Cs in %. .....	108

<b>Figure 7.15.</b> Variation of Z with respect to Rs as a function of frequency (100 Hz, 1000 Hz, 10000 Hz and 100000 Hz).....	108
<b>Figure 7.16.</b> Variation of Z with respect to Ls as a function of frequency (100 Hz, 1000 Hz, 10000 Hz and 100000 Hz).....	109
<b>Figure 7.17.</b> Variation of Z with respect to Cs as a function of frequency (100 Hz, 1000 Hz, 10000 Hz and 100000 Hz).....	109
<b>Figure 7.18.</b> 1 kV/cm (198 V) .....	110
<b>Figure 7.19.</b> 5 kV/cm (987 V) .....	110
<b>Figure 7.20.</b> 6 kV/cm (1188 V) .....	110
<b>Figure 7.21.</b> 10 kV/cm (1986 V) .....	110
<b>Figure 7.22.</b> 5 kV/cm (2865 V) .....	110
<b>Figure 7.23.</b> 1 kV/cm (Up: Before [22.7°C], Down: After [23 °C]) .....	111
<b>Figure 7.24.</b> 5 kV/cm (Up: Before [22.2°C], Down: After [22.3 °C]) .....	111
<b>Figure 7.25.</b> 6 kV/cm (Up: Before [22.2°C], Down: After [22.9 °C]) .....	112
<b>Figure 7.26.</b> 10 kV/cm (Up: Before [22.1°C], Down: After [25.1 °C]) .....	112
<b>Figure 7.27.</b> 15 kV/cm (Up: Before [22.4°C], Down: After [31.2 °C]) .....	113
<b>Figure 7.28.</b> Control sample (Ph:7-7.5).....	114
<b>Figure 7.29.</b> 1 kV/cm (Ph:7-7.5).....	114
<b>Figure 7.30.</b> 5 kV/cm (Ph:7-7.5).....	114
<b>Figure 7.31.</b> 6 kV/cm (Ph:7-7.5).....	114
<b>Figure 7.32.</b> 10 kV/cm (Ph:7-7.5).....	114
<b>Figure 7.33.</b> 15 kV/cm (Ph:7-7.5).....	114
<b>Figure 7.34.</b> Control sample (75-80 UFC).....	115
<b>Figure 7.35.</b> 1 kV/cm (17-23 UFC) .....	115
<b>Figure 7.36.</b> 5 kV/cm (34-39 UFC) .....	115

<b>Figure 7.37.</b> 6 kV/cm (6-34 UFC) .....	116
<b>Figure 7.38.</b> 10 kV/cm (12-30 UFC) .....	116
<b>Figure 7.39.</b> 15 kV/cm (+300 UFC) .....	116
<b>Figure 7.40.</b> Absorbance values for each e-field applied .....	118
<b>Figure 7.41.</b> Absorbance plots for each e-field applied.....	118

## **APPENDIXES' INDEX**

Appendix 1: Plate isolation method by serial dilutions .....	95
Appendix 2: RLC-meter equations.....	96
Appendix 3: Preliminary experimentation's lb medium protocol .....	97
Appendix 4: PRELIMINARY EXPERIMENTATION'S methodology.....	98
Appendix 5: Colony counting method results of the preliminary experimentation .....	102
Appendix 6: Discussion of the preliminary experimentation .....	104
Appendix 7: Resultados de la experimentación principal .....	110
Appendix 8: References of drinking water conductivity in Peru and in the Rimac basin (ANA, INEI and Lurin sample).....	119

## **ABSTRACT**

In the last two years, the percentage of cases in Peru linked to diarrheal diseases in children has been considerably reduced, demonstrating that even in difficult times health must always be our greatest strength. Of course, fulfilling this desire requires that all Peruvians have access to treated water sources to comply with their personal hygiene duties. However, nearly 3 million Peruvians live without access to drinking water and leave their health to the fate of natural water sources with high probabilities of containing bacteria and viruses. Under this premise, the purpose of this thesis was to show the effectiveness of an alternative water sterilization treatment that could be of great help to these Peruvians in need. A methodology based on the 'electroporation' technique was developed through the application of low and high intensity electric field pulses, seeking to damage the cell membrane of *Escherichia coli* (*E. coli*) bacteria and inactivate their growth in contaminated water volumes. The *E. coli* cell was cultured in the laboratories of the University of Engineering and Technology and diluted in 9 ml of tap water to form a theoretical suspension of 480 CFU/ml of water. To meet the objective, pulses of 1, 5, 6, 10 and 15 kV/cm were applied to the contaminated water through cuvettes (400  $\mu$ l) and the percentage of bacteria surviving the treatment was documented using the colony counting technique in Petri dishes. Respective measurements of pH, absorbance, and temperature of the water samples, as well as electrical measurements of the cuvettes, were performed moments before and after the application of the pulses. With this it was concluded that 1 kV/cm was sufficient to inactivate between 50-70 % of *E. coli* colonies when unipolar type pulses are applied in a time range of 20-22  $\mu$ s. The minimum energy required to meet this result was simulated using MATLAB software and was 0.06092 J. This study did demonstrate that electric field is an effective physical phenomenon capable of sterilizing tap water samples using cuvette containers.

### **KEY WORDS:**

Electroporation; moderate electric field pulses; cuvettes; equivalent circuit; tap water



## INTRODUCTION

The year 2020 marked the milestone of greatest social vulnerability for Peru in the health sector, being the COVID 19 pandemic the catalyst event that, on the one hand, clarified a long-lasting panorama of existing hospital deficiencies in the country. On the other hand, the situation highlighted the value of sanitary hygiene at the societal level. It is therefore encouraging to read how the Peruvian Ministry of Health (MINSA) claims a 55% decrease in the number of cases of children under 5 years of age affected by Acute Diarrheal Diseases (ADD), due to the good hygiene practices acquired in the last 2 years [1].

Naturally, water is the main medium we use to prevent these diseases, but it is also the medium through which they can be transported. This means that viruses and bacteria that cause diseases such as malaria, dengue fever, leptospirosis, hepatitis, among other microorganisms, can move through water [2]. The water to which we have access in nature is often not in hygienic conditions and generate a potential risk for about 3 million (9.3%) Peruvians [3], who today are not connected to a conventional public water network. Thus, for example, in 2017, three springs in the department of Puno (the Qayqu spring, the Condor Wachana and the Ch'akipata) presented traces of fecal and total coliforms in their waters, registering values of 330 NMP/100 mL, 250 NMP/100 mL and 170 NMP/100 mL respectively [4].

Lima usually feels the problem of disconnection to the resource from another angle. Since there are urban-marginal areas far from a water transport system, these people suffer from the ravages of poor storage of the little drinking water that reaches them. In the early 2000s, a study was carried out in the capital that revealed the situation of 224 homes with water storage in cisterns. Of these, 73.68% showed microbiological contamination with heterotrophic bacteria, total coliforms, and fecal coliforms [5], demonstrating that there is a problem that not only emphasizes a need for water, but also a deficit of characteristics and opportunities that do not allow proper care of the water already available.

These examples show that the problem of access and care of drinking water is a cross-cutting issue throughout the nation and presents an opportunity to study water sterilization techniques that contribute to improving the availability of safe water for all Peruvians. For this reason, the present thesis will investigate the process of elimination of pathogenic bacteria in water, being *Escherichia coli* (*E. coli*) the bacterium that was taken into consideration. *E. coli* was considered because it is the most common bacterium used for experimentation.

To carry out the process, the electroporation theory was used as a method to eliminate the bacteria, a procedure through which high voltage electric field pulses are used to evaluate the survival of the pathogen after their application. Likewise, the energetic cost of the electroporation process was determined by simulating the process in an electrical circuit design software. All this to obtain an idea of the energy cost required to put into operation a system that sanitizes water using this technique.

## **SCOPE**

The data of the thesis were extracted during a laboratory study conducted at the University of Engineering and Technology (UTEC) from June to October 2021. These are self-recovered data, and their analysis did not involve splicing the research with a specific real case within the society; rather, it was reduced to a laboratory-scale study, using materials, equipment, and substances from within the university itself.

Specifically, the thesis covered a study of the effect of 5 different electric field pulses on 1 dilution of *E. coli* bacteria in water. The behavior and survival of the *E. coli* after applying the different field pulses was studied to study the energetic needs involved with this experimentation and to fulfill the defined objectives.

For this purpose, the ECM 830 Square Wave pulse generator of the L509 laboratory was used, which triggered the 5 field pulses in the range of 1 to 15 kV/cm (1 kV/cm, 5 kV/cm, 6 kV/cm, 10 kV/cm, 15 kV/cm). The number of repetitions for each pulse was  $n=30$ . That is, for each field value the bacteria went through 30 pulses. In addition, the pulse type was

'quadratic wave' in direct current (DC) with a pulse time equal to 20 microseconds per pulse. The parameters for the use of the circuit design software were obtained using an 'RLC measuring instrument'. Energy analysis of these parameters was performed using electrical circuit theory by Excel calculations and the use of MATLAB ® Simulink Software.

Bacterial survival was evaluated by performing a culture comparison before and after the electroporation process. For this purpose, the bacteria were cultured in the university laboratories, having as operating conditions the conditions of the L504 laboratory. A water sample from a body of water was not taken for the experiment. The sterility of the procedure is defined using a sterilization chamber for the bacterial culture process and the care I took myself during the culture and electroporation, both processes occurring at different times and in different laboratories.

Finally, the scope of the thesis also includes pH studies and temperature variation analysis of the liquid suspension due to the applied field. This will corroborate the existence of any electrical effect such as the Joule effect in the elimination of bacteria. The aim is not to make a prototype of a sterilization system based on electroporation, nor to analyze its performance under real operating conditions, i.e., outside the university facilities.

It should be noted that a preliminary experimentation was carried out where instead of 1, 3 dilutions were made in also tap water and 3 pulses of electric field were tested. The purpose of this experimentation was to prepare for the primary experimentation and to analyze important electrical parameters.

## **BACKGROUND**

Pathogens such as *E. coli* are usually eliminated in wastewater treatment plants. However, there are alternative studies that comment on the existence of water sterilization techniques that involve advanced oxidation processes (POAs) in their treatment. Briefly, these techniques use high amounts of electromagnetic energy to form hydroxyl radicals (-

OH), micro compounds, which damage cell membranes and allow the inactivation of the bacterial organism in the liquid suspension [6].

On the other hand, shock chlorination is also a commonly used resource [7], [8] nowadays to eliminate pathogenic bacteria in water. The advantage of this process is that it can eliminate not only coliform bacteria but also bacteria from iron, manganese and sulfur. For this purpose, a certain amount of chlorine is required according to the volume of water to be disinfected. Their results show that this is a good treatment to sterilize water stored in storage tanks, since their constant exposure to the elements predisposes the contamination and infection of their contents with bacteria and unwanted organisms.

Now, the use of electricity as a resource to eliminate pathogens has been studied previously [9]-[14]. Thus, for example, in 1981, Hülshager et. al [15] determined that with applied electric field values between 8-20 kV/cm, a sterilization rate of more than 50% of *E. coli* bacteria can be achieved. It should be emphasized that their study was limited to the use of an electrolyte as a culture medium for *E. coli*. In addition, he established a statistical correlation relating the applied field value to the percentage of surviving bacteria after the application of electricity. On the other hand, the University of Arkansas determined in 2020 that the energy cost for the reduction of bacteria by using electricity is extremely low, with application powers reaching up to only 200 micro-Watts and a current in the microampere domain [16].

One of the most recent applications of electroporation occurred in 2017. For that purpose, the help of a microfluidic device was available, which performs cell sterilization bacteria at a microbiological level. The results showed that the cell damage efficiency reached 90% by applying 300 V pulses for up to three minutes [17].

## **JUSTIFICATION AND MOTIVATION**

The situation in the country presents an opportunity to study water sterilization techniques to contribute to the improvement of water quality for all Peruvians. Regarding the

phenomenon under study, electroporation is a method that damages cell membranes temporarily or irreversibly with the application of high-voltage electric fields [17]. The advantage of this technique is that it avoids the use of complex methods of cell disruption or membrane opening of a microorganism, so this technique will not need for example detergent agents (Chemical Cell Disruption) or enzymes (Enzymatic Cell Lysis) or changes in the salt concentration in the surroundings of the *E. coli* cell (Osmotic Shock) or cavitation by pressure change (Cavitation) or freezing the cell membrane (Thermal Lysis) in order to accomplish the task of sterilization [18].

The direct benefits that the population has with this type of technology is obtaining clean water with less concentration of bacteria. Families exposed to contaminated water would see in the results of this thesis an opportunity for hope in their search for clean water.

Furthermore, should there be other studies in the future that complement the results of this thesis and aim at building a prototype of small-scale disinfection based on electricity, a first integrated Peruvian disinfection model would have been created.

Thus, this thesis and its results are, on the one hand, very beneficial for the low-income society where access to electricity is scarce and expensive. However, on the other hand, a low energy cost counts as a criterion for validation and acceptance of this disinfection technique so that it can be attainable and established in the Peruvian community transversally for all socioeconomic levels.

### **GENERAL OBJECTIVE**

Evaluate the energy requirements and the inactivation percentage of *E. coli* colonies present in contaminated water samples, due to the usage of the electroporation killing method.

### **SPECIFIC OBJECTIVES**

- a. Simulate with Simulink Software the energy values transferred to 5 contaminated tap water samples based on the electrical parameters in the experiment.
- b. Evaluate the survivability of *E. coli* after electroporation using the colony counting method and OD600 absorbance analysis.
- c. Establish a correlation of survivability with respect to the established evaluation variables (electric field).
- d. Validate the threshold value (electrical field value) for which at least 50% of *E. coli* bacteria can be eliminated.

# **CHAPTER I:**

## **THEORETICAL FRAMEWORK**

This chapter will present the various applications of irreversible electroporation in different areas of science and medicine, as well as the most important data on the dimensions of *E. coli* bacteria and their relation to the electroporation process. Furthermore, the electroporation process requires physical formulas linked to fundamental electrical parameters. Specifically, capacitor theory will be necessary to understand the field strength generated inside and outside the bacterial membrane. Likewise, there is a survival equation related to the generated electric field, so defining the electric field is vital to evaluate the experimental results.

### **1.1 *E. coli* cell**

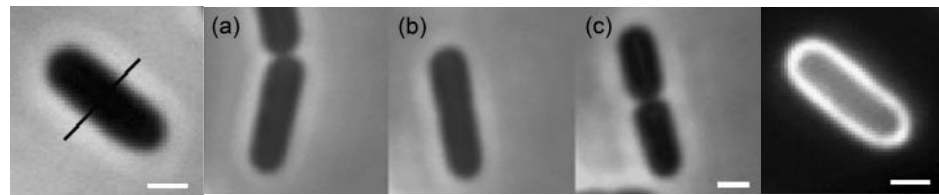
#### **1.1.1 Cell dimensions**

*Escherichia coli* has the dimensions of a rod or cylinder, where the average length of the bacterium is between 1-2 micrometers and has a radius of 0.5 micrometers [19], [20]. The dimensions are variable and there are observations of *E. coli* bacteria that, depending on the medium in which they have been cultivated, reach sizes with lengths of up to 3 micrometers and 0.8 micrometers in diameter [21], but the determining factor in their size is the length-diameter ratio, which is found to be 2.5 for cells in the exponential phase of growth [22] and between 3.7-3.9 [22], [23] for cells in the stable and final phase of growth.

Now, in terms of internal dimensions *E. coli* is a 'gram-negative' prokaryotic type bacterium enveloped by 3 protective layers defined as cytoplasmic membrane (or inner membrane), cell wall (or peptidoglycan layer) and an outer membrane [24]. The inner membrane is usually 4-4.1±0.3 nm thick [18],[25] and has the nature of being hydrophobic. The characteristic of being hydrophobic should be emphasized, since this implies that in liquid suspension and in the presence of an electric field, the membrane will not be influenced

by the aqueous medium during the application of the field until the pores in the membrane open.

On the other hand, the peptidoglycan layer or cell wall represents between 10-20% of the cell envelope, ranging between 1.2-2 nm in width [18]. In addition, it gives the bacterium its rigidity and rod-like shape (**Figure 1.1**) [24],[26]. Likewise, atomic force microscopy and small-angle neutron scattering studies showed that the periplasm presents a width in the range of 2.5-7 nm [27], with a degree of uncertainty of 4.5 nm.



**Figure 1.1.**Rod shape of *E. coli* bacteria. [24]

### 1.1.2 Dielectric *E. coli* parameters

With the help of volume dielectric force microscopy (SDFVM) procedures on 3 types of bacteria, a range of permittivities varying from 2.6 to 4.9 was established for these bacterial cells [28]. It is concluded that these values may well be considered for the study of permittivity in plasma membranes, so that these first indications provide key clues for the determination of dielectric parameters for bacteria in general. On *E. coli* there are studies that show how for lipid membranes the permittivity value is between 2.1 and 2.4 [29], while values in the range of  $K= 2-4$  [30] also show that the dielectric constant of the internal membranes of *E. coli* has an average of  $K = 3$ .

## 1.2 Electroporation Principle

Donald Chang et. al published in 1992 an extensive guide on the process of electroporation, where they define that this phenomenon allows what is known as 'destabilization' of a cell membrane for a short period of time. During that time the membrane



becomes permeable to molecules from the surrounding medium; that is, a pathway into the cell is opened due to the appearance of these pores on the surface of the membrane. [31]

More recent studies comment that the specific site of occurrence of electroporation is through the inner membrane of the cell [9] [10] and not through the entire protective envelope of the cell. Knowing this, lessens the focus of study and calculations in this thesis, since it determines the physical location on which the equations and formulas are to be applied.

It is also usual that electroporation is described as a process of charging a capacitor [17], just as it occurs in an electrical circuit. In other words, there is a charging time  $\tau_m$  required by the membrane to store energy and reach the electroporation potential  $V_{tm}$ . But it is only possible to damage the membrane and observe pore creation when  $V_{tm}$  exceeds a threshold voltage value  $V_c$ . This value has been determined and is found to be around 1 V [9], [32], [33] across the membrane; it even has a minimum value studied that is around 200 mV [11][17].

Of course, it is questionable to consider that reaching the threshold voltage value will depend on the cell type and its various attributes, because, as will be defined below, inducing such a voltage depends on the specific dimensions of each cell. Also, a particular phenomenon within cell membranes prior to electroporation must be considered. In the natural state every membrane senses an electrical potential difference, known as 'resting potential'  $\Delta V_m$ , which for *E. coli* has been studied to take values between -140 mV [34] and -135 mV [35] in steady state. It is important to recognize that this membrane potential is going to have to be considered as a starting voltage on the membrane, whose contribution influences the final potential due to the electroporation process. This voltage will have to be overcome by the induced voltage if a successful electroporation procedure is to be performed.

### **1.2.1 Irreversible Electroporation**

When the pores never close and the cell becomes permanently permeabilized, irreversible electroporation is said to have occurred [36]. In this process a mechanical rupture of the lipid membrane occurs [9], [10] and it is suggested that voltages induced in the

membrane greater than 1 V will be responsible for permanently damaging the cells in question, also leading to what is known as electroporation cell death. It is fair to state that the equations of section 1.4.4 should be oriented to calculate parameters that contemplate values of induced voltage in the membrane much higher than 1 V.

### **1.2.2 Cell death**

Eberhard Neumann et al. [33] discusses how cell death occurs after the application of repetitive pulses, but not simply due to the application of 1 pulse that reaches the threshold voltage value for pores to open. It was found in [33] that "the application of a few pulses is not lethal". Rather, the real reason for cell death occurs due to the exchange of material between the suspended medium and the contents of the cell, a process known as 'cell lysis'. It is for this reason that irreversible electroporation need not necessarily occur to achieve cell death, but only the repetition of the partial opening of the pores, so that the exchange of molecules external and internal to the cell causes the rupture of the membrane and thus cell death.

### **1.2.3 Membrane permeabilization**

The pores that open due to electroporation will allow the transport of ions and small molecules across the lipid membrane when they have reached the necessary voltage threshold. Studies such as the molecular simulation of an archaeal bacterium show how chloride ions, coming from the solution in which the membrane is immersed, cross the damaged membrane of the bacterium after being electroporated [37]. This behavior is not indistinct in *E. coli*, where it is observed that in addition to ions, ATP (Adenosine Triphosphate) molecules are released from the cell during electroporation [38], [39]. Furthermore, with respect to the ions that are released from the membrane, these are usually K<sup>+</sup> potassium ions [40]. The increase of ions in the solution in which the bacteria are suspended are an indication of the occurrence of electroporation and a simple way to measure the potassium concentration would be using ion-selective electrodes [40]. The most

important conclusion encompasses that as the electroporation electric field increases, the concentration of potassium ions in the medium increases accordingly, so future studies of conductance, resistivity, and resistance of the medium before and after electroporation are recommended for future analysis to be performed.

### 1.3 Actual irreversible electroporation studies

#### 1.3.1 Actual mathematical models

At present, different studies seek to express and analyze the behavior of electroporation from a statistical point of view as was done by H. Hülshager et. Al. [15] in the past. For instance, A. Goldberg et. Al. [41] determined that the Peleg-Fermi formulation (Equation 1) was an equation that sharpens the final survivability results given by Hülshager because the formulation takes the number of pulses ‘n’ and the electric field ‘E’ as the main independent variables for its calculations. This studies only demonstrate how probabilistic studies are important to improve the accuracy of the electroporation’s survivability correlation to dropout from the need of doing microscopic studies to determine the efficacy of this method.

$$S = \frac{1}{\frac{E}{E_{co}} \frac{E_c(n)}{E_{co}} \frac{A(n)}{E_{co}}} \frac{1}{1+e}$$

**Equation 1. Peleg-Fermi formulation [41]**

#### 1.3.2 Electroporation in the medical field

Irreversible electroporation has an application in the world of medicine linked to the treatment of tumors and cancer cells. Studies in 2018 [42] on tumor treatment in rodents demonstrate how the total elimination of tumor formations occurs successfully after the application of 150 electric field pulses of 100 μs each. This considers the use of electrodes

up to 10 mm apart (due to tumor size), an application of alternating current under a frequency of 1 Hz and an electric field of 1.5 kV/cm. The experiment shows that for low electric field values, pulse numbers in the order of 150 units were required to eliminate the tumor definitively. This value is five times the number of pulses used by effective studies in the sterilization of *E. coli* with irreversible electroporation, where 30 pulses maximum were used, but with much higher electric field ranges (up to 13 times higher) [15].

More recent studies, dating back to experiments conducted during the year 2020, have studied the effect of microampere direct current ( $\leq 100$  microamps) to sterilize and eliminate bacterial culture colonies. To achieve this, an application time of 30 minutes was required; however, even though the time of application was longer than the previous experiments early mentioned on this investigation, this shows that the use of current as a cell damage technique has convincing results. [16]

For example, it is highlighted that cell damage by means of current caused a detachment of ions, molecules, and proteins through the cell membrane, which is a fact that occurs during electroporation processes [37]. This detachment of microbiological molecules and their observation are undeniable evidence that the membrane has been damaged, thus demonstrating the effectiveness of the applicability of electrical treatment in bacteria. In addition, this paper complements the theoretical framework criteria by providing one more equation that can help to calculate the power consumption of the process which involves dividing the value of voltage applied to the sample by the resistance of the culture that holds the bacteria in it:

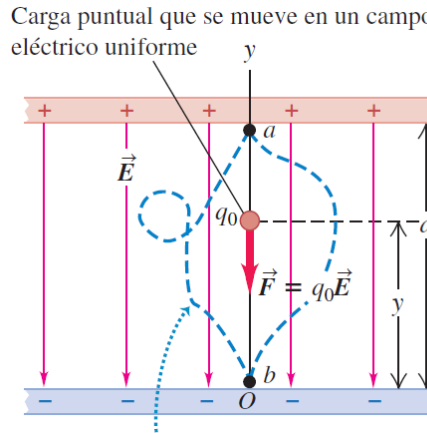
$$\text{Equation 2 } \textit{Power consumed} = \frac{\textit{Voltage}^2}{\textit{Culture resistance}} [W]$$

## 1.4 Equations and electrical formulas

### 1.4.1 External electrical field $E_e$

When the bacterial culture is placed inside a volume, such as the volume of a cuvette, it is in this space that the bacterial cells will be electroporated. The cuvette has in this space 2 electrodes, one in front of the other, usually in the form of a plate. The theory according to

Gauss's Law states that since there are 2 parallel plates, they will induce a uniform external electric field  $E_e$  [43] between them in a similar way to the observed field in the **Figure 1.2**.



**Figure 1.2.** Parallel plate capacitor concept [43]

This structure is known as a plate capacitor or plate capacitor. The equations governing the behavior of the capacitor, with distance between plates  $d = y_a - y_b$ , are listed below. However, it should be noted that these equations represent the behavior of a capacitor where the medium between the plates is vacuum or air at atmospheric pressure:

1. The potential per unit charge for an arbitrary test charge to move from  $a$  to  $b$ . Also known as the potential of the positive plate with respect to the negative plate:

$$\text{Equation 3} \quad V_{ab} = \frac{W_{a \rightarrow b}}{q_0} = E_e(y_a - y_b) = E_e d$$

2. Homogeneous electric field as a function of charge density:

$$\text{Equation 4} \quad E_e = \frac{\sigma}{\epsilon_0} = \frac{q}{A\epsilon_0}$$

3. The capacity of a capacitor to store energy, or simply capacitance.:

$$\text{Equation 5} \quad C = \frac{q}{V_{ab}} = \frac{\epsilon_0 A}{y_a - y_b} = \frac{\epsilon_0 A}{d}$$

4. Capacitance per unit area:

$$\text{Equation 6} \quad c = \frac{C}{A} = \frac{\epsilon_0}{d}$$

5. Potential energy of a capacitor with charge Q, which is the energy with which equal charges are separated between the plates of the capacitor.:

$$\text{Equation 7} \quad W = U = \frac{Q^2}{2C} = \frac{1}{2} QV_{ab} = \frac{1}{2} CV_{ab}^2$$

6. Energy stored by the electric field:

$$\text{Equation 8} \quad u = \frac{\frac{1}{2}CV^2}{Ad} = \frac{1}{2} \epsilon_0 E_e^2$$

When there is a dielectric material between the plates the parameters of voltage, electric field and capacitance usually vary as follows as a function of the dielectric constant K. This is going to be the most accurate analysis perspective for performing the calculations because the bacterial culture can be considered as dielectric material between the plates:

7. Voltage due to a dielectric:

$$\text{Equation 9} \quad V = \frac{V_{ab}}{K}$$

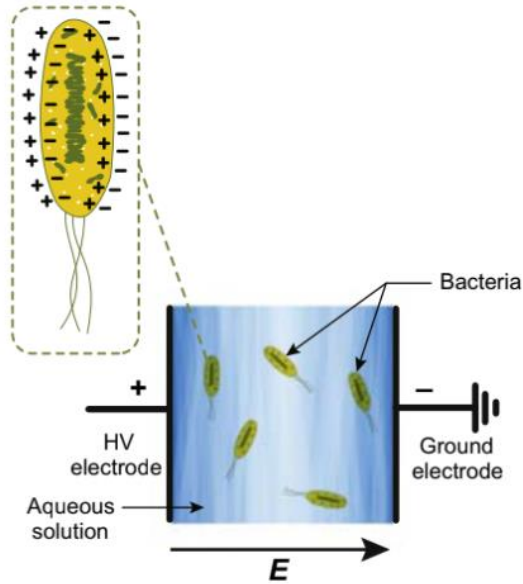
8. Electrical field due to dielectric:

$$\text{Equation 10} \quad E_{ed} = \frac{\sigma_{neta}}{\epsilon_0} = (\sigma_0 - \sigma_i)/\epsilon_0 = \sigma_0(1 - \frac{1}{K}) = V/d$$

9. Capacitance due to dielectric:

$$\text{Equation 11} \quad C_K = \frac{A\varepsilon_0}{d} K$$

It is in this sense that the  $E_{ed}$  field will be responsible for creating the induced transmembrane potential  $\Delta V_E$  in the membrane, due to a phenomenon known as polarization (Figure 1.3).



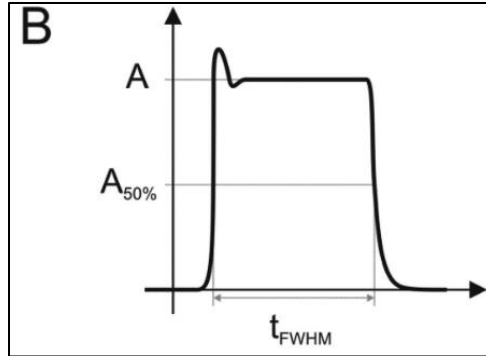
**Figure 1.3.** Polarization of bacteria due to the application of an electric field pulse [44]

Likewise, it is known that a membrane can be represented as a capacitor, so it is fair to consider that prior to the electroporation process there will exist an electric field  $E_m$  in the membrane, responsible for inducing the 'resting potential'  $\Delta V_m$  found in every lipid membrane. Therefore, the equations according to Gauss's Law for a capacitor influence the electrical analysis of the *E. coli* membrane.

#### 1.4.2 Voltage-current relation of a capacitor

This formula will have the assumption that the electrodes operate as a linear capacitor, whose capacitance is independent of the voltage. It should also be assumed that after each

pulse the capacitor discharges, i.e., at time  $t=0$  s the applied voltage reaches its peak, remains constant for a time  $\tau$  and then drops suddenly, as illustrated in **Figure 1.4**.



**Figure 1.4.** Quadratic pulse [45]

Voltage equation goes as follows:

$$\text{Equation 12 } v(t) = \frac{1}{C} \int_{t_0}^t i(t) dt + v_0$$

Measuring the current that reaches the electrodes for each pulse is indispensable to be able to calculate and estimate a theoretical capacitance value, which also helps to calculate the dielectric constant factor  $K$  of the medium or liquid suspension. If  $v(t)$  is known, considering that it is equivalent to the value established by the pulse generator, we have all the variables necessary for the calculations.

On the other hand, if we consider that the value of the current through the capacitor depends on time, we have that:

$$\text{Equation 13 } i(t) = \frac{Cdv(t)}{dt}$$

Where the voltage value  $v(t)$  is a function of time. This equation is vital for the development of the equivalent circuit and the electroporation process, since without the current it will not be possible to define a correct value of energy and power of the process.



### 1.4.3 Ohm's Law

Ohm's law of circuits is applied to determine the voltage  $V$ , current  $I$  and impedance  $Z$  parameters of an electrical system. It begins by being described as follows:

$$\text{Equation 14 } V = IZ$$

The impedance  $Z$  is the sum of the resistive part  $R$  and the imaginary part  $jX$  of a circuit, where:

$$\text{Equation 15 } Z = R + jX = |Z| \cos(\phi) + |Z| \sin(\phi)j$$

The impedance is presented together with a phase angle ' $\phi$ ' when the circuit is in the frequency domain [46]. This angle is important to perform the calculation of instantaneous apparent power  $S$ , as well as instantaneous real power  $P$  and reactive power  $Q$  for all times in a circuit.

$$\text{Equation 16 } S = VI = I^2R + I^2jX = P + jQ$$

$$\text{Equation 17 } P = I^2R = VI \cos(\phi)$$

$$\text{Equation 18 } Q = VI \sin(\phi)$$

Likewise, the resistance value of a conductive medium is represented by the following equation:

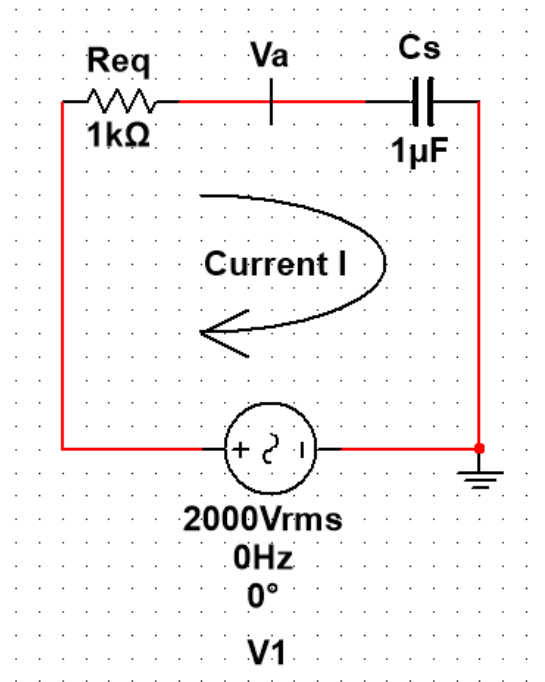
$$\text{Equation 19 } R = \frac{\rho L}{A}$$

### 1.4.4 Kirchhoff's Laws

Kirchhoff's laws are used to schematize the path of energy along a circuit. For this thesis they were used to analyze the energy transferred to the cuvette vessel where the *E. coli* suspension was stored.

### 1.4.4.1 Series Circuit

The series circuit analysis follows Kirchoff's voltage law, where a current loop  $I$  represents the current through the entire circuit as seen in **Figure 1.5**. The equivalent resistance  $R_{eq}$  is the sum of the resistances of the pulse generator leads connected to the cuvette along with the electrical parameters of the cuvette.



**Figure 1.5.** Current Loop according to Kirchoff's Voltage Law - Reference Image.

According to Kirchoff in [46], the sum of potential rises is equal to the sum of potential falls along the passive and resistive elements of the circuit. In this sense, considering that the voltage value for each pulse depends on the time; and, considering the variables of the **Figure 1.5**, the equations that govern the behavior of the circuit for all time are:

$$\text{Equation 20 } V_1(t) = (V_1 - V_a) + V_a$$

If the voltage across the capacitor is  $V_c = V_a = V_1 \left(1 - e^{\frac{-t}{R_{eq}C_s}}\right)$ , the previous equation is redistributed as:

$$\text{Equation 21 } V_1(t) = IR_{eq} + V_1 \left(1 - e^{\frac{-t}{R_{eq}C_s}}\right)$$

Where the current  $I(t)$  through the circuit is:

$$\text{Equation 22 } I(t) = \frac{C_s}{R_{eq}C_s} V_1 e^{\frac{-t}{R_{eq}C_s}}$$

Inserting Equation 22 into Equation 21, it gives the general voltage equation for all times:

$$\text{Equation 23 } V_1(t) = \left(\frac{C_s}{R_{eq}C_s} V_1 e^{\frac{-t}{R_{eq}C_s}}\right) R_{eq} + V_1 \left(1 - e^{\frac{-t}{R_{eq}C_s}}\right)$$

The power  $P(t)$  of the system is the multiplication of  $V_1(t)$  and  $I(t)$ , where the first term according to Equation 24 is the power of the resistor  $P_R$ , which is lost as heat, and the second term  $P_c$  is the measure of the energy stored in the capacitor:

$$\text{Equation 24 } P(t) = \left(\frac{C}{R_{eq}C_s} V_1 e^{\frac{-t}{R_{eq}C_s}}\right)^2 R_{eq} + V_1 \left(1 - e^{\frac{-t}{R_{eq}C_s}}\right) \left(\frac{C_s}{R_{eq}C_s} V_1 e^{\frac{-t}{R_{eq}C_s}}\right) = P_R + P_C$$

The power in the capacitor is the multiplication of  $V_a(t)I(t)$ :

$$\text{Equation 25 } P_c(t) = V_1 \left(1 - e^{\frac{-t}{R_{eq}C_s}}\right) \left(\frac{C_s}{R_{eq}C_s} V_1 e^{\frac{-t}{R_{eq}C_s}}\right)$$

Thus, the energy flowing into the capacitor in the time interval of  $t=[0,20\mu\text{s}]$  is equal to:

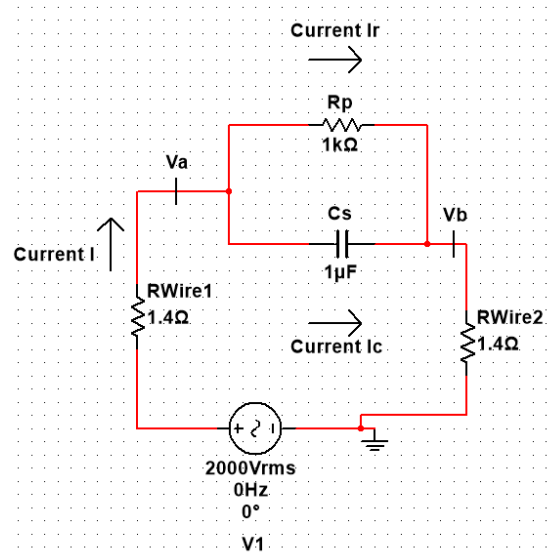
$$\text{Equation 26 } E_c = \int_0^{0.000020} P_c(t)dt$$

Finally, the energy consumed  $E$  by the whole circuit is defined by the integral in the interval of  $t=[0,20\mu\text{s}]$ :

$$\text{Equation 27 } E = \int_0^{0.000020} P(t)dt$$

#### 1.4.4.2 Parallel circuit

The parallel circuit (**Figure 1.6**) follows the same resolution logic as the series circuit. However, both the Node Law and the Voltage Law will be applied to solve it.



**Figure 1.6.** Equivalent parallel circuit and current flow.

This law states that the sum of current outputs of a node is equal to the sum of current inputs. In this case it is satisfied that:

$$\text{Equation 28 } I = I_c + I_r$$

Where it is known that  $I_c = C_S \frac{dV}{dt}$  ,  $I_r = \frac{V_a - V_b}{R_p}$  y  $\frac{dV}{dt} = \frac{d(V_a - V_b)}{dt}$ .

Consequently,

$$\text{Equation 29 } I = C_S \frac{dV}{dt} + \frac{V_a - V_b}{R_p}$$

Applying Kirchhoff's voltage law and considering that  $R_1 = R_2$ , we have that:

$$V_1 = (V_1 - V_a) + (V_a - V_b) + V_b$$

$$V_1 = IR_1 + (V_a - V_b) + V_b$$

$$V_a - V_b = V - IR_1 - IR_2$$

$$\text{Equation 30 } V_a - V_b = V - I(R_1 + R_2) = V - I(2R_1)$$

Inserting Equation 29 into Equation 30 and if  $(V_a - V_b)$  is equal to the voltage  $V_c(t)$  through the capacitor, then for  $\frac{dV}{dt} = V_c'(t)$  is followed that:

$$V_c(t) = V - [CV_c'(t) - \frac{V_c(t)}{R_p}](2R_1)$$

$$V_c(t) = V - 2R_1 CV_c'(t) - \frac{2R_1}{R_p} V_c(t)$$

Thus, the voltage across the capacitor is described by a first order linear ordinary differential equation with result equal to:

$$\text{Equation 31 } V_c(t) = c_1 e^{\frac{-t}{C_p R_p} - \frac{t}{2C_p R_1}} + \frac{R_p V}{R_p + 2R_1}$$

With the initial consideration that the voltage at time  $V(0) = 0 V$ , it is found that:

$$C_1 = \frac{-R_p V}{2R_1 + R_p}$$

And the voltage equation across the capacitor is finally,

$$\text{Equation 32 } V_c(t) = \frac{-R_p V}{2R_1 + R_p} \left( e^{\frac{-t}{C_p R_p} - \frac{t}{2C_p R_1}} \right) + \frac{R_p V}{R_p + 2R_1}$$

The final capacitor voltage at time  $t = \text{infinite}$  microseconds is that of the limit of the voltage function when time extends to infinity. This is simply described by the following relation:

$$\text{Equation 33 } V_{final} = \lim_{t \rightarrow \infty} (V_c(t)) = \frac{R_p V}{R_p + 2R_1}$$

The system power is equal to:

$$\text{Equation 34 } P(t) = VI$$

The power through the capacitor is equal to:

$$\text{Equation 35 } P_c(t) = \left( \frac{-R_p V}{2R_1 + R_p} \left( e^{\frac{-t}{C_p R_p} - \frac{t}{2C_p R_1}} \right) + \frac{R_p V}{R_p + 2R_1} \right) I_c = P_c(t) I_c(t)$$

And the energy through the capacitor is equal to:

$$\text{Equation 36 } E_c = \int_0^{0.000020} P_c(t) dt$$

#### 1.4.5 Electroporation phenomenon

There is a formula that describes the electroporation phenomenon from another point of view and depends on the initial considerations to be considered such as whether the current to be applied during electroporation is direct current (DC) or alternating current (AC). When the latter is direct current the voltage induced on the cell membrane to be evaluated is reduced

to its simplest form. This simplification of the standard has been validated by more than one author ([10]-[12], [14], [18]), being then the main formula of the Induced Transmembrane Voltage  $V(E)$  by electroporation for cells of radius  $R$  and length  $l$ :

$$\text{Equation 37 } V(E) = Rf(R, l)E\cos(\delta)$$

Where  $\delta$  is the angle between the external electric field vector  $E$  and the position of the cell membrane.  $f(R, l) = f$  is the shape factor and depends on the dimensions of the cell: on its radius  $R$  and length  $l$ . The value of the shape factor is  $f=1.5$  for cells of spherical shape (diameter equal to length) and:

$$\text{Equation 38 } f = \frac{l}{l-\frac{d}{3}}$$

For rod-shaped cells such as *E. coli* it is evident that mathematically a higher electric field level will be needed to achieve the same level of induced voltage as the cell radius decreases.

#### 1.4.6 Threshold electrical field $E_c$

Neumann [33] determines that clearing Equation 38 can serve as an 'approximation' for estimating and clearing the critical electric field strength (for electroporation to occur) as a function of the threshold voltage value  $V_c$  across the membrane. The consideration of the value of  $V_c \approx 0.2-1V$  seen in Section 1.1.1. serves as a seed value for the determination of the applied external  $E_c$  value. Also, the condition for this voltage range  $V_c$  to take place is that the electric field pulse durations are of 'short duration'. ( $\Delta t \approx 10 \mu s$ ):

$$\text{Equation 39 } E_c = \frac{V_c}{Rf}$$

### 1.4.7 Survivability equation

The equation correlating the survival of *E. coli* bacteria due to the influence of electric fields remains valid since 1981, being described in [15] and demonstrating that bacterial survival depends specifically on 6 specific variables: The experimental electric field  $E$ , the critical electric field  $E_c$ , the pulse duration  $\tau$ , the number of pulses  $n$ , a decay constant  $t_c$  and the resistivity of the medium in suspension.

In older literature,  $E_c$ , usually represents the value of the electric field with which up to 50 % of cells in a cell population are allowed to be damaged by electroporation [33]. Both Hülshager and Neumann comment that  $E_c$ , depends on cell size and it is defined that "higher fields will be required for decreasing cell diameters" [15]. However, for *E. coli* it was determined that approximately 6 kV/cm on average is sufficient to not only damage but reduce the culture population by 50%, within a range of 10 to 30 pulses and with a decay constant in the range of 12-30 microseconds [33].

The equation goes as follows:

$$\text{Equation 40 } S = \left(\frac{t}{t_c}\right)^{-\frac{(E-E_c)}{k}}$$

Where the values of  $t_c = 12 \mu s$ ,  $E_c = 4.9 \text{ kV/cm}$ ,  $k = 3.6 \text{ kV/cm}$  are defined for *E. coli* K12 bacterial cultures within the electroporation range of 8-20 kV/cm. In addition, it is known that:

$$\text{Equation 41 } t = \tau n$$

That is, the value of  $t$ , known as treatment time, which is the multiplication of the pulsation time with the number of pulses of the experiment. From this theory it is concluded that, the higher the number of pulses and the higher the resistivity of the suspension, the more bacteria will be eliminated.



## 1.5 Electroporation equipment

### 1.5.1 Unipolar pulse generator

During the electroporation process it is common to use high voltage pulses [45], where the potential induced by the electric field  $E_e$  is higher than 1 kV. To achieve such a procedure 3 pieces of equipment are necessary: a pulse generator, a sample collector, and a pair of electrodes.

For this thesis the pulse generator in question is the BTX ECM-830 (**Figure 1.7**), which generates quadratic wave pulses [47]. Which means that the voltage applied by electroporation with the instrument is only maintained for a short time interval  $\tau$  and rises to a maximum  $V_t$  which will remain constant during the mentioned time span. According to [45] the time lapse  $\tau$  tends to be in the time range between nanoseconds to milliseconds during an electroporation process. But, the BTX ECM-830 device only allows a time range in microseconds, specifically between 10 and 600 microseconds, in high voltage and the voltage range between 1-3 kV.

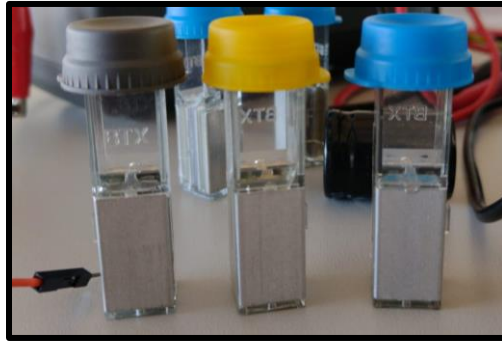


**Figure 1.7.** ECM 830 Pulse Generator [48]

### 1.5.2 BTX Disposable Cuvettes Plus

The case of the BTX pulse generator integrates in its equipment electrodes that, due to their dimensions, can be characterized as 'milli-electrodes' [45] since the separation

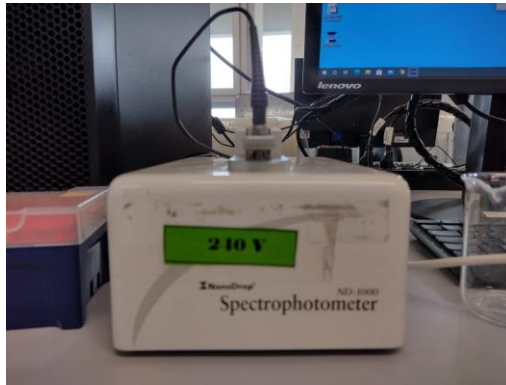
distance between one electrode and the other, known as 'gap', is in the range of millimeters. The various electrodes available from UTEC and used for experimentation were the BTX Disposable Cuvettes Plus [47] (**Figure 1.8**). They have a gap of 1 mm, 2 mm, and 4 mm, different according to the color of their cover and inside them the water sample was inoculated with *E. coli* bacteria for subsequent analysis after electroporation.



**Figure 1.8.** Disposable Electroporation Cuvettes Plus [48]

### 1.5.3 Spectrophotometer Nanodrop - ND 1000

The bioengineering laboratory has its own spectrophotometer, which requires low sample quantities to measure absorbance. Only 1-2 microliters are sufficient for measurements and the instrument (**Figure 1.9**) will be helpful to perform immediate examinations, with greater speed, to the bacterial culture at the time before and after the electroporation process.



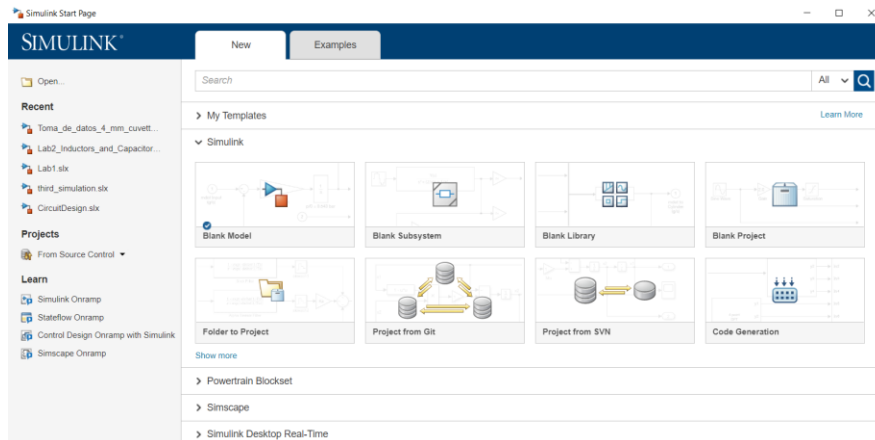
**Figure 1.9.** Spectrophotometer ND-1000.

## 1.6 Softwares

### 1.6.1 Simulink from MATLAB®

Simulink is a visualization space that allows the development of simulations of a wide variety of systems. It works in conjunction with MATLAB taking advantage of a special graphical interface to perform high-level processing models, being able to run electrical, electronic, thermodynamic, fluid mechanics, and other systems.

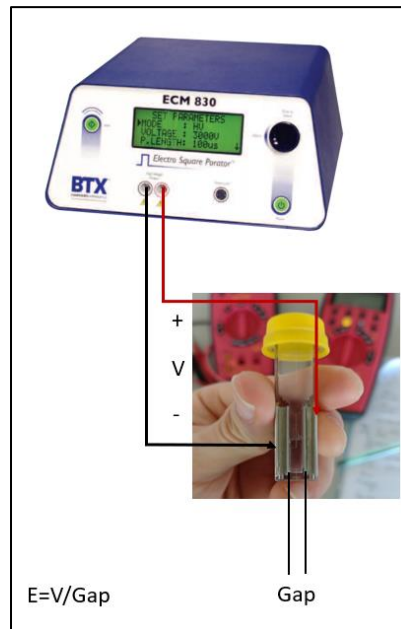
The template to create the simulation space is shown in **Figure 1.10** and in the 'Blank Model' section you can start working from a blank template.



**Figure 1.10.** Simulink from MATLAB®

## CHAPTER II: METHODOLOGY

The general analysis of the thesis contemplated the calculation of the energy and survival analysis of *E. coli* bacteria during the process of electroporation of water with bacteria in cuvette vessels. The electric field pulse applied to the water with bacteria was equal to  $E=V/\text{Gap}$ , where Gap is the distance between the plates and V is the voltage applied by the pulse generator, as shown in **Figure 2.1**. The gap used for this experimentation was 2 mm or 0.2 cm and the time duration of the electric field application to the bacteria was  $\tau=20$  microseconds. N=30 unipolar pulses were applied with a waiting time of 1 second between each pulse. Therefore, the period of the process was 1.0002 seconds with a total experimental time equal to 29.0006 seconds.



**Figure 2.1.** Application of voltage to the cuvette

The investigation was completed in 8 steps, as shown in **Figure 2.2**. The first step consisted of the preparation of the *E. coli* contaminated water sample. Then, electrical parameters of the cuvette vessel were measured with the RLC-meter, as well as the thermo-physical parameters of the vessel and the absorbance values of the contaminated water sample with the Nanodrop spectrophotometer before the electroporation procedure. Once the pulses were applied, measurements of the same parameters were performed to evaluate the differences and quantify the variations. Following the application of the electric field, the treated samples were cultured in Petri dishes, as well as untreated samples were cultured to evaluate the effect of the electric field on colony growth.

With all the data, the energy transfer during the electroporation procedure was simulated using MATLAB® programming language. Then, the evaluation of *E. coli* survival was performed using the colony count method and the absorbance of the samples that were electroporated. With this data, it was possible to establish a survival curve with which the threshold value of the electric field for which 50% concentration of the bacteria can be eliminated was finally validated.

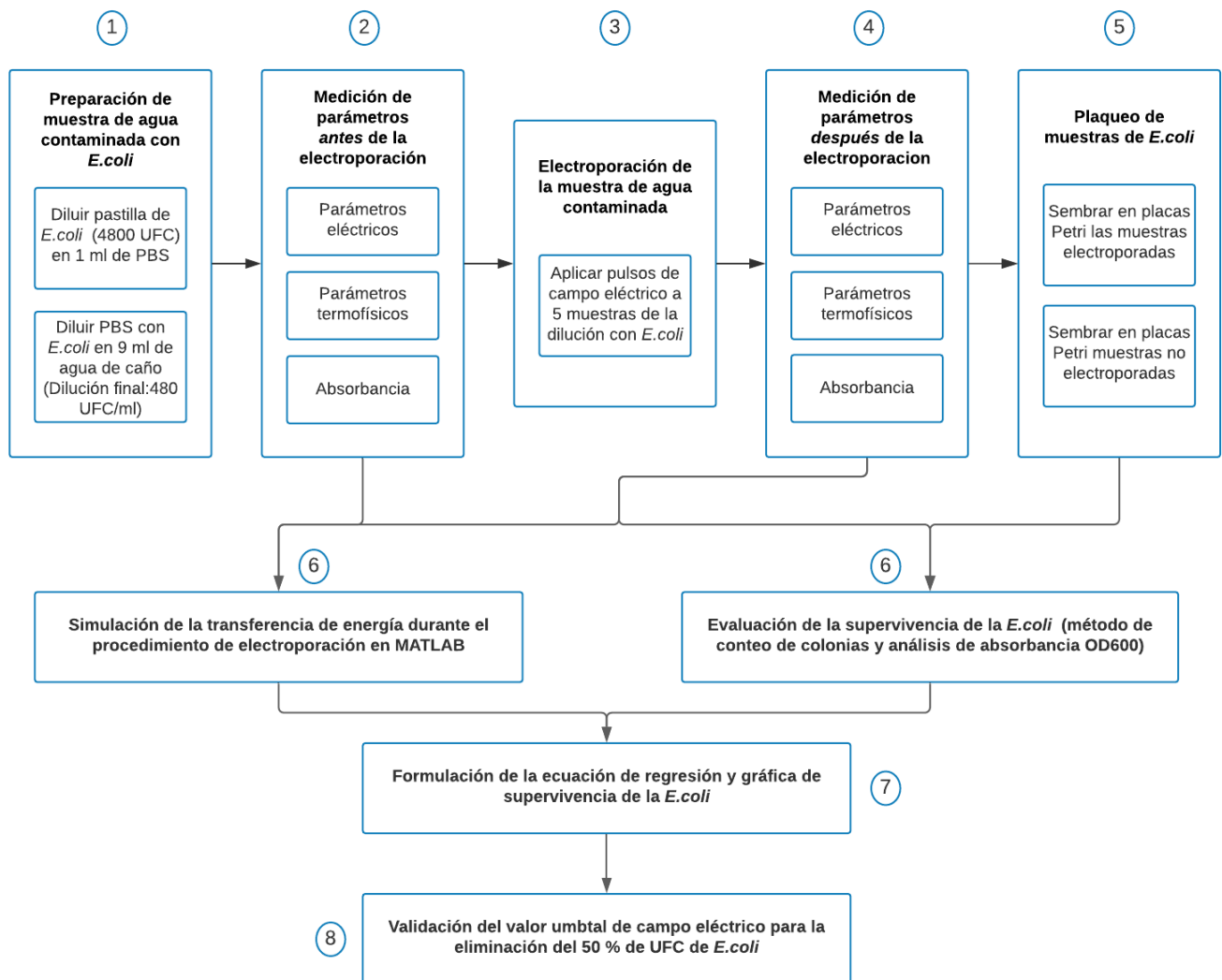


Figure 2.2. Methodology flowchart

Each step will be deepened next.

## 2.1 Preparation of the contaminated tap water sample

An *E. coli* ATCC® 8739 pellet from the Epower™ laboratory was dissolved in buffer to prepare it for subsequent use in the electroporation procedure. The dissolution protocol established by the manual of the same pellet, validated by thesis author Luis Palomino [49]

in 2019, was followed, so phosphate buffer or phosphate buffer saline (PBS) pre-warmed to 37°C was used for dilution of the pellet. Only 1 ml of PBS buffer was required for the procedure and after dissolving the pellet in PBS, the suspension was heated at 37°C for 30 minutes to dilute and hydrate the pellet properly.

The *E. coli* pellet contained 4800 CFU or colonies of bacteria and was diluted in 1 ml of PBS to obtain a statistically significant number of colonies during the plating phase of the experiment. In this sense, the *E. coli* culture in buffer had a concentration equal to 4800 CFU/ml.

## 2.2 Energy transfer simulation

**Table 2.1** shows all the electrical voltage ranges that can be applied to the 3 different cuvettes. There are limitations that will prevent reaching electric field ranges higher than 30 kV/cm due to the maximum voltage capacity (3000 V) of the BTX ECM 830 pulse generator. It was therefore decided to use the 2 mm cuvette (400 microliter capacity) for all the electric field runs to standardize the experimentation under the same geometrical conditions and physical properties of the cuvette vessel. It was chosen to apply voltage values equal to 200, 1000, 1200, 2000 and 3000 V, to evaluate 5 points of electric field, being these 1, 5, 6, 10 and 15 kV/cm respectively.

<b>E [V/cm]</b>	<b>U [V]</b>		
	<b>0.1 cm</b>	<b>0.2 cm</b>	<b>0.4 cm</b>
<b>1000</b>	100	200	400
<b>2000</b>	200	400	800
<b>3000</b>	300	600	1200
<b>4000</b>	400	800	1600
<b>5000</b>	500	1000	2000
<b>6000</b>	600	1200	2400
<b>7000</b>	700	1400	2800
<b>7500</b>	750	1500	3000
<b>8000</b>	800	1600	-
<b>9000</b>	900	1800	-

<b>10000</b>	1000	2000	-
<b>15000</b>	1500	3000	-
<b>20000</b>	2000	-	-
<b>30000</b>	3000	-	-

**Table 2.1.** Voltages attainable by each cuvette according to distance from the Gap.

## 2.2.1 Parameter's measurements

### 2.2.1.1 Electrical parameters

With the culture dilution ready, the contents were inoculated into the cuvette vessels and the field pulses were applied. Before and after electroporation, the electrical parameters of the cuvette vessels were measured with the RLC-meter IET DE-5000 (**Figure 2.3**), being the values of capacitance 'Cs', inductance 'Ls', resistance 'Rs', resistance 'DCR' and phase angle 'phy'.



**Figure 2.3.** RLC-meter IET DE-5000.

It is noted in detail in **Table 2.2** that the RLC-meter gave default values for a series circuit, with a subscript 's' of the values, coming from 'Series'. The parameters in this table were obtained by performing a test with the 4 mm cuvette inoculating only pipe water into the cuvette. A similar table was then filled in for the final measurements with the 2 mm cuvette vessel before and after the electroporation process. As there are 5 final electric field values, a total of 10 tables were filled for their respective analysis. It should be noted that the values were measured for 4 types of frequencies: 100, 1000, 10000 and 100000 Hz (first column of the table).



Frequency	Series Inductance	Series Capacitance	Series Resistance	DC-Resistance	Disipation Factor	Quality Factor	Phase Angle
Hz	Ls (H)	Cs (F)	Rs ( $\Omega$ )	$\Omega$	D	Q	$\phi$
100	-	-	-	-	-	-	-
1000	-	-	-	-	-	-	-
10000	-	-	-	-	-	-	-
100000	-	-	-	-	-	-	-

**Table 2.2.** Parameters read RLC-meter cuvette 4 mm.

With the data in **Table 2.2** and the equations located in Appendix 2, the reactance values 'Xs' or 'Xp' were calculated to obtain an equivalent impedance value Z of the system for the development of both series and parallel equivalent circuits. In addition, as it is known that the ratio  $\frac{Xs}{Rs}$  is equal to the tangent of the phase angle 'phy' of a circuit [46] and that  $Q = \frac{Xs}{Rs} = \frac{1}{D}$ , the phase angle 'phy' of the system was calculated using the following equation:

$$\text{Equation 42 } \text{phy} = \tan^{-1}(Q)$$

The values of impedance 'Z', phase angle 'phy' and reactance 'Xs' were listed before and after the electroporation procedure in tables like **Table 2.3**.

	Frequency	Impedance Z	Phase Angle phy	cos(phy)	Reactance Xs
1 kV/cm	100	-	-	-	-
	1000	-	-	-	-
	10000	-	-	-	-
	100000	-	-	-	-
5 kV/cm	100	-	-	-	-
	1000	-	-	-	-
	10000	-	-	-	-
	100000	-	-	-	-
6 kV/cm	100	-	-	-	-
	1000	-	-	-	-

	Frequency	Impedance Z	Phase Angle phy	cos(phy)	Reactance Xs
	10000	-	-	-	-
	100000	-	-	-	-
10 kV/cm	100	-	-	-	-
	1000	-	-	-	-
	10000	-	-	-	-
	100000	-	-	-	-
15 kV/cm	100	-	-	-	-
	1000	-	-	-	-
	10000	-	-	-	-
	100000	-	-	-	-

**Table 2.3.** Impedance, Phase angle and reactance per electric field (100-100000 Hz)

Current values were also measured with an AMPROBE AC50A current clamp meter (**Figure 2.4**). This instrument took 3 readings per second, i.e., 3 readings for each field pulse period applied in the experiment. In this sense, the maximum value among the 3 readings per second was considered as the corresponding value of current transferred per pulse. The values were listed appropriately in a table to evaluate the behavior of the current over time.



**Figure 2.4.** Amprobe AC50A – Current sensor

### 2.2.1.2 pH and temperature measurements

The initial pH of the stock dilution in the test tube was measured with pH strips and this was done after inoculating the contents into the cuvette containers to avoid any contamination of the sample that was going to be electroporated. After electroporation, the

samples were first plated for each electric field value onto Petri dishes. It was just after the plating process that the pH of the remaining samples in the corresponding cuvettes was measured to avoid contamination of the plates.

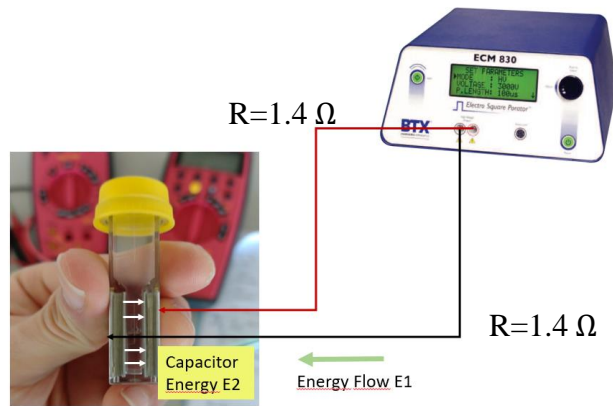
The temperature of the samples was measured with the thermographic camera FLUKE® 279 FC. Data were taken, as well as photos to record the temperature variation before and after the electroporation. The temperature and pH data were listed in the **Table 2.4**.

E-field applied [kV/cm]	Temperature before electroporation [°C]	Temperature after electroporation [°C]	pH of the medium before electroporation	pH of the medium after electroporation
1	-	-	Measurement from the test tube	-
5	-	-		-
6	-	-		-
10	-	-		-
15	-	-		-

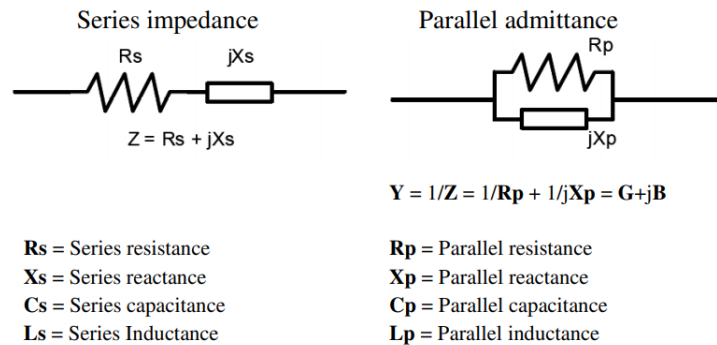
**Table 2.4.** pH and temperature measurements

### 2.2.2 Simulink simulation explanation

The actual circuit that was simulated was the one in **Figure 2.5**, where it is shown that the pulse generator is connected to the cuvette vessel through 2 wires, whose measured resistances were both equal to  $R_{wire} = 1.4 \Omega$ . The basis for the development of the equivalent circuits came from the IET 5000 RLC-meter manual [51], which shows (**Figure 2.6**) the respective equivalences for the development of both parallel and series circuits based on the resistance and reactance values measured and calculated previously.



**Figure 2.5.** Power flow from the pulse generator to the cuvette

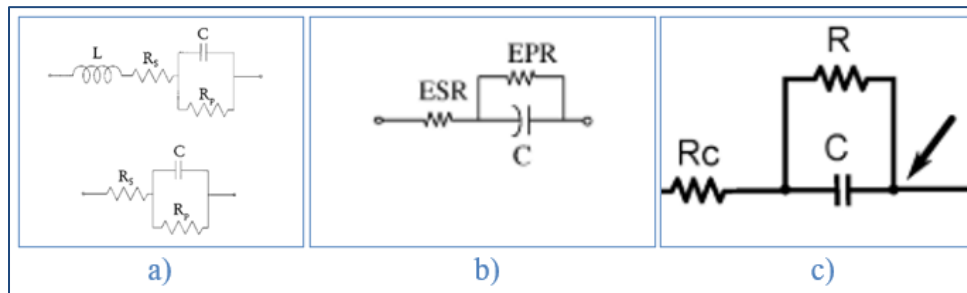


**Figure 2.6.** Series and Parallel Circuit. Source: Manual RLC-meter IET D-5000

Although there are 2 simulation schemes in parallel and series, it must be considered that the cuvette vessel has been considered as a model of a real capacitor as described in the theoretical framework. It is in this sense, that the literature from studies of the 'Institute of Electrical and Electronics Engineers' (IEEE) shows that the equivalence of a capacitor circuit can be modeled under the model of a 'compound equivalent circuit', joining a parallel resistor 'EPR' and a series resistor 'ESR' with a parallel capacitor 'C' as shown in **Figure 2.7b**).

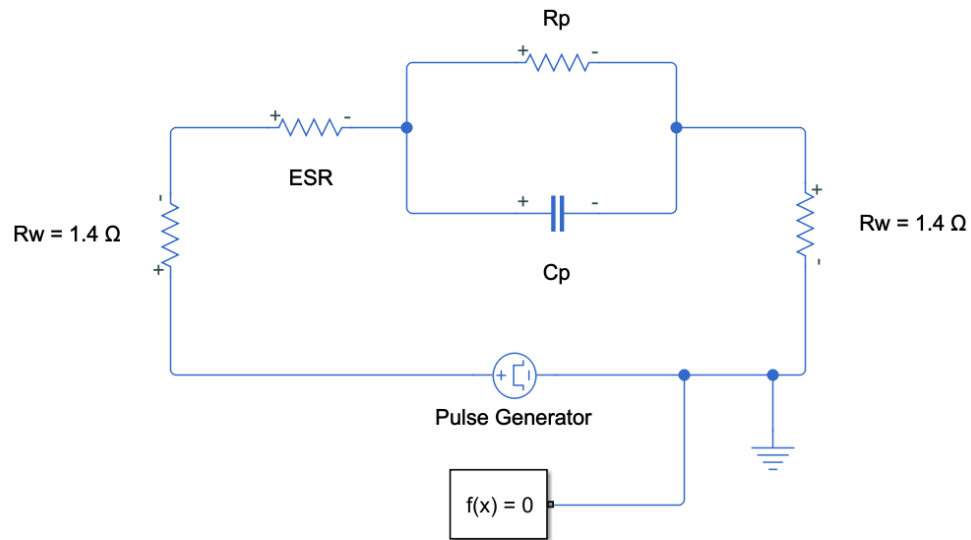
In addition to that, the study from **Figure 2.7c**) demonstrates how a cuvette vessel with liquid biological contents can be modeled under the same concept of a 'compound equivalent circuit', where the parallel resistance 'R' or 'EPR' is considered as the resistance due to the liquid inside the cuvette vessel. This model was the definitive one for the

development of the equivalent circuits in this investigation, where finally, the values of 'ESR' and 'C' were obtained from the **Table 2.2** for each of the different cuvettes using the measured values of 'Rs' and 'Cs'. The value of parallel resistance 'EPR' was obtained from the resistance of the water dilution given by its resistivity, this parameter was calculated measuring the conductivity of the tap water from UTEC using a Multiparameter YSI Professional Plus ® and transforming this value into its resistivity reciprocal.



**Figure 2.7.** a) Complete equivalent circuits modeling a real capacitor [69], b) Classical equivalent circuit of a capacitor [70] c) Cuvette filled with biological medium [71].

The final equivalent circuit model was the one in **Figure 2.8**, which was done with Simulink. In order to set the parameters for each individual electrical field pulse applied, there is a window (**Figure 2.9**) in Simulink where it is noticeable that the voltage value 'V2' was changed with respect to the pulses applied per voltage value (200, 1000, 1200, 2000 and 3000 V). The 'PW' value is the pulse length, which was 20  $\mu$ s, while 'PER' is the value of the complete period or cycle of a pulse plus the interval between each pulse, which in total is 1.00002 seconds. Five equivalent circuits were made, one per applied voltage value.



**Figure 2.8.** Final simulation of the circuit in Simulink

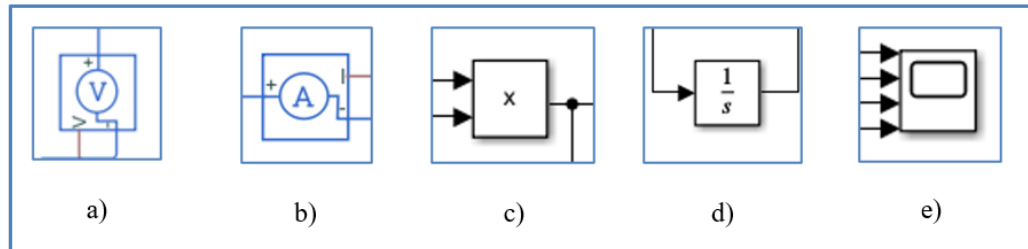
Parameters		
Initial value, V1:	0	V
Pulse value, V2:	200	V
Pulse delay time, TD:	0	s
Pulse rise time, TR:	1e-9	s
Pulse fall time, TF:	1e-9	s
Pulse width, PW:	22e-6	s
Pulse period, PER:	1.00002200001	s

**Figure 2.9.** Parameters of the simulated DC Pulse Voltage Generator

### 2.2.3 Energy measurements with Simulink

The equivalent circuits designed had a voltage sensor and a current sensor attached. A multiplier element was also incorporated to multiply the measured voltage and current signals, thus calculating the power transferred from the pulse generator to the terminals of the simulated cuvette. With the usage of an integrator element, the value of the total transferred power was obtained by integrating the measured power values from pulse  $n=1$  to pulse  $n=30$  within the applied pulse length of  $20 \mu\text{s}$ . Having done this, the values of the 4 fundamental parameters previously mentioned (voltage, current, power and energy) were

obtained. These parameters were visualized by using a 'Scope' display where the functions with respect to time for each of the 4 parameter was to be seen. All the instruments or are shown in **Figure 2.10**.






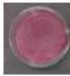



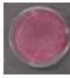



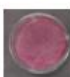



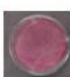




**Figure 2.10.** Simulink sensors and displays (a) voltage sensor, (b) current sensor, (c) multiplier, (d) integrator, (e) scope)

## 2.3 Survivability analysis of *E. coli*

### 2.3.1 Colonies counting in Petri Plates

In total, 400  $\mu\text{l}$  of sample were inoculated in 5 different cuvettes, as shown in **Table 2.5**. Once the cuvettes had undergone electroporation, 100  $\mu\text{l}$  of their contents were extracted for plating to analyze whether, after 24 hours of incubation, *E. coli* colonies grew in smaller amounts than in a sample that did not undergo the procedure. To achieve this objective, 3 plating procedures were performed for each cuvette to have 3 statistically significant samples and thus be able to establish arithmetic averages of the number of colonies that grew for each field value applied.

To characterize the statistical variation of colonies with respect to colonies that did not undergo the electroporation, another 4 samples (4x100 $\mu\text{l}$ ) of contaminated dilution were plated but this time directly from the test tube, whose content hosted a sane and stable number of colonies that were not electroporated. With all this information, the percentage difference in colony growth was calculated by dividing the average number of colonies that grew post-treatment by the average number of colonies that grew from the untreated sample.

Experimentación				
Campo eléctrico	Volumen total	Plaqueo 1	Plaqueo 2	Plaqueo 3
1 kV/cm	 400 µl	 100 µl	 100 µl	 100 µl
5 kV/cm	 400 µl	 100 µl	 100 µl	 100 µl
6 kV/cm	 400 µl	 100 µl	 100 µl	 100 µl
10 kV/cm	 400 µl	 100 µl	 100 µl	 100 µl
15 kV/cm	 400 µl	 100 µl	 100 µl	 100 µl

**Table 2.5.** Colony count for each field value.

### 2.3.2 Spectrophotometric analysis UV-VIS OD600

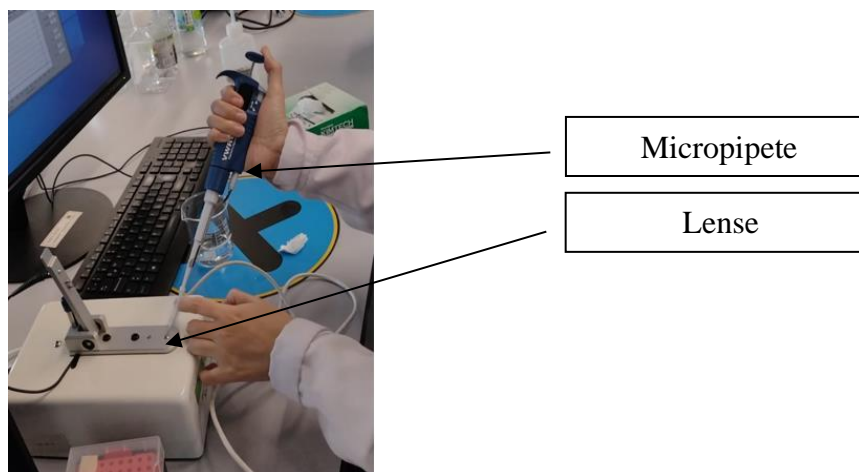
A UV-VIS test was performed with the ND-1000 spectrophotometer to account for the concentration of bacteria. With the instrument, absorbance values were obtained and due to Beer Lambert's law, it was considered that the light absorbance value of the *E. coli* bacteria sample was strictly proportional to the concentration of *E. coli* bacteria [53],[54]. The proper method of absorbance reading for *E. coli* bacteria occurred by measuring the value for the wavelength of irradiated light equal to 600 nm [55], procedure which due to this wavelength is known as OD600.

This method has been previously used with this same equipment in recent studies [49] and for this thesis the OD600 was performed using the Nanodrop software under the UV/Vis mode, inoculating 1-2 microliters of the water with bacteria with micropipette (**Figure 2.11**)



for the absorbance measurement according to the parameters established in the user's manual [56]. Thus, to know how much bacteria survived the treatment it was necessary to relate the absorbance values before and after the electroporation process, as shown in the following equation:

$$\text{Equation 43 } \frac{\text{Absorbancia post tratamiento}}{\text{Absorbancia inicial}} = \% \text{ de supervivencia}$$



**Figure 2.11.** Inoculation model for spectrophotometer usage

The initial absorbance was measured just after inoculation of the samples into the cuvette containers for electroporation, that is to maintain the sterility of the liquid to be treated. From the remaining 8 ml of sample in the stock dilution from the test tube 2 µl were inoculated into the spectrophotometer to obtain an average value of the initial absorbance. Five samples were taken.

After plating the electroporated content from the cuvettes, 100 µl sample was left over from each cuvette from which 2 absorbance tests were also performed for each electric field value applied. The whole absorbance tests' scheme is shown in **Table 2.6**.

Cuvette	Initial absorbance test OD600	Absorbance test post electroporation OD600

1 kV/cm	The initial absorbance was measured directly from the test tube (5 samples).	The absorbance was measured from the remaining sample in the cuvette (2 samples).
5 kV/cm		idem
6 kV/cm		idem
10 kV/cm		idem
15 kV/cm		idem

**Table 2.6.** Spectrophotometry tests

#### **2.4 Regression formula of survivability of the *E. coli***

A curve was developed using Excel software that represented the behavior of the decrease in *E. coli* survival with respect to the increase in the electric field applied to eliminate it. For this purpose, it was defined that the percentage values of colony survival were represented as dependent variables on the y-axis; and, that the applied electric field values are the independent variables on the x-axis.

The curve was constructed under the traditional expression of bacterial survival established by the FDA [75]. Under that concept, the 'survival percentage' of the y-axis was calculated by the relation  $\log_{10}\left(\frac{N}{N_0}\right)$ , where  $N$  represents the number of surviving bacterial colonies after each electric field application and  $N_0$  the number of colonies found in the control.

#### **2.5 Threshold value of the electrical field required for elimination 50 % of *E. coli* colonies**

Hülshager et. al [15] demonstrated that the bacterium *E. coli* K12 has a critical electric field value  $E_c$  equal to 4.9 kV/cm, i.e., that after this electric field value is applied, the bacterium begins to die and to decrease with a linear behavior with respect to the increase of the electric field. So, it is with this notion, that the experimental curve defined by the electroporation results of our experimentation was contrasted with the theoretical curve given by this author. The objective was to understand whether our results were as equal, less, or

more effective than what the literature has to say and to define the electrical field value needed to eliminate at least 50% of bacteria for both our results and Hülshager's experiment.

In addition, with the energy values previously calculated during the simulation of this experiment, it was possible to determine the electrical energy needed to achieve the threshold value.

## CHAPTER III: RESULTS AND DISCUSSIONS

### 3.1 Energy transfer simulation

#### 3.1.1 Thermo-physical parameters

The temperature of the water in the vessels varied for each value of field applied. Firstly, this parameter was relatively similar for all cuvettes with an average temperature of 22.32 °C. One of the measurements was 22.7 °C so I hypothesize that the most likely actual temperature is 23 °C at most. In that sense, **Table 3.1** shows that the temperature variation applying 1 and 5 kV/cm is practically null since the range of temperatures measured for these 2 cases is from 22.3 to 23 °C. However, from 6 kV/cm onwards there is a slight increase in temperature, being 0.7 °C the temperature variation for this electric field value and 3 °C and 8.8 °C for 10 and 15 kV/cm respectively.

E-field applied [kV/cm]	Temperature before electroporation [°C]	Temperature after electroporation [°C]	pH of the medium before electroporation	pH of the medium after electroporation	E-field applied [kV/cm]
1	22.7	23	0.3	7 – 7.5	7 – 7.5
5	22.2	22.3	0.1		7 – 7.5
6	22.2	22.9	0.7		7 – 7.5
10	22.1	25.1	3		7 – 7.5
15	22.4	31.2	8.8		7 – 7.5

**Table 3.1.** pH and temperature measurements before and after electroporation

This temperature variation allows the use of the energy equation for incompressible fluids considering water in the compressed liquid state. The enthalpy equation for a given temperature  $T$  is according to [57] described by means of the following formulation:

$$H = mc_p T = mh \quad \text{Enthalpy in Joule [J]}$$

Since there was a variation in the temperature, there will be a variation in the enthalpy  $H$ . It was taken into consideration that the dilution of water with buffer is taken as 100% water. In that sense, the density of water between 22 and 23 °C is equal to 997.71 kg/m<sup>3</sup> [57], so that, for a volume of water equal to 400 µl, the mass between the cuvette plates is equal to  $m = \rho V = 3.99084E^{-4} \text{ kg}$ .

The equation of the enthalpy variation was then equal to:

$$\Delta H = m [c_{pT_2} T_2 - c_{pT_1} T_1] = m[h_2 - h_1]$$

Listed in **Table 3.2**, in the fifth column, are the final thermal energy variations  $\Delta H$  transferred to the water as a product of the power transfer through the plates to the dilution. Considering that the treatment involved applying 30 pulses per experiment it was possible to calculate an average power value  $P$  (second last column of **Table 3.2**) for each pulse by dividing  $\Delta H$  over the time of each pulse and again over 30 pulses. It is to be noted that in general the energy or enthalpy difference  $\Delta H$  increases with the rise in electrical field or voltage value applied.

Voltage applied [V]	Specific enthalpy before treatment h1 [J/kg]	Specific enthalpy after treatment h2 [J/kg]	$\Delta h$ Specific enthalpy difference [J/kg]	$\Delta H$ Enthalpy difference [J]	$\Delta H$ per pulse [J]	$P$ per pulse [W]
198	95263	96520	1257	0.5016	0.01672	760
987	93168	93587	419	0.1672	0.0055733	253.33
1188	93168	96101	2933	1.1705	0.039017	1773.5
1986	92749	105308	12559	5.0121	0.16707	7594.09
2865	94006	130806	36800	14.686	0.489533	22251.5

**Table 3.2.** Thermal energy and power transferred to the cuvette per pulse

It should be noted that the first column of the table shows that the voltage values vary slightly from the initial theoretical values (200, 1000, 1200, 2000 and 3000 V) that were going to be applied since the pulse generator decided by itself to regulate these values automatically. That is, 100% of the theoretical voltage and electric field were not transmitted to the samples. So, this circumstance was considered during the simulation with Simulink, for which this voltage values were finally the ones that were set as initial values during the simulation. Furthermore, each pulse had a real application time (pulse length) equal to  $t=22 \mu\text{s}$  instead of  $20 \mu\text{s}$  since this value was also defined automatically by the pulse generator. All these measurements can be observed in the Appendix 7.

Finally, it should also be mentioned with certainty that the only reason for there to be a temperature rise in the water dilution is that there was a leakage current flowing through the medium that dissipated the thermal energy  $\Delta H$  according to the expression  $P = I^2R$ , where  $R$  is the resistance due to water dilution and  $I$  is the leakage current through it. This phenomenon will eventually be discussed in this research.

### 3.1.2 Electrical parameters' measurements

#### 3.1.2.1 RLC-meter's measurements

The parameters measured with the RLC-meter were listed in **Table 3.3** and they show that from 12 out of 20 measurements (each row of the table counts as one measurement) the trend of variation of inductance 'Ls', capacitance 'Cs' and resistance 'Rs' after the appliance of the pulses corresponds with an increase, a decrease, and an increase of their values respectively. The same trend was to be seen in the results of a preliminary experimentation (**Table 7.7**) done before this primary investigation for which their results are to be found in Appendix 6. Although the explanation of this trend is beyond from the scope of this primary investigation the results of the preliminary part detail that there is a dependance of the variation of impedance of the system  $\Delta Z$  on the variation of the main parameters  $\Delta Ls$ ,  $\Delta Cs$ , and  $\Delta Rs$ .

	Frequency Hz	Before electroporation			After electroporation			$\Delta Ls$	$\Delta Cs$	$\Delta Rs$
		Ls (H)	Cs (F)	Rs (Ohm)	Ls (H)	Cs (F)	Rs (Ohm)			
1 kV/cm	100	1.569	1.6168E-06	221.2	1.525	0.000001658	229.1	-2.8%	2.5%	3.6%
	1000	0.0205	1.2342E-06	70.46	0.02022	0.000001252	73.82	-1.4%	1.4%	4.8%
	10000	0.0002539	9.976E-07	52.22	0.0002538	0.000000998	54.47	0.0%	0.0%	4.3%
	100000	0.00000328	7.723E-07	50.53	0	0	0	0.0%	0.0%	0.0%
5 kV/cm	100	1.087	0.000002328	351.2	1.207	0.000002095	392.7	11.0%	-10.0%	11.8%
	1000	0.0215	1.1771E-06	109.9	0.02369	0.000001068	115.38	10.2%	-9.3%	5.0%
	10000	0.0003665	0.000000691	60.5	0.0004032	6.284E-07	61.66	10.0%	-9.1%	1.9%
	100000	0.000006225	4.054E-07	53.56	0.0000068	3.744E-07	54.61	9.2%	-7.6%	2.0%
6 kV/cm	100	1.038	0.000002436	342.1	1.183	0.000002141	399	14.0%	-12.1%	16.6%
	1000	0.021	0.000001205	113.4	0.02436	1.0397E-06	122.6	16.0%	-13.7%	8.1%
	10000	0.0003888	6.496E-07	59.2	0.0004438	5.707E-07	61.56	14.1%	-12.1%	4.0%
	100000	0.000006614	3.823E-07	51	0.000007342	3.448E-07	53	11.0%	-9.8%	3.9%
10 kV/cm	100	1.7628	0.000001436	730	1.913	0.00000132	764.2	8.5%	-8.1%	4.7%
	1000	0.042	0.000000604	172	0.0448	0.000000565	195	6.7%	-6.5%	13.4%
	10000	0.000701	3.611E-07	64.84	0.000728	3.223E-07	70.18	3.9%	-10.7%	8.2%
	100000	0.00001077	2.352E-07	54.3	0.0000118	2.147E-07	56.74	9.6%	-8.7%	4.5%

	Frequency Hz	Before electroporation			After electroporation			$\Delta L_s$	$\Delta C_s$	$\Delta R_s$
		Ls (H)	Cs (F)	Rs (Ohm)	Ls (H)	Cs (F)	Rs (Ohm)			
15 kV/cm	100	1.2686	0.000001967	438	1.2815	0.000001997	428.2	1.0%	1.5%	-2.2%
	1000	0.02636	0.00000096	122.3	0.02544	0.000000996	121.55	-3.5%	3.7%	-0.6%
	10000	0.0004331	0.000000585	61.13	0.0004386	0.000000578	61.16	1.3%	-1.2%	0.0%
	100000	0.000007	3.614E-07	54	0.0000069	3.686E-07	53.86	-1.4%	2.0%	-0.3%

**Table 3.3.** Inductance, capacitance, and series resistance measured by the RLC instrument, before and after the electroporation procedure. Last three columns show the variation of the parameters with respect to the initial values.

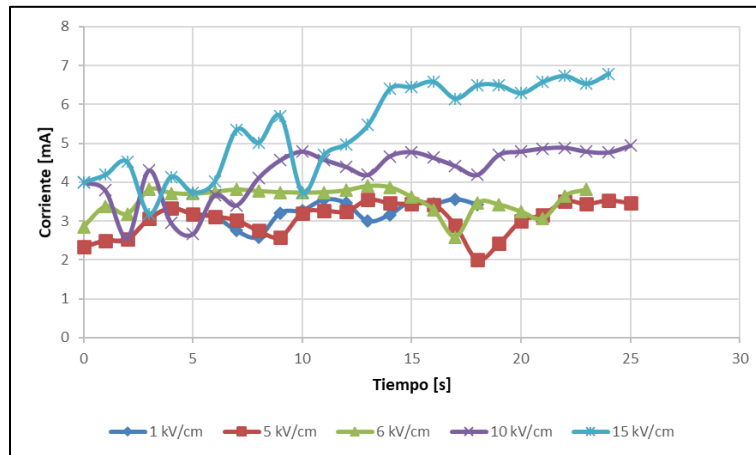
From these values, the most important ones are the Cs and Rs values because they represent the ESR, and Cp values needed for the development of the equivalent circuit in Simulink. Out of these parameters, the values at 100 Hz were needed because that frequency value was the one that approached the most to 0 Hz, since DC pulses were applied. The importance of this values will be furthered discussed.

### 3.1.3 AMPROBE AC50A current measurements

It was recorded on videos how the current values supplied to the cuvette vessel increased with respect to time. The data were recorded in **Table 7.9** in Appendix 7 and, as explained in section 2.2.2.1, the data was gathered by selecting at the maximum current peak value measured within the pulses' intervals.

From **Table 7.9** it is noticeable how with respect to the advance of time, the current peaks increase considerably, and this increase was able to be visualized in **Figure 3.1**. This increase in current only denotes that as both the electric field and the electroporation time increase, the current values increase as well.





**Figure 3.1.** Variation of peak current with respect to time

Current increase suggests 2 important analytical considerations and one important fact, which is that the electrical energy transmitted into the system rises with respect to time. However, on the one hand, the first analytical consideration concerns Ohm's Law. This law explains that the only reason for an increase of current in an electrical system to occur is that a decrease on its electrical impedance takes place. On the other hand, the second perspective takes the law of current through a capacitor into consideration, which implies that, as the current reaching a capacitor depends on its capacitance value 'C' and this in turn on the value of the dielectric constant 'K' of the dielectric between its plates, the increase in current during this experiment would be explained by an increase in the value 'K' of the water and therefore in the capacitance 'C' of the cuvette vessels that were used during the electroporation.

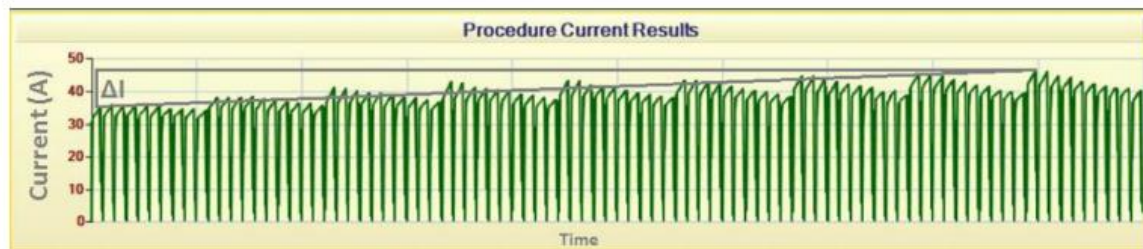
In the following, the two perspectives of analysis were discussed.

### 3.1.3.1 Analysis Consideration 1: Change in the resistivity $\rho$ of the medium

About the first consideration of analysis, there are studies about the variation of water resistivity ' $\rho$ ' with respect to temperature ([60]-[62]) that guarantee that water resistivity and resistance decrease with increasing temperature. Such studies involve the use of 'ultrapure water' and not pipe water as is the case in the thesis, however, since the element is the same, it can be hypothesized that the temperature increase recorded in section 3.1.1 represents a

decrease in the dilution resistivity of water as the electric field and temperature of the medium increases.

To corroborate this hypothesis, we appealed to the explanation seen in [63] which has described how an increase in the current reading through a cuvette vessel effectively responds to an increase in the temperature of the medium [63]. Similar cases, such as that of A. Ruarus et Al. [64], have been able to demonstrate with theory and amperage measurements that indeed the physical phenomenon that explains an increase in current during an electroporation procedure is an increase in electrical conductivity of the medium because of its increase in temperature. The results have been measured and illustrated in **Figure 3.2** and for each electric field pulse applied in the irreversible electroporation studies there was an increase in the measured current.



**Figure 3.2.** Increase in current during applied pulses in an irreversible electroporation experiment [64]

Furthermore, when the temperature of the medium in [64] returned to the initial temperature, the amperage of the pulses also returned to its initial values. Therefore, it is concluded that temperature is a parameter that affects the correct measurements of parameters during electroporation procedures and will be a fundamental variable when performing other electroporation experiments. Having established the basics of the temperature and current behaviors during electroporation, it could be then concluded that as the conductivity of the tap water during this investigation increased due to a temperature raise, its resistivity decreased fulfilling Ohm's law, and thus reading increments in the current that passed through the current sensor.

### 3.1.3.2 Analysis Consideration 2: Change in the electrical conductivity K of the medium

Regarding the second analysis consideration, it was previously explained that capacitance is a value that depends on the dielectric constant of the medium between the plates of a capacitor. Now, three studies ([65]-[67]) mention how the dielectric constant 'K' of water (either distilled or tap water) will tend to decrease with the increase in its temperature T; and, in [66] an equation (Equation 44) is given as a function of temperature T for the calculation of 'K' in distilled water. That function was used in this thesis according to the experimental temperatures defined in **Table 3.1**. The equation is not said to be valid for tap water but because the value of the dielectric constant at 25°C ( $K \approx 78.5$ ) behaves quite similarly for all types of water, it gives an estimate on the capacitance change of the cuvette due the temperature increase of its medium.

$$\text{Equation 44 } K = 87.740 - 0.4008t + 9.398(10^{-4})t^2 - 1.410(10^{-6})t^3$$

By applying Equation 11 ( $C_K = \frac{A\epsilon_0}{d}K$ ) the capacitances of each of the 5 different cuvettes were then calculated and listed in **Table 3.4**. As expected, if the value of 'K' decreases (see columns 5 and 6), the capacitance values decrease, too (see columns 7 and 8).

Applied Voltage [V]	E-field applied [kV/cm]	Temp. Before treatment [°C]	Temp. After treatment [°C]	Dielectric constant K before	Dielectric constant K after	Capacitance C before [F]	Capacitance C after [F]
198	0.99	22.7	23	79.1096167	79.0015987	7.00451E-11	6.99495E-11
987	4.935	22.2	22.3	79.2899842	79.2538769	7.02048E-11	7.01729E-11
1188	5.94	22.2	22.9	79.2899842	79.0375878	7.02048E-11	6.99814E-11
1986	9.93	22.1	25.1	79.3261084	78.2497067	7.02368E-11	6.92838E-11
2865	14.325	22.4	31.2	79.2177865	76.1070553	7.01409E-11	6.73866E-11

**Table 3.4.** Dielectric constant K and capacitance C values according to pre- and post-electroporation temperatures.

This behavior on the capacitance is not indistinct from that observed in both the preliminary and primary experimentation when the parameters of Cs were measured with the RLC-meter (**Table 3.3** and **Table 7.7**). Thus, given the experimental results measured with the RLC-meter, as well as given the theoretical results in **Table 3.4**, it is demonstrated that the capacitance 'C' of the cuvette vessel tends to decrease as a product of the electroporation procedure. However, despite this, the decrease in capacitance 'C' would not explain the increase in current 'I' observed in **Figure 3.1**. On the contrary, given Equation 13, a decrease in the capacitance of a capacitor translates directly into a decrease in the current that passes through it, in this case, the current that passes through the cuvettes.

### 3.1.3.3 Final current discussion

To sum up, it can only be concluded that the increase in current measured during the experiment is explained only, if at the same time, there is a reduction in both the resistivity of the tap water and the capacitance of cuvettes, where the variation of the resistivity with respect to time is much greater than the variation of the capacitance. ( $\frac{\partial \rho}{\partial t} \gg \frac{\partial C}{\partial t}$ ). Only in this way, the current would increase because of the decrease of the resistivity of the medium and would not decrease due to the decrease of the capacitance.

In the end, it is noticeable that the energy transfer into the water will actually tend to increase as the current increases. In other words, this thesis demonstrates that electroporation in cuvette vessels is a procedure that will always require a higher power flow per pulse applied due to the decrease in the resistivity of the medium, making the electroporation process a thermodynamically transient and non-stationary system.

In the following section, the electroporation system was modeled, and the values of thermal energy dissipated and seen in **Table 3.2** were validated with the usage of an equivalent circuit analysis.

### 3.1.4 Simulink simulation

As explained in the methodology the values of ESR, EPR and C were obtained to simulate the equivalent circuit. As known, ESR corresponds to the value of 'Rs' measured with the RLC-meter; 'Rp' was the resistance due to the resistivity 'ρ' of the dielectric (tap water) between the cuvette vessel plates [68], [52], [68] and the capacitance C corresponds to the value of 'Cs' which was also measured with the RLC-meter.

Both Cs and Rs values used were those measured at 100 Hz frequency before electroporation (from **Table 3.3**), as they were the closest to 0 Hz. The simulation was not performed with the values measured after electroporation, because the values measured in this state were not completely constant and tended to vary much. The final values used for the simulation of each of the 5 equivalent circuits were organized in **Table 3.5**.

Frequency Hz	Series capacitance Cs	Series resistance Rs
1 kV/cm	1.62E-06	221.2
5 kV/cm	2.33E-06	351.2
6 kV/cm	2.44E-06	342.1
10 kV/cm	1.44E-06	730
15 kV/cm	1.97E-06	438

**Table 3.5.** Capacitance Cs and Resistance Rs measured from the 2mm cuvette

Now, since the values of Cs and Rs were measured from the same vessel with 'gap' equal to 2 mm, then each row of **Table 3.5** represents an individual measurement from which an average and the standard deviation (S.D.) of the measurements was calculated and established in **Table 3.6**.

	Cs	Rs
D.E.	4.34E-07	191.4980679
Mean	1.96E-06	416.5

**Table 3.6.** Capacitance and resistivity (average and standard deviation)

The only parameter that was missing was the  $R_p$  value which was considered as constant to facilitate the calculations and the development of the circuit. As already discussed, resistance  $R_p$  was calculated from the tap water conductivity measurement, which was taken directly from the tap water of UTEC and had a value equal to  $567 \mu\text{S}/\text{cm}$  or  $1763.66 \text{ Ohm}\cdot\text{cm}$ .

It is important to mention that SUNASS [72] claims that in Peru all drinking water must have a conductivity lower than  $1500 \mu\text{S}/\text{cm}$  or resistivity higher than  $666.66 \text{ Ohm}\cdot\text{cm}$ ; in that sense, the measured conductivity of UTEC's tap water falls within the range established by law and can be valid to use. In addition,  $567 \mu\text{S}/\text{cm}$  falls within the range of Rimac river's conductivity given by INEI and the Autoridad Nacional del Agua (ANA), as well as within the range of conductivity of various samples of tap water measured from Lurín district that were found on an undergrad investigation. The information and sources of this values can be found in Appendix 8.

Now, to calculate the value of  $R_p$ , given the previously measured resistivity, Equation 19 was used. For this, it was important to first analyze the geometry of the cuvette, especially the surface area  $A$  of its plates and its gap, which we already know it to be  $0.2 \text{ cm}$  ( $2 \text{ mm}$ ). So, if the area of the cuvette vessels' plates is considered to have a surface area  $A$  equal to:

$$A = \frac{\text{Cuvette volume}}{\text{Gap}} = \frac{400 \mu\text{L}}{0.2 \text{ cm}} = 2E^{-4}\text{m}^2 = 2 \text{ cm}^2$$

Then, the resistance value ' $R_p$ ' of the UTEC water is equal to:

$$R_p = \frac{\rho L}{A} = \frac{\rho \text{Gap}}{A} = 1763.66 \Omega\text{cm} * \frac{0.2 \text{ cm}}{2 \text{ cm}^2} = 176.36 \Omega$$

#### 3.1.4.1 Enthalpy $\Delta H$ simulation

Since the enthalpy  $\Delta H$  calculated in **Table 3.2** represents a thermal loss, this energy was simulated as the sum of the energy dissipated in the resistors ' $R_s$ ' and ' $R_p$ ' after the 30 pulses applied for each electric field value, since the energy dissipated in resistors represents

thermal losses according to circuit theory. The purpose of this simulation is to define a curve that represents the energy lost as heat for each of the 5 e-field pulses applied.

However, to define the curve that best models the behavior of thermal losses, 4 scenarios were simulated to validate which values of 'ERS' and 'Cs' best fit to simulate the actual measured enthalpy. These were the scenarios where:

- a. The average capacitance Cs and average resistance Rs were used.
- b. The maximum capacitance Cs and maximum measured resistance Rs were used.
- c. The minimum capacitance Cs and minimum measured resistance Rs were used.
- d. The respective parameters from **Table 3.5** were used.

Having the values of Cs, Rp and Rs ordered in **Table 3.7** for each of the 4 scenarios, we proceeded to carry out the simulations.

Scenarios	Conditions	Cs	Rs	Rp	
(1)	Mean Cs y Rs	1.96E-06	416.5	176.33	
(2)	Max. Cs y Rs	2.44E-06	730	176.33	
(3)	Min Cs y Rs	1.44E-06	221.2	176.33	
(4)	Respective Cs and Rs values	1 kV/cm	1.62E-06	221.2	176.33
		5 kV/cm	2.33E-06	351.2	176.33
		6 kV/cm	2.44E-06	342.1	176.33
		10 kV/cm	1.44E-06	730	176.33
		15 kV/cm	1.97E-06	438	176.33

**Table 3.7.** Values of Cs, Rp and Rs per simulated scenario

The sums of energy dissipated in the resistors 'Rp' and 'Rs' for each applied pulse were very similar to those measured during the experimentation for the scenario of average values (Scenario 1) and that of the respective measured values (Scenario 4). However, as

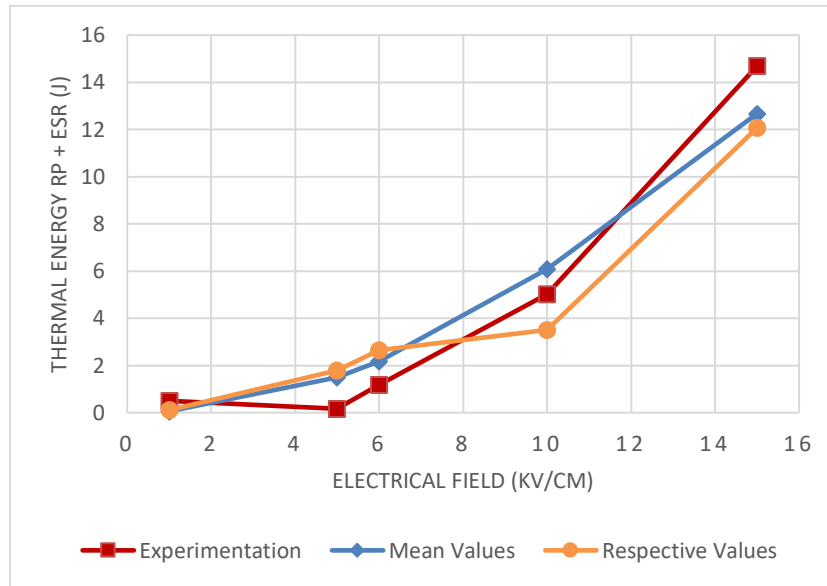
seen in **Table 3.8**, the rest of the scenarios (2 and 3) presented energy values very far from the real ones, so it was decided to resign their significance in the explanation of the results.

Real e-field applied [kV/cm]	Energy in Joule [J]				
	Real enthalpy $\Delta H$ measured	Mean Cs y Rs (Scenario 1)	Max. Cs y Rs (Scenario 2)	Min Cs y Rs (Scenario 3)	Respective Cs and Rs values (Scenario 4)
0.99	0.5016	0.06053	0.03497	0.1106	0.1109
4.935	0.1672	1.504	0.8689	2.747	1.779
5.94	1.1705	2.179	1.259	3.98	2.646
9.93	5.0121	6.09	3.518	11.12	3.504
14.325	14.686	12.67	7.322	23.15	12.07

**Table 3.8.** Thermal energy dissipated in the cuvette vessel according to scenario and actual enthalpy

So, with the values of **Table 3.8** the energy curves were plotted in **Figure 3.3**. This results only denote that for values of Rs and Cs measured with a conventional RLC meter for a frequency of 100 Hz, it is possible to achieve a similarity in the energy results that is not far from the real enthalpy transferred into the tap water. It is important to notice that average values (Scenario 1) adjust the energy values much better to the real ones than the other scenarios. Let's don't forget either that the resistance value Rp was considered as constant during the simulations. This means that it was possible to obtain close energy values without having to consider the possibility of a variation on the resistance of the tap water, effect previously discussed to be of great possibility of having to happen during the electroporation.





**Figure 3.3.** Plots of dissipated energy per electric field value (red: experimentation, blue: simulation with average values, yellow: simulation with values measured with RLC-meter).

The total electrical energy through the system (between the terminals of the pulse generator) was also simulated and for simplicity only the total electrical energy according to the average value scenario (Scenario 4) was listed in **Table 3.9**. It was calculated that, of the total electrical energy delivered by the pulse generator, 99.36% of the energy was dissipated as heat through the cuvette vessel, leaving a remaining 0.64% of energy that was either dissipated through the conductive wires ( $R_w = 1.4 \text{ Ohm}$ ) or stored in the electric field of the capacitor. It should be noted that it was also possible to simulate the current through the resistor  $R_p$ , or, in other words, the leakage current. However, it is beyond the scope of this thesis to show these parameters.

	Energy simulated in Joule for the scenario 4 [J]		
E-field [kV/cm]	Whole system energy [J]	ERS+Rp energy [J]	Percentage from the whole
0.99	0.06092	0.06053	99.36%
4.935	1.514	1.504	99.34%
5.94	2.193	2.179	99.36%
9.93	6.129	6.09	99.36%
14.325	12.75	12.67	99.37%

**Table 3.9.** Percentage of energy dissipated as heat to the vessel

## 3.2 Survivability equation of *E. coli*

### 3.2.1 Colonies counting in Petri plates

A noticeable decrease in the value of colonies grown in the range of 1-10 kV/cm was obtained. The photos of the experience are all in Appendix 7 and the plates do not show a visual trend that dictates that the percentage of colonies eliminated is proportional to the increase in the electric field value. Of the 3 samples for each value of electric field applied that was plated, uneven results were obtained as shown in **Table 3.10** and even in the case of sample 3 for 1 and 6 kV/cm, 2 colony counts could not be recorded due to a cultivation error.

	UFC amount per sample plate		
Cuvette	Sample 1	Sample 2	Sample 3
1 kV/cm	23	17	-
5 kV/cm	~34	~39	<36
6 kV/cm	>34	6	-
10 kV/cm	~12	~30	~19

	UFC amount per sample plate		
Cuvette	Sample 1	Sample 2	Sample 3
15 kV/cm	<100	~300	~300

**Table 3.10.** Surviving colonies per electric field value

In **Table 3.11** it was determined that on average the colonies from the untreated water sample equaled 75 units per 100  $\mu$ l of sample, With this value, if the corresponding change ratio is performed by dividing the values in **Table 3.10** by the 75 units, the percentage of colonies eliminated can be calculated. This percentage exceeded 50% in most cases, except for sample 2 for 5 kV/cm and its results can be reviewed in **Table 3.12**.

	UFC amount per sample plate				Average UFC value
Control	Sample 1	Sample 2	Sample 3	Sample 4	
	75	60-80	<49	<60	75

**Table 3.11.** Control samples

	% Of survivability (UFC)		
Cuvette	Muestra 1	Muestra 2	Muestra 3
1 kV/cm	30.7 %	22.3 %	-
5 kV/cm	~45.4 %	~52 %	<48 %
6 kV/cm	<45.3 %	8 %	-
10 kV/cm	~16 %	~40 %	~25.3 %
15 kV/cm	-	-	-

**Table 3.12.** Percentage of colonies that survived the treatment (3 samples per e-field pulse)

It is worth noting that, after applying the value of 15 kV/cm, more colonies grew than the original control number which we already know was 75 UFC. The increase was more than double the control and on 2 occasions, the colonies formed exceeded 300 units.

Understanding this effect is beyond the scope of this thesis, so only the survivability of the 1-10 kV/cm samples have been taken as significant.

### 3.2.1.1 Discussion of the survivability trend

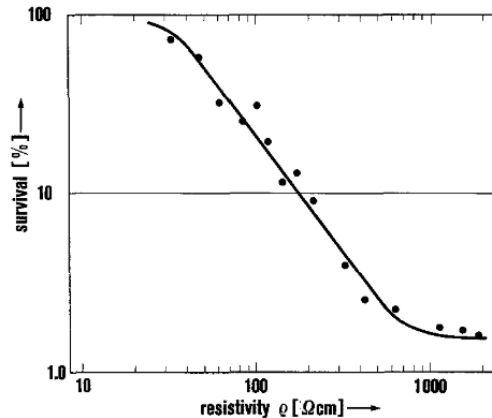
Qualitatively the visual results (Appendix 7) show some inverse trend to the expected as the applied electric field increased during the experimentation. It appears visually that as the electric field increased, fewer bacteria were inactivated. At best, one would notice the clear tendency of the colonies to decrease as demonstrated in the experimental studies by Hülshager et. Al. [15] or in the theoretical studies described by A. Goldberg and B. Rubinsky [41]. However, in 9 out of 10 cases (not counting the 15 kV/cm samples) more than 50% of colonies were inactivated, even at the lowest applied electric field value which was 0.99 kV/cm.

This event found its answer in the literature found in [73], where electroporation studies on volumetric flows of orange juice and coconut water characterized the effectiveness of different field pulses on the survivability of *E. coli*, *L. monocytogenes*, *S. cerevisiae*, *S. senftenberg* and *L. plantarum* microorganisms. The results correlated that the effectiveness in inactivating the microorganisms was higher for the condition in which moderate bipolar electric field pulses of 2.7 kV/cm in the range of 15-1000  $\mu$ s were applied, than for high monopolar pulses between 10-20 kV/cm in the range of 2  $\mu$ s. In other words, while applying the same amount of electrical and thermal energy for both configurations (moderate and high), more bacteria were inactivated with the moderate electric field value than with the higher one.

Under this concept, it is not wrong to think that the lowest values of e-field applied had a better efficiency than the highest one. This inverse effect even demonstrates that the inactivation effectiveness of electroporation procedures does not depend exclusively on a specific and determinant value of energy transferred to the medium; but rather, on the conditions under which this energy is transferred, i.e., the applied electric field value and the applied pulse duration. The experimental setup had also constant pulse duration (which was

22  $\mu$ s), so the only parameter left which might have represented the only influence on the result was the e-field applied.

This experiment only shows that for a range of time in the domain of the microseconds, 1 kV/cm is more than enough to eliminate more than 50% of *E. coli* bacteria on tap water. The only reason that might have played against higher efficiency in higher field pulses could be linked to the increase in temperature that decreases the resistivity of the dilution and increases its conductivity. In that sense, Hülshager et. al. (**Figure 3.4**) and F. Espino-Cortes et. al. [74] mention that increasing the conductivity of the medium reduces the inactivation efficiency of the electroporation treatment. Therefore, it makes sense to believe that the electroporation efficiency also decreased with increasing temperature and with increasing applied voltage. However, it has not been possible to quantify how much the efficiency decreased due to the increase in temperature and it is left as a recommendation to investigate.



**Figure 3.4.** Increased electroporation efficiency in *E. coli* removal with increasing resistivity. [15]

### 3.2.2 Spectrophotometric analysis UV-VIS OD600

A spectrophotometry analysis was performed (see curves and data measured with the Nanodrop ND-1000 in Appendix 7) whose values for the wavelength equal to 600 nm have been listed in **Table 3.13**. The curves in fact show no significant variation in the absorbance

values, and this is to be seen in **Table 3.13** because the mean absorbance post treatment values for each individual e-field value applied tended to be like the initial absorbance value which was 0.011. This fact is significant, because it only shows that the plate results seen in section 3.2.1 are not correlated with a variation in absorbance.

<b>Cuvette</b>	<b>Initial absorbance test OD600</b>	<b>Absorbance test post treatment OD600</b>	<b>Mean absorbance post treatment</b>
1 kV/cm	Sample 1: 0.014 Sample 2: 0.014 Sample 3: 0.006 Sample 4: 0.009 Sample 5: 0.012 Mean: 0.011	Sample 1: 0.014 Sample 2: 0.012	0.013
5 kV/cm		Sample 1: 0.014 Sample 2: 0.011	0.125
6 kV/cm		Sample 1: 0.014 Sample 2: 0.021 Sample 3: 0.011	0.153
10 kV/cm		Sample 1: 0.008 Sample 2: 0.013 Sample 3: 0.018	0.013
15 kV/cm		Sample 1: 0.007 Sample 2: 0.009 Sample 3: 0.013 Sample 4: 0.013	0.105

**Table 3.13.** Pre- and post-electroporation treatment absorbance values

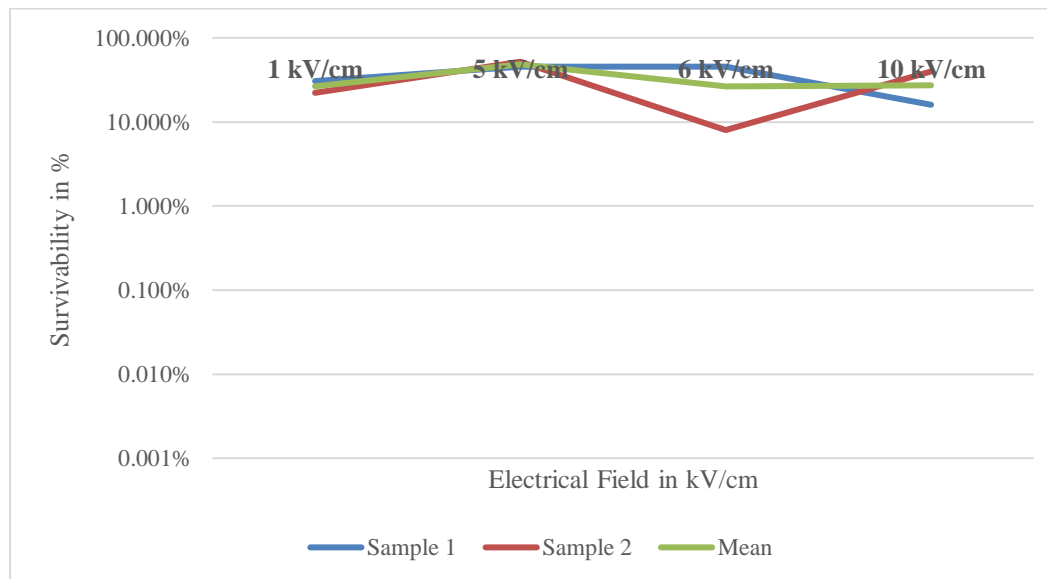
These results show that the inactivation by electroporation of *E. coli* did not alter the absorbance of the medium, for which the absorbance values were not useful to establish a survivability percentage rate based on Equation 43. It should be noted that from the beginning it was specified that the instrument was not calibrated, and this may have been a reason for the lack of variation.

### 3.3 Regression formula for *E. coli* survivability

**Table 3.14** summarizes the applied electric field values versus survival values for each of the three samples. The last column of the table comprises the average survivability values for each applied field value given the 3 samples. Because sample N°3 had cultivation issues, with the values for sample N°1 and 2, the curves defining the survivability with respect to the applied electric field were plotted in **Figure 3.5**. The average survivability was plotted, too

E-field value kV/cm	% Of survivability (UFC)			Average Survivability
	Sample 1	Sample 2	Sample 3	
0.99 (1)	30.70%	22.30%	-	26.50%
4.94 (5)	45.40%	52%	48%	48.47%
5.94 (6)	45.30%	8%	-	26.65%
9.93 (10)	16%	40%	25.30%	27.10%

**Table 3.14.** Average survivability per e-field value applied.



**Figure 3.5.** Experimental survival curves

Unfortunately, due to the cuvette gap (2 mm) and the maximum applicable voltage of 3000 V of the available pulse generator, it was impossible to achieve electric field ranges

above 15 kV/cm for which the final analysis had only 4 points for the construction of the curves. This was not enough data for establishing a significant correlation formula with the Excel software, not either a correlation coefficient  $R^2$ . Therefore, the second last specific objective of this research could not be accomplished.

Nevertheless, **Figure 3.5** shows that over the working range of the experiment the percentage of bacteria removal was almost constant, approach that serves for establishing that the e-field range of electroporation efficacy for killing *E. coli* colonies on tap water was 1-10 kV/cm. Moreover, within this electroporation range, 1 kV/cm can be considered as the most efficient e-field because, as **Table 3.15** illustrates, this value required the less energy for inactivating a similar amount of *E. coli* colonies among all the other higher e-field pulses applied.

Survivability (%)		Mean energy simulated [J]
Electrical Field	Mean	
1 kV/cm	26.50%	0.06092
5 kV/cm	48.47%	1.514
6 kV/cm	26.65%	2.193
10 kV/cm	27.10%	6.129

**Table 3.15.** Energy for eliminating a specific percentage of colonies per e-field pulse applied

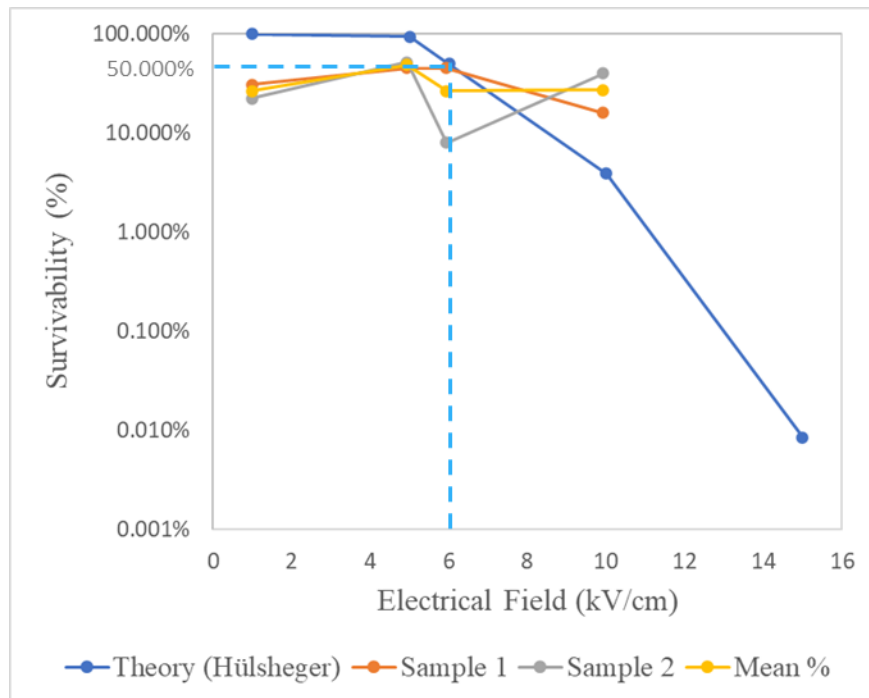
### 3.4 Threshold electrical value for killing 50% of *E. coli*

With the results already discussed, it is evident that it has not been possible to establish an experimental curve that would define a mathematical correlation between the increase of the electric field with the percentage of survival of the *E. coli* bacteria. However, it was decided to compare the experimental curve against the curve defined by the author Hülshager in 1996. For this purpose, the theoretical survival correspondence was described by the relationship seen in Equation 40 in the theoretical framework. The parameters used in the equation were the constants  $t_c = 12 \mu s$ ,  $E_c = 4.9 kV/cm$ ,  $k = 3.6 kV/cm$  and the



treatment time  $t$ , which was equal to the multiplication of the applied pulse duration ( $\tau=22\mu\text{s}$ ) with the total number of applied pulses  $n=30$ , i.e.  $t=0.00066$  seconds.

Once the parameters were defined, the curve was plotted by varying the electric field values according to the values applied in this experimentation (1, 5, 6, 10 and 15 kV/cm). The result is a blue curve visible in the **Figure 3.6**, which shows the descending trend of survivability with respect to the increase in e-field. When compared with the experimental curves defined in **Figure 3.5**, the theoretical curve tends to be more inefficient because it is shifted upwards along the y-axis. Besides, the sky-blue line seen on the graph shows that 6 kV/cm was the theoretical threshold value for which 50% of *E. coli* bacteria was inactivated. Hence, if we consider that 1 kV/cm was our experimental threshold value because it eliminated between 50-70% of *E. coli* colonies, the electroporation procedure performed for this research tended to be 6 times more efficient than theoretically.



**Figure 3.6.** Comparison of experimental survival vs. theoretical survival.

### 3.5 Final discussion

To sum up, the whole experimentation demonstrated that with only the application of 30 pulses of 1 kV/cm with a duration per pulse of 22  $\mu$ s, it was possible to eliminate up to 70% of *E. coli* bacteria found in a 400  $\mu$ l sample of tap water. It can be concluded that 1 kV/cm was the threshold electric field value at which 50 to more percentage values of *E. coli* colonies could be eliminated using cuvette vessels with 2 mm gap, where the simulated electric energy to achieve that goal was around 0.06092 Joule, or in other words, it was less than 1 Joule.

Finally, **Table 3.16** shows the summary of the total results.

Dilution Factor	Gap [mm]	Voltage Applied [V]	E-field applied [kV/cm]	Mean survivability percentage (%)	Mean electrical energy dissipated through resistors Rp and ESR simulated [J]	$\Delta H$ Enthalpy difference transferred to the tap water [J]
10 <sup>-1</sup>	2	198	0.99	26.50%	0.06092	0.5016
		987	4.935	48.47%	1.514	0.1672
		1188	5.94	26.65%	2.193	1.1705
		1986	9.93	27.10%	6.129	5.0121
		2865	14.325	-	12.75	14.686

**Table 3.16.** Result after analysis of data and result

## CONCLUSIONS

The energy values simulated with Simulink showed that the measurements of series resistance  $R_s$  and series capacitance  $C_s$  for 100 Hz with a conventional RLC-meter allowed simulating, with the archetype of a compound equivalent circuit for representing the cuvette, the energy losses of the system in a very similar way as in reality, where on average 0.06 J, 1.504 J, 2.179 J, 6.09 J and 12.67 J were simulated to be lost as heat respectively for each applied electric field pulse. This electrical energy can be similarly represented by the change of enthalpy  $\Delta H$  of the tap water and the results of this research show how good electrical simulations can closely represent a real heat dissipation effect of an electroporation circuit.

It should also be noted that the thermal losses according to the simulations with Simulink represent the 99.36% of the total energy supplied by the pulse generator. In addition, for the simulation to work efficiently, the losses should be represented as electrical energy values dissipated through a resistor  $R_p$ , due to the dielectric (tap water) between the cuvette's plates, and through a resistor ESR, due to the parasitic losses of the capacitor (cuvette).

The interpretation of the colony counting methodology showed that in 9 of 13 plated samples there was a decrease of more than 50% of *E. coli* colonies formed. That is, the applied field range between 0.99 and 9.93 kV/cm was able to inactivate approximately 50-70% of colonies stored in 400  $\mu$ l of pipe water from a population of between 750-800 CFU/ml of water. Unfortunately, the absorbance test did not bring any important variation results for describing the relation between a spectrophotometric analysis and a survivability change. The lack of absorbance variation might have occurred due to the poor calibration of the instrument and/or due to the little amount of sample that was used for the procedure (2  $\mu$ l).

Due to the low variability of the data, it was not possible to establish a survival correlation that mathematically models the percentage removal of *E. coli* colonies as a function of increasing applied electric field. However, if one were to choose the most effective electric field value to inactivate *E. coli* in tap water, 0.99 kV/cm would be the

appropriate value, since despite being the lowest field value applied, it eliminated similar or more colonies than the higher field values used.

In this sense, it can be defined that 1 kV/cm was the threshold electric field value with which it was possible to eliminate even more than 50% of *E. coli* bacteria in tap water and with which the last specific objective would be met. It should be noted that the technical specifications of the pulses were: a type of unipolar pulse applied, a pulse duration equal to 22  $\mu$ s, an interval between each pulse equal to 1 second and a total of n=30 pulses applied. The total electrical energy simulated with 1 kV/cm was 0.06092 J and the measured resistivity of the pipe water was equal to 1763.66843 Ohm-cm.

Finally, it should be noted that the increase in temperature of the tap water is the key for understanding the increase in current flow recorded during the experimentation. The literature studied established that a heat transfer to a capacitor's dielectric is most probably related to an increase in its conductivity which therefore translates into a resistivity decrease. Therefore, due to Ohm's Law current must increase within an electrical circuit if impedance or resistance must diminish. Temperature increase might have also been the reason for a capacitance decrease, but understanding this phenomenon was beyond the scope of this thesis.

All in all, the electroporation process proved to be a procedure whose energy consumption follows a transient and non-stationary behavior with respect to time, due to the increase in current that conditions the system to demand always higher power flows for each e-field pulse applied over time. It could be said that the energy demand of this type of system is not constant, but variable, thus a proper simulation of electroporation might only be done if current and voltage values are measured with sensitive, precise sensors that measure the variations of parameters precisely with respect to time. In addition, survivability was proved to be efficient for this electroporation procedure, especially for tap water, so it might be a good opportunity to test this same setup for a bigger scale in order to prove its efficacy on larger volumes of contaminated tap water.

## RECOMENDATIONS

The experimental results allowed the development of an experimental survival curve in the range of 1 to 10 kV/cm without the possibility of determining a mathematical correlation equation. It is suggested to extend the experimental electric field range from 15 kV/cm to 40 kV/cm to have a larger amount of work data to which regression statistics can be applied.

Similarly, the sample volume for this procedure should be expanded from 400  $\mu$ l to a bigger sample capable of running in a higher power spectrophotometer because the probability of having performed a non-significant absorbance test in this thesis is high due to the uncalibrated Nanodrop instrument and the application of only 2  $\mu$ l of sample for the respective analyses. For this new absorbance test, it is suggested to continue with the OD600 protocol.

Likewise, it would be an excellent recommendation to evaluate the efficacy of the electric field pulses in different types of water, specifically in water from natural sources or storage tanks with potential *E. coli* content. In this way, the actual effectiveness of electroporation as a method to sterilize water could be tested with real field data and the data could be compared with those defined in this thesis. It is suggested to test the same type of pulse, i.e., unipolar, with the same pulse duration and only 1 kV/cm, to check if this electric field value is efficient for different types of water.

To perform a better energy analysis, it is highly recommended to install better voltage and current sensors. Specifically, the voltage sensor should be directly connected to the plate terminals between the water volume to properly read the voltage transferred in-situ and see if there is any potential drop or rise for each applied field pulse. As for the current, it is sufficient to use a clamp ammeter that senses in the microsecond range in the same way as the voltage. Consequently, the multiplication of voltage and current will have a better power value and thus a more realistic integral energy calculation without the need for a MATLAB simulation.

Finally, it is recommended to perform an ANOVA statistical analysis for the survival analysis with the colony counting method, to calculate with statistical precision, the average number of colonies that survived per value of electric field applied, as well as the average number of colonies found in the control water sample. Moreover, instead of leaving the Petri dishes incubating for 24 hours, it would be good to remove them after 15 hours, so that the samples do not dry out and the colonies formed are in perfect condition to be counted.

## BIBLIOGRAPHY

- [1] MINSA, “En un 55% se redujeron los casos de enfermedades diarreicas en niños gracias al lavado de manos | Gobierno del Perú,” 2020. <https://www.gob.pe/institucion/minsa/noticias/307310-en-un-55-se-redujeron-los-casos-de-enfermedades-diarreicas-en-ninos-gracias-al-lavado-de-manos/> (accessed Sep. 06, 2021).
- [2] C. Cabezas Sánchez, “Enfermedades infecciosas relacionadas con el agua en el Perú,” *Rev. Peru. Med. Exp. Salud Publica*, vol. 35, no. 2, pp. 309–316, Apr. 2018, doi: 10.17843/RPMESP.2018.352.3761.
- [3] INEI, “Perú: formas de acceso al agua y saneamiento básico,” *Boletín Agua y Saneam.*, vol. 9, p. 70, 2020, [Online]. Available: <https://www.inei.gob.pe/biblioteca-virtual/boletines/formas-de-acceso-al-agua-y-saneamiento-basico-9343/1/>.
- [4] D. A. Quispe, “Calidad bacteriológica y físico-química del agua de seis manantiales del distrito de Santa Rosa-Melgar,” p. 85, 2017, [Online]. Available: <http://hdl.handle.net/11056/13212>.
- [5] E. O. Marchand Pajares, “Microorganismos indicadores de la calidad de agua de consumo humano.” [https://sisbib.unmsm.edu.pe/bibvirtual/tesis/basic/marchand\\_p\\_e/discusion.htm](https://sisbib.unmsm.edu.pe/bibvirtual/tesis/basic/marchand_p_e/discusion.htm) (accessed Sep. 07, 2021).
- [6] A. K. Carrascal Camacho, J. C. Salcedo Reyes, N. Rojas Higuera, A. M. Pedroza Rodríguez, A. Sánchez Garibello, and A. Matiz Villamil, “Evaluación de tres métodos para la inactivación de coliformes y *Escherichia coli* presentes en agua residual doméstica, empleada para riego,” *Univ. Sci.*, vol. 15, no. 2, p. 139, 2015, [Online]. Available: <http://www.scielo.org.co/pdf/unsc/v15n2/v15n2a05.pdf>.
- [7] S. O. Skipton *et al.*, “Tratamiento de agua potable: La cloración de choque.”
- [8] M. C. Dozier, P. Asistente, D. Extensión, and R. Hidráulicos, “Tratando agua almacenada con cloro,” pp. 6–8.

- [9] W. K. Neu and J. C. Neu, "Theory of electroporation," *Card. Bioelectric Ther. Mech. Pract. Implic.*, pp. 133–161, 2009, doi: 10.1007/978-0-387-79403-7\_7.
- [10] J. C. Weaver and Y. A. Chizmadzhev, "Theory of electroporation: A review," *Bioelectrochemistry Bioenerg.*, vol. 41, no. 2, pp. 135–160, 1996, doi: 10.1016/S0302-4598(96)05062-3.
- [11] J. Gehl, "Electroporation: Theory and methods, perspectives for drug delivery, gene therapy and research," *Acta Physiol. Scand.*, vol. 177, no. 4, pp. 437–447, 2003, doi: 10.1046/j.1365-201X.2003.01093.x.
- [12] K. H. Schoenbach, A. Abou-Ghazala, T. Vithoukas, R. W. Alden, R. Turner, and S. Beebe, "Effect of pulsed electrical fields on biological cells," *Dig. Tech. Pap. Int. Pulsed Power Conf.*, vol. 1, no. 2, pp. 73–78, 1997, doi: 10.1109/ppc.1997.679279.
- [13] P. Ellappan and R. Sundararajan, "A simulation study of the electrical model of a biological cell," *J. Electrostat.*, vol. 63, no. 3-4 SPEC. ISS., pp. 297–307, 2005, doi: 10.1016/j.elstat.2004.11.007.
- [14] S. B. Dev, D. P. Rabussay, G. Widera, and G. A. Hofmann, "Medical applications of electroporation," *IEEE Trans. Plasma Sci.*, vol. 28, no. 1, pp. 206–223, 2000, doi: 10.1109/27.842905.
- [15] H. Hülshager, J. Potel, and E. G. Niemann, "Killing of bacteria with electric pulses of high field strength," *Radiat. Environ. Biophys.*, vol. 20, no. 1, pp. 53–65, 1981, doi: 10.1007/BF01323926.
- [16] V. R. Krishnamurthi, A. Rogers, J. Peifer, I. I. Niyonshuti, J. Chen, and Y. Wang, "Microampere electric current causes bacterial membrane damage and two-way leakage in a short period of time," *Appl. Environ. Microbiol.*, vol. 86, no. 16, pp. 1–10, 2020, doi: 10.1128/AEM.01015-20.
- [17] M. S. Islam, A. Shahid, K. Kuryllo, Y. Li, M. J. Deen, and P. R. Selvaganapathy, "Electrophoretic concentration and electrical lysis of bacteria in a microfluidic device using a nanoporous membrane," *Micromachines*, vol. 8, no. 2, 2017, doi: 10.3390/mi8020045.



- [18] M. S. Islam, A. Aryasomayajula, and P. R. Selvaganapathy, “A review on macroscale and microscale cell lysis methods,” *Micromachines*, vol. 8, no. 3, 2017, doi: 10.3390/mi8030083.
- [19] “Bacteria - Diversity of structure of bacteria | Britannica.” <https://www.britannica.com/science/bacteria/Diversity-of-structure-of-bacteria> (accessed Jun. 07, 2021).
- [20] M. Riley, “Correlates of Smallest Sizes for Microorganisms The Size and Contents of an Average Gram-Negative Organism The Effect of Growth Conditions on Cell Constituents Distribution of Genetic Determinants of *E. coli* K-12 Essentials of Conceptually Pared Down Ave,” no. Dc, 1999.
- [21] O. Pierucci, “Dimensions of *Escherichia coli* at various growth rates: model for envelope growth,” *J. Bacteriol.*, vol. 135, no. 2, pp. 559–574, 1978, doi: 10.1128/jb.135.2.559-574.1978.
- [22] K. D. Young, “The Selective Value of Bacterial Shape,” *Microbiol. Mol. Biol. Rev.*, vol. 70, no. 3, pp. 660–703, 2006, doi: 10.1128/mubr.00001-06.
- [23] S. Cooper and M. W. Denny, “A conjecture on the relationship of bacterial shape to motility in rod-shaped bacteria,” *FEMS Microbiol. Lett.*, vol. 148, no. 2, pp. 227–231, 1997, doi: 10.1016/S0378-1097(97)00038-4.
- [24] G. Reshes, S. Vanounou, I. Fishov, and M. Feingold, “Cell shape dynamics in *Escherichia coli*,” *Biophys. J.*, vol. 94, no. 1, pp. 251–264, 2008, doi: 10.1529/biophysj.107.104398.
- [25] K. Pluhackova and A. Horner, “Native-like membrane models of *E. coli* polar lipid extract shed light on the importance of lipid composition complexity,” *BMC Biol.*, vol. 19, no. 1, pp. 1–22, 2021, doi: 10.1186/s12915-020-00936-8.
- [26] T. J. Silhavy, D. Kahne, and S. Walker, “The bacterial cell envelope.,” *Cold Spring Harb. Perspect. Biol.*, vol. 2, no. 5, 2010, doi: 10.1101/cshperspect.a000414.
- [27] W. Vollmer and P. Born, “Bacterial cell envelope peptidoglycan,” in *Microbial*

*Glycobiology*, First edit., Elsevier, 2010, pp. 15–28.

- [28] M. Checa, R. Millan-solsona, and E. Torrents, “Mapping the dielectric constant of a single bacterial cell at the nanoscale with scanning dielectric force volume microscopy †,” pp. 20809–20819, 2019, doi: 10.1039/c9nr07659j.
- [29] W. Huang, “THEORETICAL CALCULATION OF THE DIELECTRIC CONSTANT OF A BILAYER MEMBRANE,” vol. 17, 1977.
- [30] T. Heimburg, “The Capacitance and Electromechanical Coupling of Lipid Membranes Close to Transitions : The Effect of Electrostriction,” vol. 103, no. 5, pp. 918–929, 2012, doi: 10.1016/j.bpj.2012.07.010.
- [31] D. C. Chang, B. M. Chassy, J. A. Saunders, and A. E. Sowers, *Guide to Electroporation and Electrofusion*. 1992.
- [32] H. Berg, “Guide to Electroporation and Electrofusion.,” *Bioelectrochemistry and Bioenergetics*, vol. 29, no. 2. pp. 248–249, 1992, doi: 10.1016/0302-4598(92)80073-p.
- [33] E. Neumann, A. E. Sowers, and C. A. Jordan, *Electroporation and Electrofusion in Cell Biology*, 1st ed. Springer US, 1989.
- [34] C. T. Bot and C. Prodan, “Quantifying the membrane potential during *E. coli* growth stages,” *Biophys. Chem.*, vol. 146, no. 2–3, pp. 133–137, 2010, doi: 10.1016/j.bpc.2009.11.005.
- [35] D. Zilberstein, V. Agmon, S. Schuldiner, and E. Padan, “Escherichia coli intracellular pH, membrane potential, and cell growth,” *J. Bacteriol.*, vol. 158, no. 1, pp. 246–252, 1984, doi: 10.1128/jb.158.1.246-252.1984.
- [36] B. Rubinsky, “Irreversible electroporation in medicine,” *Technol. Cancer Res. Treat.*, vol. 6, no. 4, pp. 255–259, 2007, doi: 10.1177/153303460700600401.
- [37] A. Polak *et al.*, “Electroporation of archaeal lipid membranes using MD simulations,” *Bioelectrochemistry*, vol. 100, pp. 18–26, 2014, doi: 10.1016/j.bioelechem.2013.12.006.

- [38] T. B. Napotnik and D. Miklavčič, “In vitro electroporation detection methods - An overview.” Elsevier, pp. 166–182.
- [39] “Electrooptics Studies of Escherichia coli Electropulsation\_ Orientation, Permeabilization, and Gene Transfer \_ Elsevier Enhanced Reader.pdf.” .
- [40] R. Pranevic, “Determination of cell electroporation from the release of intracellular potassium ions,” vol. 360, pp. 273–281, 2007, doi: 10.1016/j.ab.2006.10.028.
- [41] A. Golberg and B. Rubinsky, “A statistical model for multidimensional irreversible electroporation cell death in tissue,” *Biomed. Eng. Online*, vol. 9, pp. 1–13, 2010, doi: 10.1186/1475-925X-9-13.
- [42] J. S. S. Narayanan, P. Ray, I. Naqvi, and R. White, “A syngeneic pancreatic cancer mouse model to study the effects of irreversible electroporation,” *J. Vis. Exp.*, vol. 2018, no. 136, pp. 1–7, 2018, doi: 10.3791/57265.
- [43] F. W. Sears and M. W. Zemansky, *Física Universitaria con Física Moderna. Volumen 2*, 12th ed. 2008.
- [44] G. Rajauria and K. T. Brijesh, *Fruit Juices - Extraction, Composition, Quality and Analysis*. Elsevier, 2017.
- [45] M. Reberšek, D. Miklavčič, C. Bertacchini, and M. Sack, “Cell membrane electroporation-Part 3: The equipment,” *IEEE Electr. Insul. Mag.*, vol. 30, no. 3, pp. 8–18, 2014, doi: 10.1109/MEI.2014.6804737.
- [46] C. Alexander and M. Sadiku, *Fundamentos de circuitos eléctricos*, 5th ed. Mexico, 2006.
- [47] “Square Wave Electroporation System User’s Manual,” pp. 1–43, [Online]. Available: [www.btxonline.com](http://www.btxonline.com).
- [48] RTI, “User ’ s Manual User ’ s Manual ユーザーズマニュアル,” vol. 2886, no. 408, pp. 1–38, 2010.
- [49] L. A. Palomino Marcelo, “Evaluación de la interacción de nanopartículas de plata con factor de crecimiento epidermal para su uso potencial en sistemas que mejoren la

regeneración de tejidos epiteliales,” *Univ. Nac. Mayor San Marcos*, 2019, [Online]. Available: <https://cybertesis.unmsm.edu.pe/handle/20.500.12672/11788>.

- [50] S. A. Servera, “Prácticas de microbiología,” Universidad de La Rioja, 2011.
- [51] I. E. T. Labs, “DE-6000 Portable , Full-Featured LCR Meter User and Service Manual,” no. April, 2014.
- [52] BK Precision, “LCR Meter Guide.” [https://bkpmedia.s3.amazonaws.com/downloads/guides/en-us/lcr\\_meter\\_guide.pdf](https://bkpmedia.s3.amazonaws.com/downloads/guides/en-us/lcr_meter_guide.pdf).
- [53] “The Beer-Lambert Law - Chemistry LibreTexts.” [https://chem.libretexts.org/Bookshelves/Physical\\_and\\_Theoretical\\_Chemistry\\_Textbook\\_Maps/Supplemental\\_Modules\\_\(Physical\\_and\\_Theoretical\\_Chemistry\)/Spectroscopy/Electronic\\_Spectroscopy/Electronic\\_Spectroscopy\\_Basics/The\\_Beer-Lambert\\_Law](https://chem.libretexts.org/Bookshelves/Physical_and_Theoretical_Chemistry_Textbook_Maps/Supplemental_Modules_(Physical_and_Theoretical_Chemistry)/Spectroscopy/Electronic_Spectroscopy/Electronic_Spectroscopy_Basics/The_Beer-Lambert_Law) (accessed Jul. 01, 2021).
- [54] “The OD600 Basics | Best OD600 Tool To Generate Microbial Growth Curves.” <https://www.implen.de/od600-diluphotometer/od600/> (accessed Oct. 03, 2021).
- [55] P. Y. Yap and D. Trau, “Direct E . coli cell count at OD600,” *Tip Biosyst.*, vol. 1, no. March, pp. 101–103, 2019.
- [56] BioRad, “NanoDrop 1000 Spectrophotometer V3 . 8 User ’ s Manual,” *No J.*, vol. 11, no. 1, p. 10, 2012, [Online]. Available: [www.nanodrop.com](http://www.nanodrop.com).
- [57] M. Moran and H. Shapiro, “Fundamentos de Termodinamica Técnica,” *J. Chem. Inf. Model.*, vol. 53, no. 9, p. 1699, 2018.
- [58] M. Say and G. Jones, “Electrotechnology,” in *Electrical Engineer’s Reference Book*, 16th ed., 2003, pp. 2–1, 2-3-2–30.
- [59] J. C. Rawlins, “RL Circuit Analysis,” in *Basic AC Circuits*, 2000, pp. 303–334.
- [60] C. D. of O. P. Issue, “CONDUCTIVITY MEASUREMENT IN HIGH PURITY WATER SAMPLES below 10  $\mu$  SIEMENS / cm High Purity Water Resistivity / Conductivity Measurement,” *IC Control. Process Water Anal. Equipments*, no. 4, 2012.

- [61] T. S. Light, S. Licht, A. C. Bevilacqua, and K. R. Morash, "The fundamental conductivity and resistivity of water," *Electrochem. Solid-State Lett.*, vol. 8, no. 1, 2005, doi: 10.1149/1.1836121.
- [62] A. C. Bevilacqua, "Ultrapure Water—The Standard for Resistivity Measurements of Ultrapure Water," *1998 Semicond. Pure Water Chem. Conf.*, pp. 2–5, 1998, [Online]. Available: <http://www.snowpure.com/docs/thornton-upw-resistivity-measurement.pdf>.
- [63] V. Stankevic *et al.*, "Compact square-wave pulse electroporator with controlled electroporation efficiency and cell viability," *Symmetry (Basel)*, vol. 12, no. 3, 2020, doi: 10.3390/sym12030412.
- [64] A. H. Ruarus, L. G. P. H. Vroomen, R. S. Puijk, H. J. Scheffer, T. J. C. Faes, and M. R. Meijerink, "Conductivity Rise During Irreversible Electroporation: True Permeabilization or Heat?," *Cardiovasc. Intervent. Radiol.*, vol. 41, no. 8, p. 1257, Aug. 2018, doi: 10.1007/S00270-018-1971-7.
- [65] "Measurement of the dielectric constant and index of refraction of water and aqueous solutions of  $\text{KCl}$  at high frequencies," vol. 4, no. 4, pp. 613–622, 1930.
- [66] C. G. Malmberg and A. A. Maryott, "Dielectric constant of water from 0 to 100 C," *J. Res. Natl. Bur. Stand. (1934)*, vol. 56, no. 1, p. 1, 1956, doi: 10.6028/jres.056.001.
- [67] S. C. Moldoveanu and V. David, *Mobile Phases and Their Properties*. 2013.
- [68] KEMET Co., "Introduction to Capacitor Technologies," p. 16, 2013.
- [69] J. Bisquert, G. Garcia-Belmonte, and F. Fabregat-Santiago, "The role of instrumentation in the process of modeling real capacitors," *IEEE Trans. Educ.*, vol. 43, no. 4, pp. 439–442, 2000, doi: 10.1109/13.883355.
- [70] R. L. Spyker, "Classical equivalent circuit parameters for a double-layer capacitor," *IEEE Trans. Aerosp. Electron. Syst.*, vol. 36, no. 3 PART 1, pp. 829–836, 2000, doi: 10.1109/7.869502.

- [71] C. Merla *et al.*, “A 10- $\Omega$  high-voltage nanosecond pulse generator,” *IEEE Trans. Microw. Theory Tech.*, vol. 58, no. 12 PART 2, pp. 4079–4085, 2010, doi: 10.1109/TMTT.2010.2086470.
- [72] Superintendencia Nacional de Servicios de Saneamiento, *La calidad del agua potable en el Perú*. 2004.
- [73] R. A. H. Timmermans *et al.*, “Moderate intensity Pulsed Electric Fields (PEF) as alternative mild preservation technology for fruit juice,” *Int. J. Food Microbiol.*, vol. 298, pp. 63–73, 2019, doi: 10.1016/j.ijfoodmicro.2019.02.015.
- [74] F. Espino-Cortes, A. H. El-Hag, O. Adedayo, S. Jayaram, and W. Anderson, “Water processing by high intensity pulsed electric fields,” *Annu. Rep. - Conf. Electr. Insul. Dielectr. Phenomena, CEIDP*, pp. 684–687, 2006, doi: 10.1109/CEIDP.2006.312024.
- [75] FDA, “Kinetics of Microbial Inactivation for Alternative Food Processing Technologies -Ultraviolet Light,” *Safe Pract. Food Process.*, no. 2, pp. 1–37, 2014, [Online]. Available: <http://www.fda.gov/Food/FoodScienceResearch/SafePracticesforFoodProcesses/ucm103137.htm>.
- [76] Autoridad Nacional del Agua, “Segundo monitoreo participativo de la calidad de agua superficial de la cuenca del río Rímac,” *Autoridades Adm. del agua*, pp. 1–31, 2014, [Online]. Available: <http://repositorio.ana.gob.pe/handle/ANA/2075>.
- [77] INEI, “PROVINCIA DE LIMA: MONITOREO DE AGUA DEL RÍO RÍMAC, SEGÚN PARÁMETRO FÍSICO Y QUÍMICO, 2001-2011.” [https://view.officeapps.live.com/op/view.aspx?src=https%3A%2F%2Fwww.inei.gob.pe%2Fmedia%2FMenuRecursivo%2Fpublicaciones\\_digitaless%2FEst%2FLib1149%2Fcuadros%2Fc02003.xls&wdOrigin=BROWSELINK](https://view.officeapps.live.com/op/view.aspx?src=https%3A%2F%2Fwww.inei.gob.pe%2Fmedia%2FMenuRecursivo%2Fpublicaciones_digitaless%2FEst%2FLib1149%2Fcuadros%2Fc02003.xls&wdOrigin=BROWSELINK).
- [78] N. ESPITIA, *Universidad Nacional Mayor de San Marcos Unidad de Posgrado Análisis de calidad de agua potable con relación a sus parámetros fisicoquímicos , biológicos , y crecimiento de Lemna minor en la estancia de Lurín , Lima 2015-2016 TESIS Para optar el Grado Aca.* 2019.

## **APPENDIXES**

## APPENDIX 1: PLATE ISOLATION METHOD BY SERIAL DILUTIONS

Materials: Sterile micropipettes, tap water, sterile tubes, and sample (*E. coli* suspension immersed in PBS buffer at 37°C).

1. The tap water will be in a beaker that will have been sterilized with UV light in the sterilization chamber prior to performing dilutions.
2. Take a sterile micropipette of 100-1000 microliters and place the tip without touching with the hands more than just the upper part of the instrument with which the inoculation will be manipulated. Flame the mouth of the beaker with water and take 9 ml of its content.
3. Transfer the 9 ml to one of the sterile tubes, flaming the mouth of the tube after removing the cap and before replacing it. Remember that the stoppers must be kept in the hand and not left on the table during the operation. Avoid touching the tip to any object. Always work in the vicinity of the flame.
4. With the same tip, if it has not been contaminated, transfer again 9 ml of the Beaker water following the instructions given in 2 and 3.
5. Repeat 4 as many times as necessary. Finally discard the used tip.
6. With a new tip take 1 ml of sample and transfer it to the first of the tubes with 9 ml of water. Deposit the tip in 'contaminated material' and mark the tube as 1/10 (or  $10^{-1}$ ).
7. Shake the tube with the first dilution well by rotating it between the palms of the hands and, with a new sterile tip, transfer 1 ml of this first dilution to the second tube with 9 ml of water. Discard the tip and shake the tube. Mark it as 1/100 (or  $10^{-2}$ ).



## APPENDIX 2: RLC-METER EQUATIONS

$$\begin{aligned}
 \mathbf{Z} &= R_s + \frac{1}{j\omega C_s} = \frac{\frac{R_p}{j\omega C_p}}{R_p + \frac{1}{j\omega C_p}} = \frac{D^2 R_p + \frac{1}{j\omega C_p}}{1 + D^2} \\
 D &= \frac{1}{Q} = \omega R_s C_s = \frac{1}{\omega R_p C_p} \\
 R_s R_p C_s C_p &= \frac{1}{\omega^2} \\
 C_p &= C_s \left( \frac{1}{1 + D^2} \right) \\
 C_s &= C_p (1 + D^2) \\
 R_p &= R_s \left( \frac{1 + D^2}{D^2} \right) = \frac{1}{\omega C_p D} \\
 R_s &= R_p \left( \frac{D^2}{1 + D^2} \right) = \frac{D}{\omega C_s}
 \end{aligned}$$

Figure 7.1. Capacitance equations

$$\begin{aligned}
 Q &= 1/D = \tan\Theta \\
 Q &= X_s/R_s = 2\pi f L_s/R_s = 1/2\pi f C_s R_s \\
 Q &= B/G = R_p/|X_p| = R_p/2\pi f L_p = 2\pi f C_p R_p
 \end{aligned}$$

Figure 7.2. Quality factor relations

### **APPENDIX 3: PRELIMINARY EXPERIMENTATION'S LB MEDIUM PROTOCOL**

1. Weigh 11.25 g of Agar and 10 g of Lb. Medium.
2. Dilute in distilled water to obtain half a liter of Agar solution and L.B. medium. Each solution is placed in Erlenmeyer flasks.
3. Sterilize 15 test tube lids, 15 test tubes, 15 petri dishes and the Erlenmeyer flasks at 121°C (15 lbs. of pressure) for 1.5 hours (until adequate temperature is reached). Once ready, remove the elements and wait for them to cool to a suitable temperature for touching.
4. Pour all the Agar solution into the 15 petri dishes, until it is all gone, in a uniform way. Work in the fume hood. Light a burner to maintain sterility in the working area. Leave the petri dishes and wait for the agar to solidify. Once that happens, cover the plates with film and refrigerate 24 hours.
5. Pack 40 mL of Lb. medium solution into a bottle with one tablet of *E. coli* bacteria.
6. Shake the bottle with broth in the shaker at 37°C for 2 hours. Then leave, shaking for another 24 hours.
7. Make dilutions of medium with the bacterial culture.

## APPENDIX 4: PRELIMINARY EXPERIMENTATION'S METHODOLOGY

The *E. coli* culture medium for preliminary experimentation was Luria Bertani (LB) medium. The *E. coli* ATCC® 8739 pellet from Epower™ Laboratory was nourished and replicated in this medium for 24 hours inside a New Brunswick Scientific G24 incubator at a temperature of 37°C. For this purpose, the pellet was arbitrarily diluted in 40 mL of LB as described in Appendix 3, the result being a yellowish liquid rich in nutrients with which we then proceeded to perform serial dilutions in tap water for the performance of the experiment (Figure 7.3).

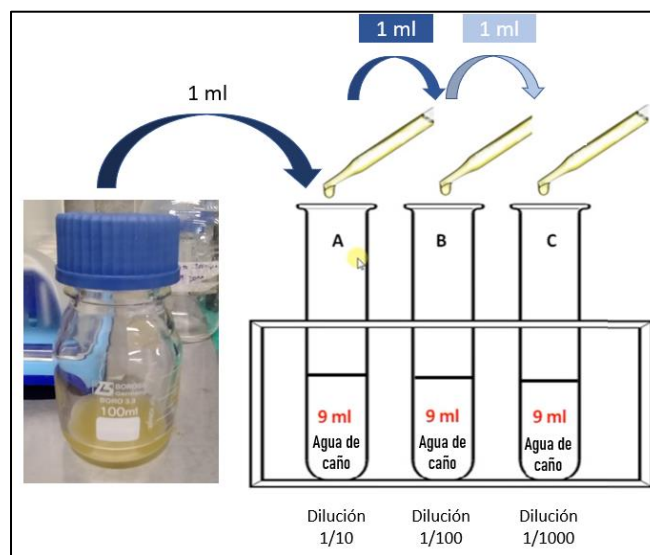


Figure 7.3. LB and serial dilutions

The protocol for performing the dilutions was the same as that of the main experiment with the only difference being that the tablet dilution medium was LB medium and not PBS buffer. Three dilutions were performed (the first 3 on the left in Figure 7.3) and from each dilution different volumes of sample were extracted and inoculated into two of the cuvettes in Figure 8.6. These were specifically the gray lid cuvette (1 mm gap) and the blue lid cuvette (2 mm gap). Now, the volume that was inoculated into the vessels was not the same for the

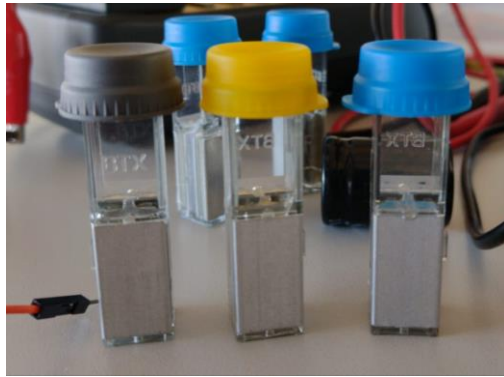
2 cuvettes, but rather, the volume was respective of the geometric dimensions that the vessels themselves offer between their plates. We inoculated 90  $\mu\text{l}$  of in the gray cuvette and 400  $\mu\text{l}$  in the blue cuvette.

In total, 3 electric field pulses were launched on each of the 3 working dilutions. It is worth mentioning that the blue cuvette or 2 mm gap was used for the application of the field equal to 10 kV/cm, while the gray container with a gap of 1 mm was used for the application of 20 and 30 kV/cm of electric field, respectively. Thus, the samples inoculated in the vessels passed through the electric field values according to each dilution as specified in the matrix in Table 8.2 and a total of 6 cuvettes were used.










The electroporated contents of the cuvettes were inoculated into Petri dishes to compare the variation of colony growth or CFU of *E. coli* post-treatment with the number of colonies that grew from the same volume that did not pass through the electroporation treatment. The agar used for colony growth was MacConkey agar due to its selective predisposition to nurture the growth of gram-negative bacteria.



**Figure 7.4.** Test tubes containing 6 different concentrations of bacteria in tap water (from highest concentration to lowest concentration in left to right direction).



**Figure 7.5.** Cuvette yellow (4 mm), cuvette blue (2 mm), cuvette gray (1 mm)

	E-field values		
	10 kV/cm	20 kV/cm	30 kV/cm
Dilution 1			
Dilution 2			
Dilution 3			

**Table 7.1.** Matrix of cuvettes per electric field value

The electrical parameters for each cuvette were measured using an RLC-meter, specifically the IET DE-5000. The parameters were measured for different test frequencies and were listed in tables such as the one seen in **Table 2.2** and the electrical parameters measured were inductance 'Ls', capacitance 'Cs', series resistance 'Rs', resistance 'DCR', dissipation factor 'D', quality factor 'Q' and phase angle 'phy'.

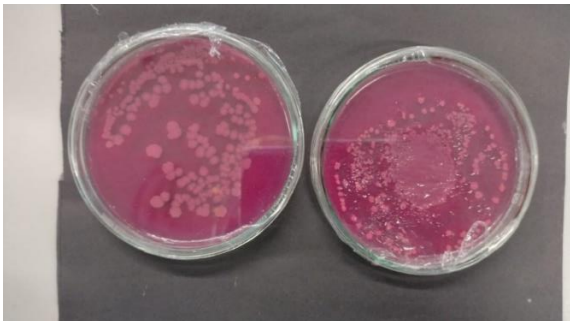
The Appendix 2 relationship equal to  $X_s = QR_s$  was applied to obtain the reactance value 'Xs-D' seen in the **Table 7.2**; the relationship  $Z = \sqrt{R_s^2 + X_s^2}$  to obtain the impedance value 'Z'; and the Equation 42 to obtain the impedance phase shift angle for each of the 6 different cuvettes. With all the electrical parameters (impedance Z, resistance Rs, inductance Ls and capacitance Cs) we proceeded to perform a correlation analysis between them using Excel software. This sought to understand the dependence of the variation of the measured RLC parameters ( $\Delta L_s$ ,  $\Delta C_s$  and  $\Delta R_s$ ) on the variation of the impedance  $\Delta Z$  to leave an analysis on the trend of variation of the parameters.

Frequency Hz	Z	Phase angle calculation	cos(phy)	Xs-D
100	-	-	-	-
1000	-	-	-	-
10000	-	-	-	-
100000	-	-	-	-

**Table 7.2.** Final electrical parameters

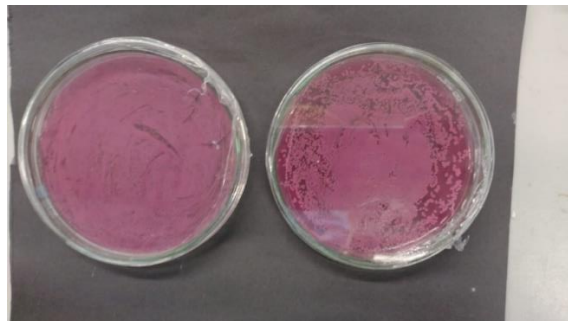
## APPENDIX 5: COLONY COUNTING METHOD RESULTS OF THE PRELIMINARY EXPERIMENTATION

1. 20 kV/cm – 3rd dilution



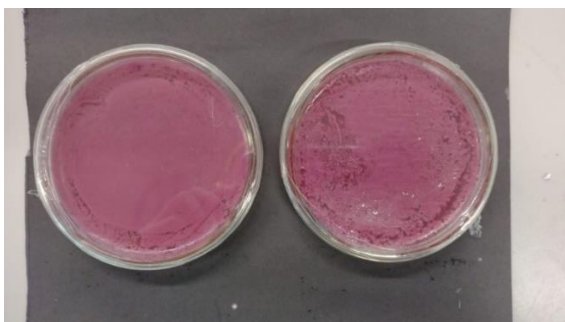
**Figure 7.6.** Left: pre-treatment control, right: electroporated sample after treatment.

2. 20 kV/cm – 2nd dilution



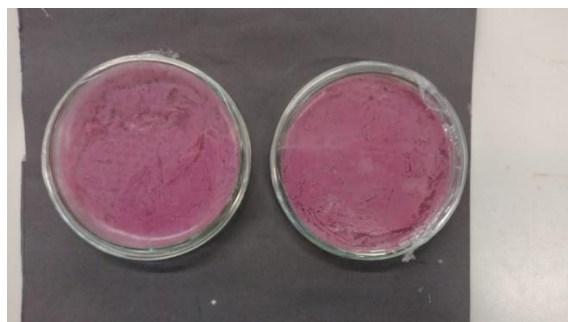
**Figure 7.7.** Left: pre-treatment control, right: electroporated sample after treatment.

3. 10 kV/cm - 3rd dilution



**Figure 7.8.** Left: pre-treatment control, right: electroporated sample after treatment.

4. 10 kV/cm – 2nd dilution



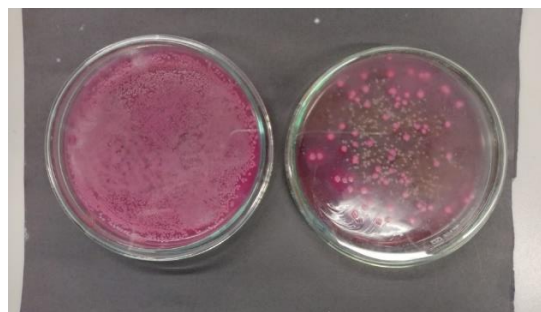
**Figure 7.9.** Left: pre-treatment control, right: electroporated sample after treatment.

5. 10 kV/cm – 1st dilution



**Figure 7.10.** Left: pre-treatment control, right: electroporated sample after treatment.

6. 30 kV/cm - 3rd dilution



**Figure 7.11.** Left: pre-treatment control, right: electroporated sample after treatment.



## APPENDIX 6: DISCUSSION OF THE PRELIMINARY EXPERIMENTATION

Electrical parameters were taken from the cuvettes and electric field pulses were applied according to each cuvette as shown in **Table 7.3**. There was one case where the treatment was applied 2 times, so the final number of pulses for this cuvette was a total of  $n = 60$  pulses and counts as a special case of analysis.

# de dilución	Campo eléctrico	Cuvette	# pulsos
1	10 kV/cm	2 mm	30
	30 kV/cm	1mm	30
2	20 kV/cm	1mm	30
	30 kV/cm	1mm	30
3	20 kV/cm	1mm	30
	30 kV/cm	1mm	60

**Table 7.3.** Pulses applied to each dilution

Regarding the variation of the electrical parameters, the percentage variations of the reading of parameters before and after the electroporation procedure are presented in **Table 7.4**, **Table 7.5** and **Table 7.6**. In yellow are the variations that did not exceed the percentage of uncertainty or 'accuracy' according to the specifications of the RLC IET-5000 instrument and therefore were considered with 0% variation.

To begin with, **Table 7.4** shows that applying 10 kV/cm to dilution No. 1 lead to an increasing trend both in the inductance value  $L_s$  and in the resistance value  $R_s$ ; as well as to a decreasing trend in the capacitance value  $C_s$ . Applying 20 kV/cm (**Table 7.5**), showed a trend very similar to the previous one in both dilutions  $N^\circ 2$  and  $N^\circ 3$ ; however, applying 30 kV/cm (**Table 7.6**) reversed the trend for inductance, resistance and capacitance in dilutions 1 and 2, while for dilution  $N^\circ 3$  a behavior more similar to the case of the application of 20 and 10 kV/cm was observed.

		Parameters								
		10 kV/cm								
		Before			After					
1st Dilution	Frequency Hz	Ls H	Cs	Rs	Ls H	Cs	Rs	delta Ls (1D)	delta Cs (1D)	delta Rs (1D)
	100	1.600870	1.582E-06	687	1.941537	1.305E-06	760	21.280%	-17.546%	10.626%
	1000	0.038236	6.625E-07	198.2	0.040161	6.307E-07	189	5.034%	-4.793%	-4.642%
	10000	0.000667	3.797E-07	96	0.000720	3.516E-07	110	7.982%	-7.39%	14.583%
	100000	0.000011	2.362E-07	84.64	0.000011	2.377E-07	92	0.000%	0.000%	8.696%

**Table 7.4.** Parameter variation - 10 kV/cm- Dilution 1

		Parameters								
		20 kV/cm								
		Before			After					
2nd Dilution	Frequency Hz	Ls H	Cs	Rs	Ls H	Cs	Rs	delta Ls (2D)	delta Cs (2D)	delta Rs (2D)
	100	5.829008	4.346E-07	1747	5.931240	4.271E-07	1800	1.754%	-1.724%	3.034%
	1000	0.102792	2.464E-07	445	0.107145	2.364E-07	480	4.234%	-4.062%	7.865%
	10000	0.001754	1.444E-07	238	0.001883	1.345E-07	249.7	7.402%	-6.892%	4.916%
	100000	0.000031	8.273E-08	207	0.000034	7.535E-08	212.9	9.789%	-8.916%	2.850%
3rd Dilution	Frequency Hz	Ls H	Cs	Rs	Ls H	Cs	Rs	delta Ls (3D)	delta Cs (3D)	delta Rs (3D)
	100	2.600037	9.742E-07	1253	2.925326	8.659E-07	1498	12.511%	-11.120%	19.572%
	1000	0.059243	4.276E-07	437	0.072543	3.492E-07	495	22.451%	-18.335%	13.272%
	10000	0.001121	2.259E-07	279	0.001390	1.822E-07	297	23.985%	-19.345%	6.452%
	100000	0.000024	1.040E-07	255	0.000030	8.407E-08	262	23.680%	-19.146%	2.745%

**Table 7.5.** Parameter variation - 20 kV/cm - Dilutions 2 and 3

		Parameters								
		30 kV/cm								
		Before			After					
1st Dilution	Frequency Hz	Ls H	Cs	Rs	Ls H	Cs	Rs	delta Ls (1D)	delta Cs (1D)	delta Rs (1D)
	100	5.12E+00	4.948E-07	1709	4.934217	5.134E-07	1630	-3.609%	3.744%	-4.623%
	1000	9.93E-02	2.550E-07	532	0.095533	2.651E-07	527	-3.811%	3.962%	-0.940%
	10000	1.77E-03	1.433E-07	306	0.001767	1.434E-07	300	0.000%	0.000%	-1.961%
	100000	3.39E-05	7.462E-08	270	0.000034	7.347E-08	261	0.000%	0.000%	-3.333%
2nd Dilution	Frequency Hz	Ls H	Cs	Rs	Ls H	Cs	Rs	delta Ls (2D)	delta Cs (2D)	delta Rs (2D)
	100	6.30E+00	4.021E-07	2068	6.012156	4.213E-07	2019	-4.563%	4.781%	-2.369%
	1000	1.19E-01	2.129E-07	598	0.114391	2.214E-07	594	-3.847%	4.001%	-0.669%
	10000	2.03E-03	1.251E-07	334	0.002048	1.237E-07	330	0.000%	0.000%	-1.198%
	100000	3.81E-05	6.649E-08	303	0.000040	6.369E-08	294	4.399%	-4.214%	-2.970%
3rd Dilution	Frequency Hz	Ls H	Cs	Rs	Ls H	Cs	Rs	delta Ls (3D)	delta Cs (3D)	delta Rs (3D)
	100	3.07E+00	8.244E-07	1547	3.936637	6.435E-07	1871	28.115%	-21.945%	20.944%
	1000	7.49E-02	3.382E-07	536	0.090056	2.813E-07	643	20.236%	-16.830%	19.963%
	10000	1.45E-03	1.745E-07	320	0.001645	1.540E-07	396	13.329%	-11.761%	23.750%
	100000	3.14E-05	8.065E-08	286	0.000035	7.328E-08	362	10.064%	-9.144%	26.573%

**Table 7.6.** Parameter variation - 20 kV/cm - Dilutions 1, 2 and 3

All in all, of the 24 measurements, the tendency of the variation of the inductive parameter 'Ls', capacitive 'Cs' and resistive 'Rs', is to vary positively, negatively, and

positively respectively. A special frequency analysis was developed, for which, the frequency of positive or negative variations were ordered in **Table 7.7** according to the reading of the parameters.

	Cases in %			Cases in N°		
	delta Ls	delta Cs	delta Rs	delta Ls	delta Cs	delta Rs
Positive Variation	66.7%	16.7%	62.5%	16	4	15
Negative Variation	16.7%	66.7%	37.5%	4	16	9
No variation	16.7%	16.7%	0.0%	4	4	0

**Table 7.7.** Frequency analysis of inductance, capacitance, and resistance.

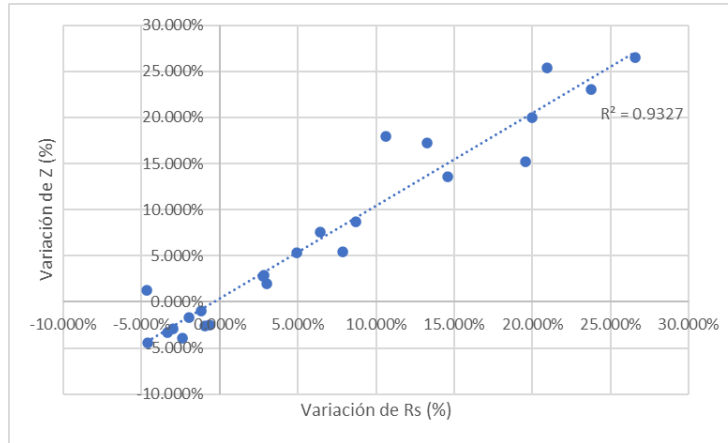
With the appropriate calculation of the impedance according to  $Z = \sqrt{Rs^2 + Xs^2}$ , the variations of impedance before and after electroporation were obtained, and these are listed in **Table 7.8**, where it can be seen that the tendency in 16 of the 24 cases was to increase. Only in 8 cases did it vary negatively and there was never a non-significant variation.

	Cases in %	Cases in N°
	delta Z	delta Z
Positive Variation	66.7%	16
Negative Variation	33.3%	8
No variation	0.0%	0

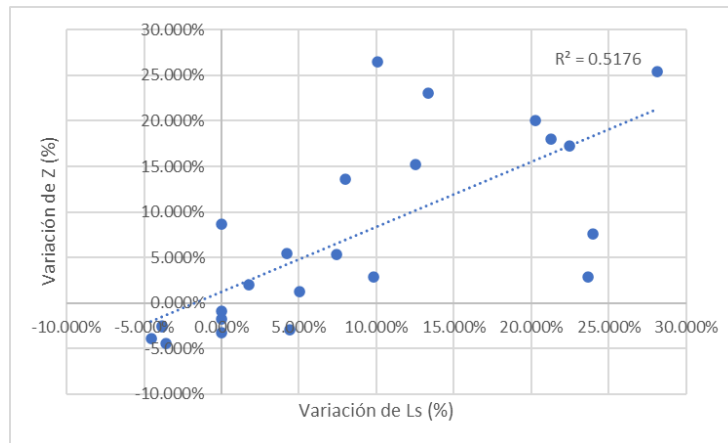
**Table 7.8.** Frequency analysis of impedance.

After obtaining these results, the correlation between the variation of the parameters 'Ls', 'Cs' and 'Rs' with the variation of the impedance 'Z' was studied for the 24 cases, showing in **Figure 7.12** that there is a positive correlation with  $R^2 = 0.9327$  between the variation of the impedance with the variation of the resistance 'Rs' measured. Unfortunately, the situation for the inductive and capacitive variation does not follow a correlational pattern as seen in **Figure 7.13** and **Figure 7.14**; whose graphs present a correlation quite far from  $R^2 = 1$ . This

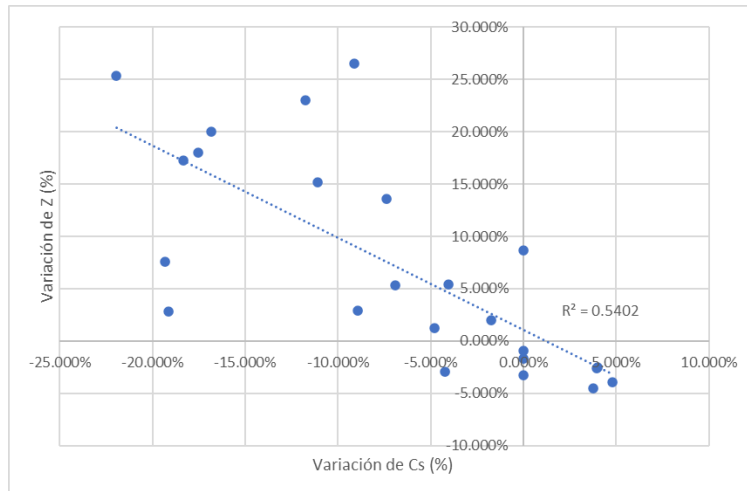
only means that the resistance measured in the cuvettes as parasitic resistance value has a strong influence in the impedance of the cuvette and thus in the energy that flows through the circuit into the tap water dilution.



**Figure 7.12.** Variation of  $Z$  with respect to the variation of  $R_s$  in %.

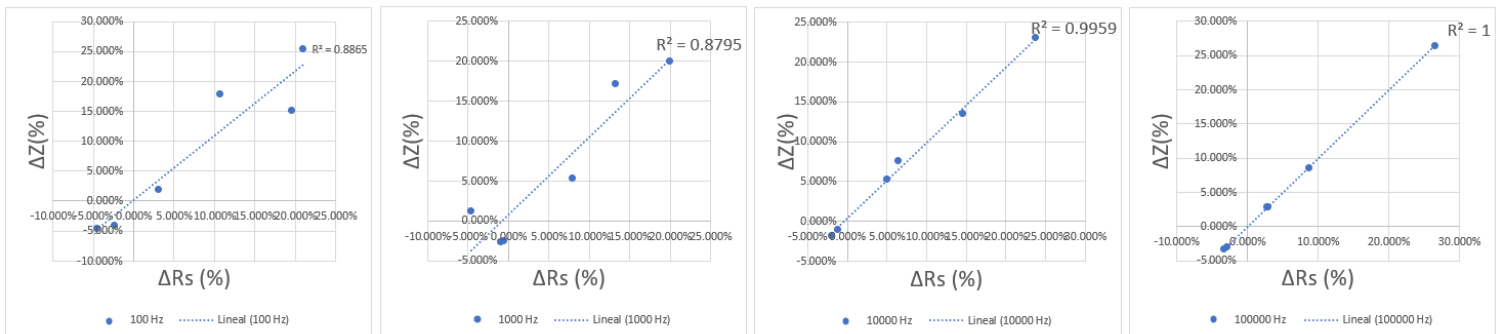


**Figure 7.13.** Variation of  $Z$  with respect to the variation of  $L_s$  in %.

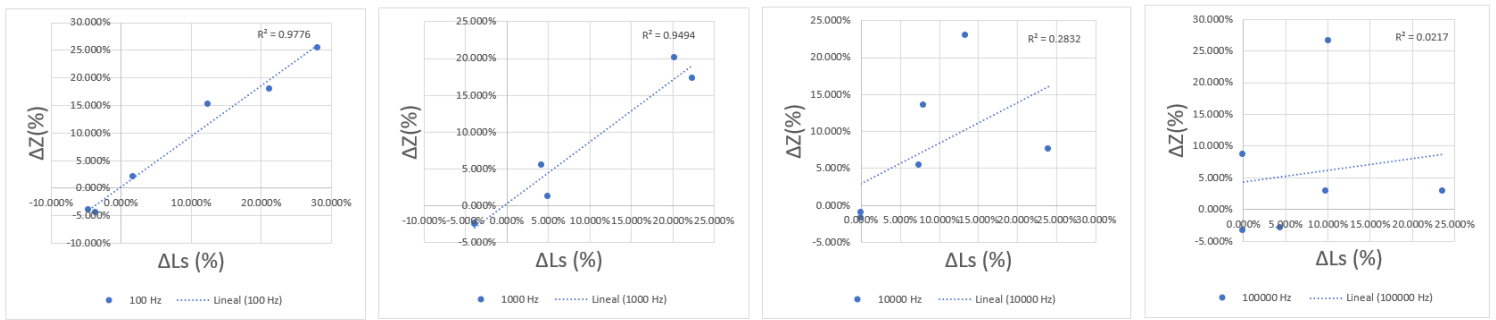


**Figure 7.14.** Variation of Z with respect to the variation of Cs in %.

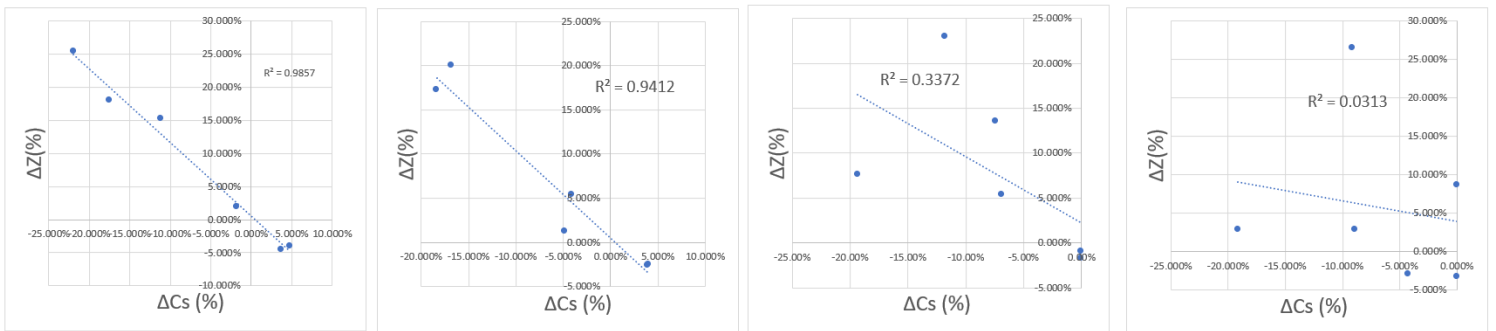
However, when performing the same analysis as a function of frequency (**Figure 7.15**), it was shown that the correlation varies with respect to the variation in frequency. For frequencies higher than 10 kHz, the impedance variation depends almost with a correlation  $R^2 = 1$  on the resistance variation (**Figure 7.15**), while the dependence of the inductive (**Figure 7.16**) and capacitive (**Figure 7.17**) variation is practically null. However, for frequencies lower than 10 kHz and tending to 0 Hz, the situation is reversed, presenting a greater dependence of the inductive and capacitive effect with a correlation  $R^2$  equal to 0.9776 and 0.9857 respectively. The dependence of the resistance remains high with an  $R^2$  equal to 0.8865 (**Figure 7.15**) for frequency values equal to 100 Hz and tending to 0 Hz.



**Figure 7.15.** Variation of Z with respect to Rs as a function of frequency (100 Hz, 1000 Hz, 10000 Hz and 100000 Hz)



**Figure 7.16.** Variation of Z with respect to Ls as a function of frequency (100 Hz, 1000 Hz, 10000 Hz and 100000 Hz)



**Figure 7.17.** Variation of Z with respect to Cs as a function of frequency (100 Hz, 1000 Hz, 10000 Hz and 100000 Hz)

## APPENDIX 7: RESULTADOS DE LA EXPERIMENTACIÓN PRINCIPAL

1. Voltage per pulse applied:



Figure 7.18. 1 kV/cm (198 V)



Figure 7.19. 5 kV/cm (987 V)



Figure 7.20. 6 kV/cm (1188 V)



Figure 7.21. 10 kV/cm (1986 V)



Figure 7.22. 5 kV/cm (2865 V)

2. Cuvettes' temperature:



**Figure 7.23.** 1 kV/cm (Up: Before [22.7°C],  
Down: After [23 °C])



**Figure 7.24.** 5 kV/cm (Up: Before [22.2°C],  
Down: After [22.3 °C])





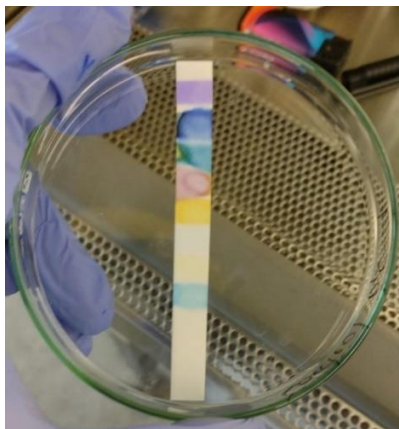
**Figure 7.25.** 6 kV/cm (Up: Before [22.2°C],  
Down: After [22.9 °C])

**Figure 7.26.** 10 kV/cm (Up: Before [22.1°C],  
Down: After [25.1 °C])

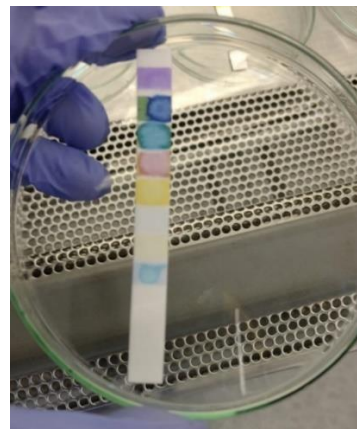


**Figure 7.27.** 15 kV/cm (Up: Before [22.4°C], Down: After [31.2 °C])

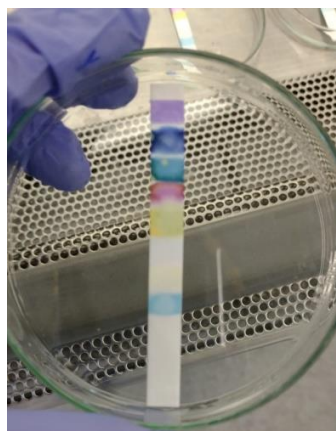
### 3. Ph measurements of the cuvettes' samples



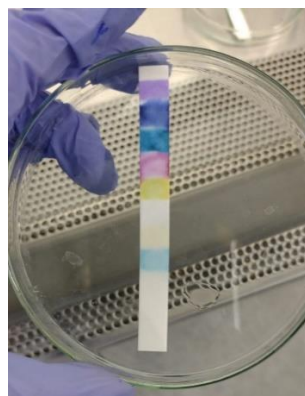
**Figure 7.28.** Control sample (Ph:7-7.5)



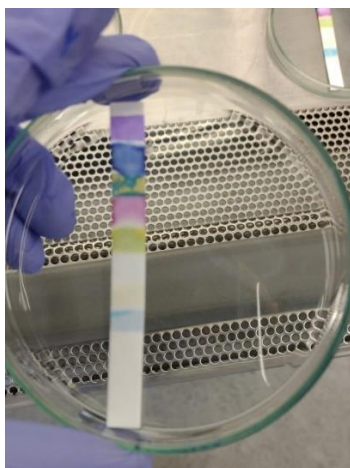
**Figure 7.29.** 1 kV/cm (Ph:7-7.5)



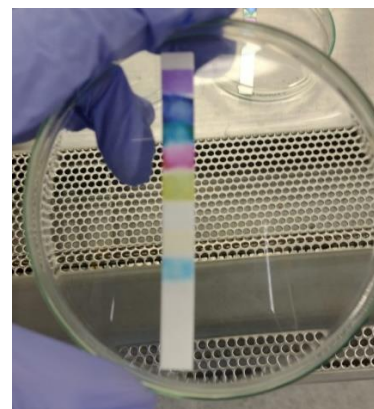
**Figure 7.30.** 5 kV/cm (Ph:7-7.5)



**Figure 7.31.** 6 kV/cm (Ph:7-7.5)

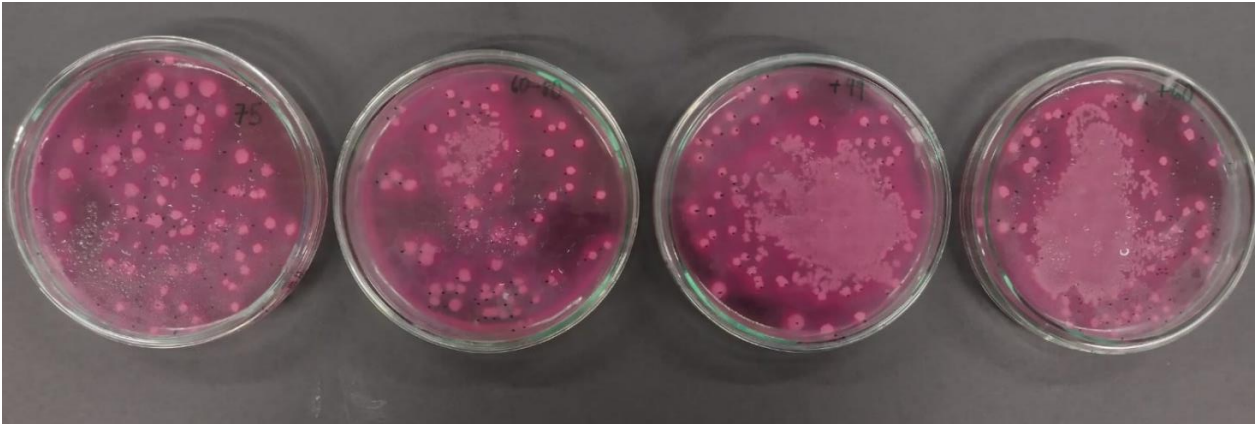


**Figure 7.32.** 10 kV/cm (Ph:7-7.5)

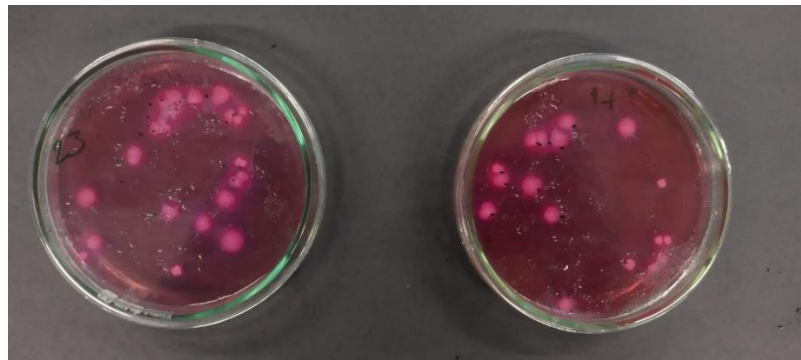


**Figure 7.33.** 15 kV/cm (Ph:7-7.5)

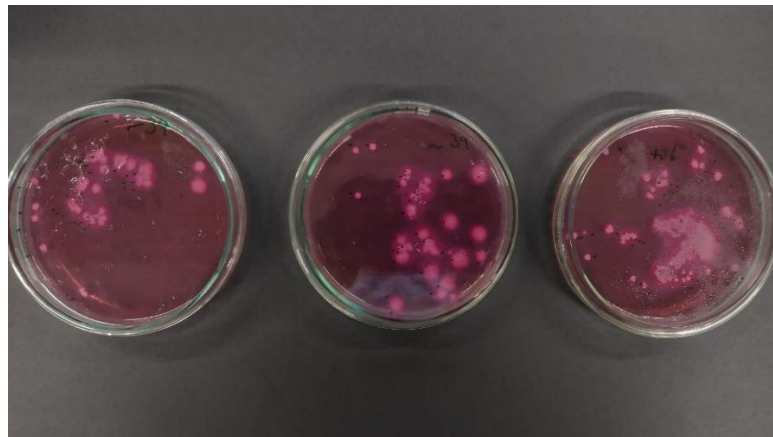
#### 4. Colony counting method in Petri Dishes



**Figure 7.34.** Control sample (75-80 UFC)

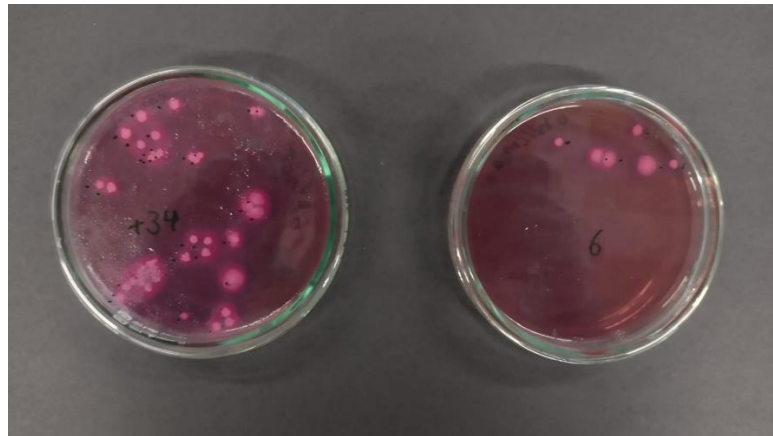


**Figure 7.35.** 1 kV/cm (17-23 UFC)

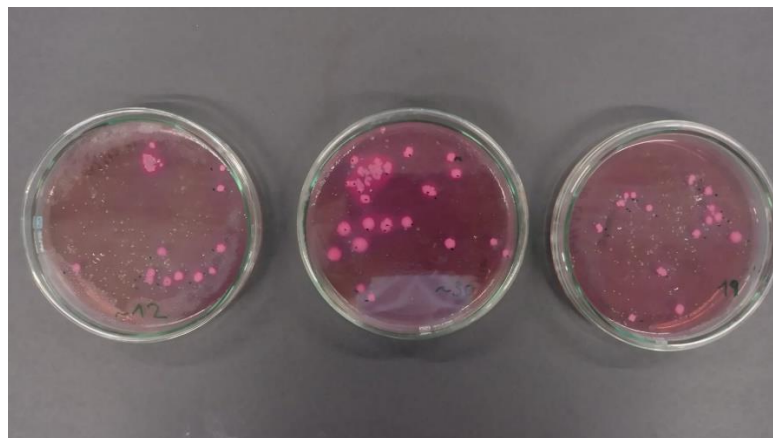


**Figure 7.36.** 5 kV/cm (34-39 UFC)

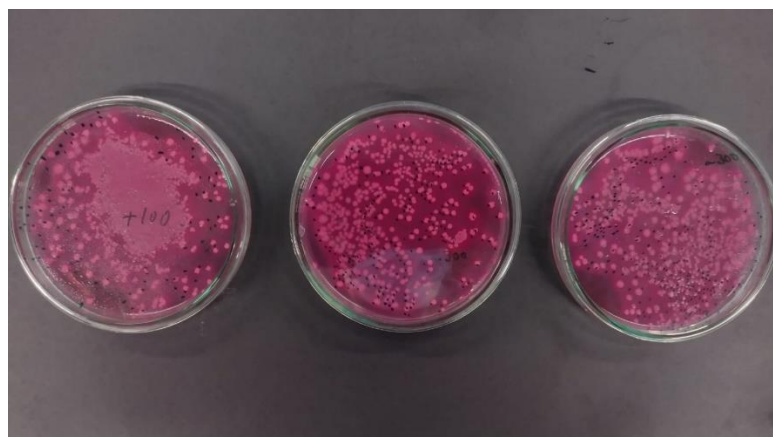




**Figure 7.37.** 6 kV/cm (6-34 UFC)



**Figure 7.38.** 10 kV/cm (12-30 UFC)



**Figure 7.39.** 15 kV/cm (+300 UFC)

## 5. Current measurements

N° of pulse	Time	Current in mA				
		1 kV/cm	5 kV/cm	6 kV/cm	10 kV/cm	15 kV/cm
1	0	2.33	2.33	2.85	4	4
2	1.000022	2.5	2.5	3.37	3.79	4.19
3	2.000044	2.52	2.54	3.18	2.58	4.52
4	3.000066	3.06	3.06	3.81	4.31	3.19
5	4.000088	3.33	3.33	3.72	2.96	4.14
6	5.00011	3.18	3.18	3.7	2.67	3.74
7	6.000132	3.12	3.12	3.75	3.67	4.02
8	7.000154	2.75	3.02	3.81	3.41	5.35
9	8.000176	2.59	2.75	3.77	4.11	5.02
10	9.000198	3.21	2.59	3.74	4.57	5.7
11	10.00022	3.27	3.21	3.73	4.79	3.74
12	11.000242	3.55	3.27	3.74	4.58	4.71
13	12.000264	3.46	3.24	3.79	4.4	4.98
14	13.000286	3	3.55	3.9	4.19	5.47
15	14.000308	3.16	3.46	3.87	4.67	6.4
16	15.00033	3.51	3.44	3.62	4.78	6.45
17	16.000352	3.44	3.43	3.29	4.63	6.58
18	17.000374	3.56	2.89	2.59	4.42	6.15
19	18.000396	3.43	2.01	3.46	4.19	6.49
20	19.000418	-	2.42	3.42	4.71	6.49
21	20.00044	-	3	3.24	4.79	6.29
22	21.000462	-	3.16	3.06	4.87	6.58
23	22.000484	-	3.51	3.65	4.89	6.73
24	23.000506	-	3.44	3.81	4.79	6.53
25	24.000528	-	3.53	-	4.77	6.79
26	25.00055	-	3.46	-	4.94	-
27	26.000572	-	-	-	-	-
28	27.000594	-	-	-	-	-
29	28.000616	-	-	-	-	-
30	29.000638	-	-	-	-	-

**Table 7.9.** Variation of the current measured for each pulse with respect to time.

## 6. Absorbance test (Plots and data)

me  Report Full Mode  Ignore

Sample ID	User ID	Date	Time	Baseline	Cursor 1 Pos.	Cursor 1 Abs.	Cursor 2 Pos.	Cursor 2 Abs.	Norm nm	Norm Abs
control abs 1	Default	19/10/2021	13:59	0.000	300	0.029	600	0.014	695	0.006
control abs 2	Default	19/10/2021	14:00	0.000	300	0.025	600	0.014	695	-0.001
control abs 3	Default	19/10/2021	14:01	0.000	300	0.022	600	0.006	609	-0.001
15 kV/cm-1	Default	19/10/2021	14:04	0.000	300	0.032	600	0.007	707	0.001
15 kV/cm-2	Default	19/10/2021	14:05	0.000	300	0.036	600	0.009	636	0.002
10 kV/cm-1	Default	19/10/2021	14:07	0.000	300	0.032	600	0.008	652	0.001
10 kV/cm-2	Default	19/10/2021	14:08	0.000	300	0.028	600	0.013	694	0.005
10 kV/cm-2-bien	Default	19/10/2021	14:10	0.000	300	0.037	600	0.018	695	-0.003
6 kV/cm-1	Default	19/10/2021	14:11	0.000	300	0.033	600	0.014	695	-0.007
6 kV/cm-2	Default	19/10/2021	14:12	0.000	300	0.034	600	0.021	742	0.051
6 kV/cm-bien	Default	19/10/2021	14:14	0.000	300	0.033	600	0.011	572	-0.000
5 kV/cm-1	Default	19/10/2021	14:15	0.000	300	0.032	600	0.014	696	-0.004
5 kV/cm-2	Default	19/10/2021	14:16	0.000	300	0.026	600	0.012	695	-0.003
1 kV/cm-1	Default	19/10/2021	14:18	0.000	300	0.027	600	0.014	695	-0.003
1 kV/cm-2	Default	19/10/2021	14:19	0.000	300	0.022	600	0.011	497	-0.003
control abs 4	Default	19/10/2021	14:21	0.000	300	0.023	600	0.009	694	-0.001
control abs 5	Default	19/10/2021	14:22	0.000	300	0.028	600	0.012	695	-0.002
15 kv/cm 3	Default	19/10/2021	14:23	0.000	300	0.028	600	0.013	652	0.001
15 kv/cm 4	Default	19/10/2021	14:25	0.000	300	0.030	600	0.013	695	-0.003

Figure 7.40. Absorbance values for each e-field applied

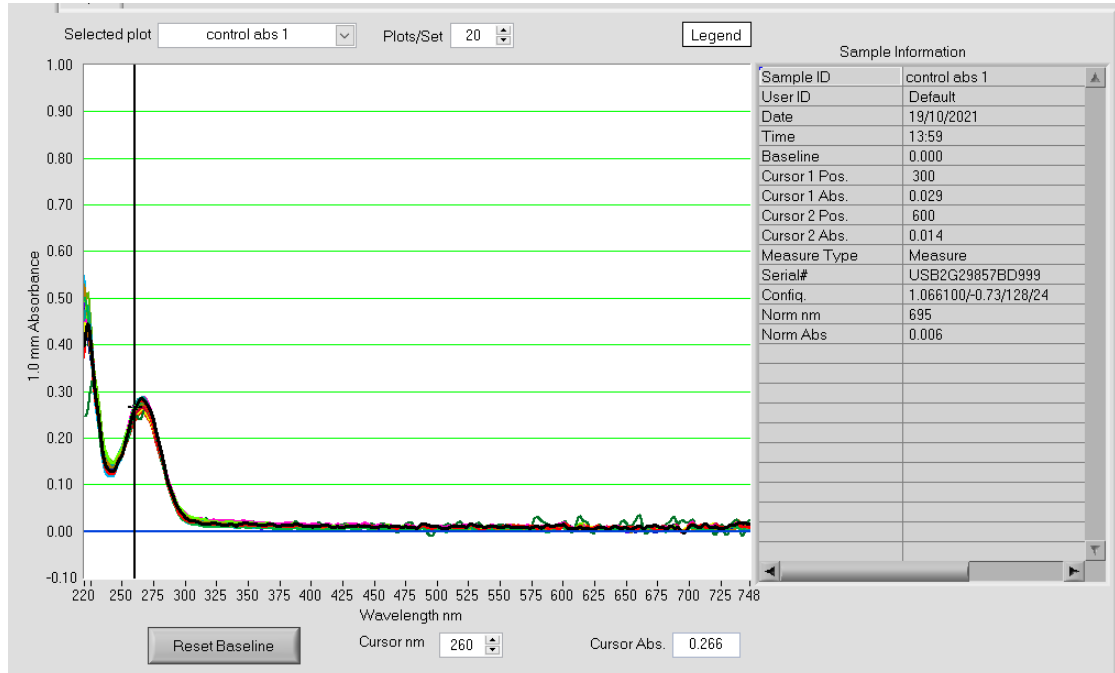


Figure 7.41. Absorbance plots for each e-field applied

## APPENDIX 8: REFERENCES OF DRINKING WATER CONDUCTIVITY IN PERU AND IN THE RIMAC BASIN (ANA, INEI AND LURIN SAMPLE)

Source	Conductivity	Resistivity	Resistance
	$\mu\text{S/cm}$	Ohm-cm	Ohm
Autoridad Nacional del Agua	263.8	3790.75057	379.075057
	300.8	3324.46809	332.446809
	362.9	2755.58005	275.558005
	478.1	2091.61263	209.161263
	494.1	2023.88181	202.388181
	506.9	1972.7757	197.27757
	515.3	1940.61712	194.061712
	516.9	1934.61018	193.461018
	528.5	1892.14759	189.214759
	591.8	1689.76005	168.976005
	617.4	1619.6955	161.96955
	650.7	1536.80652	153.680652
	657.7	1520.45005	152.045005
	716.2	1396.25803	139.625803
	730	1369.86301	136.986301
	739.6	1352.08221	135.208221
	990.6	1009.4892	100.94892
	1030	970.873786	97.0873786
1229	813.66965	81.366965	
2009.1	497.735304	49.7735304	
INEI	504.46	1982.31773	198.231773
	518.75	1927.71084	192.771084
	525.208	1904.00756	190.400756
	536.17	1865.08011	186.508011
	562.791667	1776.85644	177.685644
	564.5	1771.47919	177.147919
	573.645833	1743.23588	174.323588
	591.875	1689.54593	168.954593
	593.33	1685.40273	168.540273
	597	1675.04188	167.504188
	625.48	1598.77214	159.877214
Lurin	1038	963.391137	96.3391137
	878	1138.95216	113.895216
	929	1076.42626	107.642626
	987	1013.17123	101.317123
	1013.5	986.679822	98.6679822
	1071	933.706816	93.3706816

**Table 7.10.** Resistivity, conductance and resistance values of water samples from Rimac basin and Lurin tapwater (Autoridad Nacional del Agua [76], INEI [77], Lurín [78])